# Least Squares Based Adaptive Control and Extremum Seeking with Active Vehicle Safety System Applications

by

Nursefa Zengin

A thesis
presented to the University of Waterloo
in fulfilment of the
thesis requirement for the degree of
Doctor of Philosophy
in
Systems Design Engineering

Waterloo, Ontario, Canada, 2020

**Examining Committee Membership**

The following served on the Examining Committee for this thesis. The decision of the Examining Committee is by majority vote.

| | |
|---|---|
| External Examiner | NAME: Chun-Yi Su<br>Title: Professor |
| Supervisor | NAME: Baris Fidan<br>Title: Associate Professor |
| Internal Member | NAME: Eihab Abdel-Rahman<br>Title: Professor |
| Internal-External Member | NAME: Amir Khajepour<br>Title: Professor |
| Internal-External Member | NAME: John W. Simpson-Porco<br>Title: Assistant Professor |

## Author's Declaration

I hereby declare that I am the sole author of this thesis. This is a true copy of the thesis, including any required final revisions, as accepted by my examiners.

I understand that my thesis may be made electronically available to the public.

## Abstract

On-line parameter estimation is one of the two key components of a typical adaptive control scheme, beside the particular control law to be used. Gradient and recursive least squares (RLS) based parameter estimation algorithms are the most widely used ones among others. Adaptive control studies in the literature mostly utilize gradient based parameter estimators for convenience in nonlinear analysis and Lyapunov analysis based constructive design. However, simulations and real-time experiments reveal that, compared to gradient based parameter estimators, RLS based parameter estimators, with proper selection of design parameters, exhibit better transient performance from the aspects of speed of convergence and robustness to measurement noise.

One reason for the control theory researchers' preference of gradient algorithms to RLS ones is that there does not exist a well-established stability and convergence analysis framework for adaptive control schemes involving RLS based parameter estimation. Having this fact as one of the motivators, this thesis is on systematic design, formal stability and convergence analysis, and comparative numerical analysis of RLS parameter estimation based adaptive control schemes and extension of the same framework to adaptive extremum seeking, viz. adaptive search for (local) extremum points of a certain field. Extremum seeking designs apply to (i) finding locations of physical signal sources, (ii) minimum or maximum points of (vector) cost or potential functions for optimization, (iii) calculating optimal control parameters within a feedback control design.

In this thesis, firstly, gradient and RLS based on-line parameter estimation schemes are comparatively analysed and a literature review on RLS estimation based adaptive control is provided. The comparative analysis is supported with a set of simulation examples exhibiting transient performance characteristics of RLS based parameter estimators, noting absence of such a detailed comparison study in the literature.

The existing literature on RLS based adaptive control mostly follows the indirect adaptive control approach as opposed to the direct one, because of the difficulty in integrating an RLS based adaptive law within the direct approaches starting with a certain Lyapunov-like cost function to be driven to (a neighborhood) of zero. A formal constructive analysis framework for integration of RLS based estimation to direct adaptive control is proposed following the typical steps for gradient adaptive law based direct model reference adaptive control, but constructing a new Lyapunov-like function for the analysis. After illustration of the improved performance with RLS adaptive law via some simple numerical examples, the proposed RLS parameter estimation based direct adaptive control scheme is successfully applied to vehicle antilock braking system control and adaptive cruise control. The perfor-

mance of the proposed scheme is numerically analysed and verified via Matlab/Simulink and CarSim based simulation tests.

Similar to the direct adaptive control works, the extremum seeking approaches proposed in the literature commonly use gradient/Newton based search algorithms. As an alternative to these search algorithms, this thesis studies RLS based on-line estimation in extremum seeking aiming to enhance the transient performance compared to the existing gradient based extremum seeking. The proposed RLS estimation based extremum seeking approach is applied to active vehicle safety system control problems, including antilock braking system control and traction control, supported by Matlab/Simulink and CarSim based simulation results demonstrating the effectiveness of the proposed approach.

## Acknowledgements

First and foremost, I would like to thank my supervisor, Prof. Baris Fidan for his support, patience and immense knowledge. Besides my supervisor, I would like to thank my committee members: Prof. Amir Khajepour, Prof. Eihab Abdel-Rahman, Prof. John Simpson-Porco, and Prof. Chun-Yi Su for their insightful comments, discussions, and encouragement.

I am deeply grateful to my family for supporting me in every step of my life. Most importantly, none of this would have been possible without the love, patience and continuous support of my husband, Halit Zengin. Lastly, I would like to thank to very few but precious people who support me not only in my good times but in my hard times as well.

I also would like to acknowledge the financial support of University of Waterloo and General Motors.

## Dedication

To my family.

# Table of Contents

# List of Figures

# Nomenclature

| | |
|---|---|
| *ABS* | Antilock Braking System |
| *ACC* | Adaptive Cruise Control |
| *APPC* | Adaptive Pole Placement Control |
| *ES* | Extremum Seeking |
| *LPV* | Linear Parameter Variant |
| *LS* | Least Squares |
| *LTI* | Linear Time Invariant |
| *MISO* | Multiple input single output |
| *MRAC* | Model Reference Adaptive Control |
| *PE* | Persistence of Excitation |
| *PES* | Perturbation based Extremum Seeking |
| *RLS* | Recursive Least Squares |
| *SISO* | Single input single output |
| *TCS* | Traction Control System |

# Chapter 1

# Introduction

## 1.1 Motivation

Control systems in practice typically bear complicated and uncertain dynamics. It is infeasible to form a mathematical model for these systems accurately based on experimental data or first principles of physics. To compensate the modelling uncertainties and time variations, it is desirable to control such systems adaptively, i.e. execute on-line system identification based on real time measurements and tune the control parameters while the system is running.

Adaptive control finds itself a place in linear [60, 61] and nonlinear systems [68]. Adaptive control has two important approaches based on two different control objectives: model reference control (MRC) and pole placement control (PPC). In MRC, the objective is asymptotic tracking of a large class of signals via designing the controller such that the closed loop matches with a predefined reference model; whereas, the objective of PPC is stability and assigning a desired set of closed loop poles. MRC designs typically require the plants to be minimum phase while the minimum phase property is not required for PPC.

On-line parameter estimation is an important part of designing an adaptive control scheme. Most of the studies in the adaptive control literature have utilized gradient based parameter estimation and adaptive laws, and examined the stability and convergence of the developed schemes accordingly. Gradient based estimation algorithms are widely used in adaptive control due to their intuitive and convenient structures for Lyapunov function based system stability and convergence analysis. However, gradient based parameter estimation often does not provide the best possible transient performance and best possible level of robustness to measurement noises.

As another on-line parameter estimation method, least squares (LS) based parameter estimation is used for data fitting in almost all scientific and engineering applications such as statistics, equation solving, signal processing, system identification and most recently machine learning. Recursive least squares (RLS) parameter estimation algorithm is the recursive application of LS that provides high performance solutions to adaptive control of parametrically uncertain systems, although there does not exist a well-established stability and convergence analysis framework in the literature for adaptive control schemes involving RLS based parameter estimation. Moreover, RLS based adaptive control mostly follows the indirect adaptive control approach as opposed to the direct one, because of the difficulty in integrating an RLS based adaptive law within the direct approaches starting with a certain Lyapunov-like cost function.

Closely related to adaptive control, where the system or control parameters are estimated by minimizing a certain cost function, the field of adaptive search and optimization deals with the problem of reaching the extremum of a signal field or cost function, which could be a maximum or a minimum. There are many optimization methods to find the extremum of a function either analytically or numerically including gradient, Newton, Lagrangian, and Hamiltonian methods. In recent years, extremum seeking (ES) approaches have constituted a popular form of adaptive search and update schemes due to their convenience for non-model based analysis and a wide range of implementation areas. These approaches have been mostly used with gradient/Newton based search algorithms. Since RLS algorithms are typically observed to be superior, in terms of convergence speed and robustness to measurement noises, over gradient algorithms, it is predictable that RLS parameter estimation based ES schemes will also provide faster convergence and robustness to sensor noises.

Considering the aforementioned facts, this thesis focuses on RLS parameter estimation based adaptive control and ES schemes, providing systematic design, formal stability and convergence analysis, and comparative numerical analysis, aiming to enhance the transient performance compared to the existing gradient parameter estimation based adaptive control and adaptive ES schemes. In addition, active vehicle safety system applications of the systematically developed RLS parameter estimation based adaptive control and ES schemes are studied in the thesis.

## 1.2 Objective

Unlike the existing literature, which has mainly focused on gradient parameter estimation, this thesis investigates RLS parameter estimation based adaptive control and adaptive ES schemes:

i. Indirect adaptive PPC and MRC based on RLS parameter estimation is comparatively analysed in detail, with respect to gradient based schemes, and transient performances are exhibited via numerical simulation examples.

ii. A formal constructive analysis framework for integration of RLS based estimation to direct adaptive control is proposed following the typical steps for gradient adaptive law based direct model reference adaptive control, but constructing a new Lyapunov-like function for the analysis.

iii. An RLS estimation based ES scheme is designed and analysed for application to scalar parameter and vector parameter static map and dynamic systems. Asymptotic convergence to the extremum is established for all the cases.

iv. The proposed RLS parameter estimation based direct adaptive control and RLS parameter estimation based ES schemes are applied to active vehicle safety systems. Adaptive cruise control (ACC), anti-lock braking system (ABS), and traction control system (TCS) are considered for demonstrating the effectiveness of proposed schemes supported by Matlab/Simulink and CarSim based simulation results.

## 1.3 Organization

Later chapters of the thesis are organised as follows. Chapter 2 provides background and literature review on adaptive control and adaptive ES. Gradient and RLS on-line parameter estimation based adaptive control as well as the previous studies on RLS parameter estimation are elaborately examined. Adaptive ES with its basics and cornerstone studies on this research area are given in detail. Application areas for both schemes are presented.

Chapter 3 is devoted to introducing RLS on-line parameter estimation based indirect and direct adaptive control schemes with a set of numerical and simulation examples. Later in the chapter, the analysis of RLS parameter estimation based direct adaptive control defining new Lyapunov functions is given. The implementation of RLS parameter estimation based direct adaptive control on ACC and ABS are presented to demonstrate the validity of the design with Matlab/Simulink and CarSim simulation results.

In Chapter 4, formal problem statement of RLS based ES scheme is given for static map and dynamic systems. Existing ES scheme developed by [73] is redesigned utilizing RLS parameter estimation. Later, an RLS estimation based ES scheme is designed and analysed. Asymptotic convergence to the extremum is prer for all the cases. The performance of the proposed control schemes is examined in Matlab/Simulink and CarSim simulations with ABS and TCS. Several driving scenarios are designed to evaluate the capability of the proposed designs in longitudinal vehicle safety systems.

Chapter 5 provides concluding remarks. In addition, some possible future research directions beyond the studies in this thesis are stated.

# Chapter 2

# Background and Literature Review

This chapter provides the background for the later contribution chapters of the thesis as well as the relevant literature review. We first summarize background notions and tools of adaptive control in general. As a key component of adaptive control systems, we focus on on-line parameter estimators, particularly the gradient and LS based ones. Later, as another optimization, identification, and control approach, we provide background on ES, explaining the links with gradient and LS based parameter estimators. The background and the literature review are presented in a way to highlight the influence of the on-line parameter estimator selection as well as established and potential benefits of using LS based parameter estimators.

## 2.1 Preliminaries

This section gives some definitions from the systems theory and is intended to be the base for the work in Chapter 3.

Consider a dynamical system with the generic state-space model

$$\begin{aligned} \dot{x}(t) &= f(x(t), u(t), t), \quad x(t_0) = x_0, \\ y(t) &= g((x(t), u(t), t), \end{aligned} \tag{2.1}$$

where $x(t) \in \mathcal{R}^n$, $u(t) \in \mathcal{R}^r$, and $y(t) \in \mathcal{R}^l$, are, respectively, the state, the control input, and the output of the system at time instant $t$. When $f, g$ are linear time-invariant functions of $x, u$, (2.1) becomes

$$
\begin{aligned}
\dot{x} &= Ax + Bu, \quad x(t_0) = x_0, \\
y &= C^T x + Du,
\end{aligned}
\tag{2.2}
$$

where $A \in \mathcal{R}^{n \times n}, B \in \mathcal{R}^{n \times r}, C \in \mathcal{R}^{n \times l}$, and $D \in \mathcal{R}^{l \times r}$ are constant matrices.

The solution of (2.2) can be written as

$$
\begin{aligned}
x(t) &= e^{A(t-t_0)} x_0 + \int_{t_0}^{t} e^{A(t-\tau)} Bu(\tau) d\tau, \\
y &= C^T x + Du,
\end{aligned}
\tag{2.3}
$$

where $e^{At}$ is identified to be

$$
e^{At} \triangleq \mathcal{L}^{-1}[(sI - A)^{-1}], \tag{2.4}
$$

where $\mathcal{L}^{-1}$ and $s$ denote, respectively, the inverse Laplace transform and the Laplace variable. If we take the Laplace transform of both sides of (2.2) setting initial conditions $x(0) = 0$, we have

$$
G(s) \triangleq \frac{Y(s)}{U(s)} = C^T (sI - A)^{-1} B + D, \tag{2.5}
$$

where $Y(s), U(s)$ are Laplace transforms of $y, u$, and $G(s)$ is the transfer function of (2.2). $G(s)$ can be written as

$$
G(s) = \frac{Z(s)}{R(s)} = \frac{b_m s^m + b_{m-1} s^{m-1} + \cdots + b_0}{s^n + a_{n-1} s^{n-1} + \cdots + a_0}, \tag{2.6}
$$

where $Z(s), R(s)$ are polynomials. (2.5) leads to

$$
G(s) = \frac{C^T (adj(sI - A)) B}{det(sI - A)} + D, \tag{2.7}
$$

where $adj(sI - A)$ denotes the adjoint of the square matrix $(sI - A)$. If all the eigenvalues of $A$ lie in $\mathcal{R}[s] < 0$ then $A$ is called a stable matrix, and $G(s)$ is a stable transfer function.

Moreover, under zero inial conditions, the Laplace variable $s$ can be considered as differential operator $s(x) \triangleq \dot{x}$. In this thesis, $s$ will be used to denote both the differential operator and Laplace variable, i.e. we also use the notation

$$y = G(s)u, \tag{2.8}$$

when $s$ is considered as the differential operator. $G(s) = \frac{Z(s)}{R(s)}$ in (2.8) shall denote the filter with input $u(t)$ and output $y(t)$.

## 2.2 Adaptive Control and On-line System Identification

### 2.2.1 Adaptive Control

The main motivator of adaptive control is compensation of plant uncertainties [60, 61, 104] and variations while performing a specified control task. To perform this compensation, adaptive control parameters change with time following a certain adaptive law. Considering the dependence of this adaptive law on plant estimates vs. closed-loop system performance, adaptive control schemes are classified as identifier-based vs. non-identifier-based [60]. Former involves on-line parameter estimators which yield estimates of unknown plant parameters at each instant time. Rather than having on-line plant parameter estimators, latter involves different methods including gain scheduling and switching systems to select or form the best controller from a set of candidate controllers.

Adaptive control design typically involves a parametric model, which has unknown parameters and known signals, and an adaptive law or update law to adjust the control parameters directly based on closed-loop system perfomance or indirectly based on estimation of plant parameters. The adaptive law estimating the plant or control parameters can be combined with a control structure in two different ways, leading to direct adaptive control and indirect adaptive control. In indirect adaptive control, the plant parameters are continuously estimated and, simultaneously, the control parameters are calculated using the plant parameter estimates. In direct adaptive control, the control parameters are directly adjusted on-line to values minimizing a certain closed-loop system error based on an implicit parametric model of the closed loop system in terms of these control parameters, without requiring estimation of the plant parameters [60], as illustrated in Fig. 2.1.

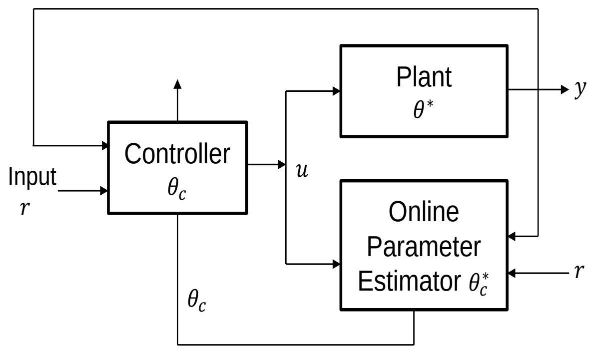


(a) Direct adaptive control structure.

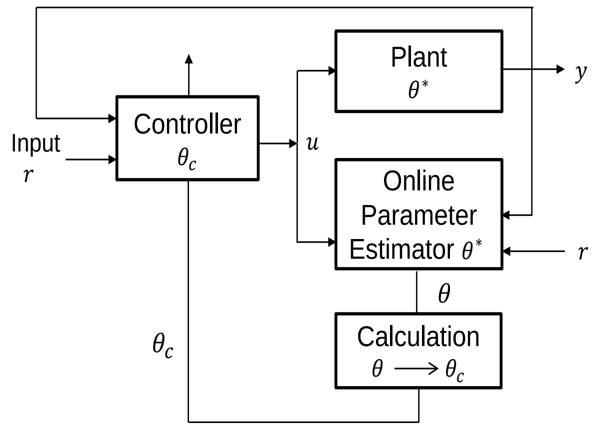


(b) Indirect adaptive control structure.

Figure 2.1: Direct and indirect adaptive control structures [60].

In indirect adaptive control design, a model, whose parameters are unknown, is formulated for the plant, and the plant parameters are recursively estimated utilizing this parametric model. The controller gains are calculated based on a predefined mapping from plant parameters to control parameters and utilizing the plant parameter estimates. In order to estimate the unknown plant parameters, parameter identification steps can be implemented accordingly.

### 2.2.2 On-line Parameter Identification

Parameter identification problem is defined as finding the best estimate of the parameters that govern a dynamical system, using the measured data of the system behaviour. System parameters can be in the form of entries of matrices, transfer function coefficients, or special model coefficients. On-line parameter identification algorithms generate estimates of such system parameters at each time by using past and current signal measurements, and convergence is often asymptotically achieved in time. These algorithms are referred as recursive parameter identification algorithms because of dependence on past and current measurements and since they are expressed in the form of a law generating the time derivatives or time updates of the parameter estimates.

A systematic on-line parameter identification design consists of three main components or steps: parametric model, estimation model, and adaptive law.

**Step 1: Parametric Model**

A parametric model (preferably linear, or bilinear) is defined. Linear parametric models are formed as

$$z = {\theta^*}^T \phi, \tag{2.9}$$

where $z \in \mathbb{R}$ and $\phi \in \mathbb{R}^n$ are signals available for measurement, and $\theta^* \in \mathbb{R}^n$ is the vector with all unknown parameters. Further varieties of linear and bilinear parametric models can be seen in [60].

**Step 2: Estimation Model**

The estimation model and estimation error are formed. For the linear parametric model (2.9), the estimation model is constructed in the same form as the parametric model, as

$$\hat{z} = \theta^T \phi, \tag{2.10}$$

where $\theta$ is the estimate of $\theta^*$, and $\hat{z}$ is the output of this estimation model. To feed the adaptive laws, the measurable (or observed) estimation error is defined as the difference between the measured output $z$ of (2.9) and output estimate $\hat{z}$ produced by (2.10), either in the unnormalized form

$$\varepsilon = z - \hat{z} \tag{2.11}$$

or in the normalized form

$$\varepsilon = \frac{z - \hat{z}}{m_s^2}, \quad m_s^2 = 1 + \alpha \|\phi\|^2, \quad \alpha \geq 0, \tag{2.12}$$

where $m_s^2$ is a normalizing signal which guarantees that $\frac{\phi}{m_s}$ bounded. The case for $\alpha = 0$ is equivalent to (2.11). Note here the observed estimation error $\varepsilon$ and the parameter estimation error $\tilde{\theta} = \theta - \theta^*$ are directly related via

$$\varepsilon = \frac{-\tilde{\theta}^T \phi}{m_s^2}. \tag{2.13}$$

**Step 3: Adaptive Law**

In continuous time, the adaptive law is usually a differential equation whose state is $\theta(t)$. It is designed following some optimization and stabilization techniques to minimize the estimation error magnitude $|\varepsilon(t)|$ at each time $t$. As the two main approaches used in the literature we briefly present the gradient and LS based adaptive laws in the next section.

## 2.3 Gradient and Least Squares Based Parameter Identification

### 2.3.1 Gradient Based Parameter Identification

Gradient based parameter estimation for the system (2.9) aims to recursively produce the estimate $\theta(t)$ of $\theta^*$ that would minimize the cost function

$$J(\theta) = \frac{\varepsilon^2 m_s^2}{2} = \frac{\left(z - \theta^T \phi\right)^2}{2m_s^2}. \tag{2.14}$$

which penalizes the mismatch between the actual output $z$ and the output estimate $\hat{z}$. The gradient based solution is given by

$$\dot{\theta} = -\Gamma \nabla J(\theta) \tag{2.15}$$

where $\nabla J(\theta) = -\frac{\left(z-\theta^T\phi\right)}{m_s^2}\phi = -\varepsilon\phi$ is the gradient of $J$ evaluated at $\theta(t)$ and $\Gamma$ is a positive definite symmetric gain matrix, called the adaptive gain. Hence, the gradient based parameter estimator (adaptive law) is obtained as

$$\dot{\theta} = \Gamma \varepsilon \phi \quad \theta(0) = \theta_0. \tag{2.16}$$

Gradient based adaptive laws are widely used in adaptive control design because of their intuitive and convenient structures for Lyapunov based system stability and signal convergence analysis. However, in terms of transient performance, requirements for guaranteed parameter convergence, and robustness to measurement noises, it is observed that gradient based parameter estimation, often, is not the best approach. To overcome such issues, LS based parameter estimation is considered.

### 2.3.2 Least Squares Based Parameter Identification

The underlying idea of LS based parameter estimation is, in place of minimizing an instantaneous (memoryless) cost function, to minimize an integral cost function that penalizes the estimation mismatches with the past data as well as the mismatch with the current instantaneous data. To give less waiting to older data mismatches and more to newer one, it is beneficial to introduce a time-indexed forgetting factor to this integral cost function. Hence, instead of the instantaneous cost function (2.14), one can consider the cost function

$$J(\theta) = \frac{1}{2}\int_0^t e^{-\beta(t-\tau)} \frac{\left[z(\tau) - \theta^T(t)\phi(\tau)\right]^2}{m_s^2(\tau)} d\tau + \frac{1}{2} e^{-\beta t}(\theta - \theta_0)^T Q_0 (\theta - \theta_0), \tag{2.17}$$

with design parameters $Q_0 = Q_0^T > 0, \beta > 0$ and initial estimate is $\theta_0 = \theta(0)$. (2.17) includes estimation errors for past data and a penalty on deviation from the initial estimate $\theta_0$. Since normalization guarantees that $\frac{z}{m_s}, \frac{\phi}{m_s} \in \mathcal{L}_\infty$, $J(\theta)$ is a bounded convex function of $\theta$ over $\mathcal{R}^n$ at each time $t$. Therefore, at each time $t$, there is a unique local (and hence global) minimum $\theta_{min}$ satisfying

$$\nabla J(\theta_{min}) = 0. \tag{2.18}$$

LS algorithm aims to generate $\theta(t)$ that satisfies

$$\nabla J(\theta) = e^{-\beta t} Q_0 (\theta - \theta_0) - \int_0^t e^{-\beta(t-\tau)} \frac{z(\tau) - \theta^T \phi(\tau)}{m_s^2(\tau)} \phi(\tau) d\tau = 0. \tag{2.19}$$

Direct solution of (2.19) for $\theta$ gives the ***non-recursive LS algorithm***

$$\theta(t) = P(t)\left[e^{-\beta t} Q_0 \theta_0 + \int_0^t e^{-\beta(t-\tau)} \frac{z(\tau)\phi(\tau)}{m_s^2(\tau)} d\tau\right], \tag{2.20}$$

where

$$P(t) = \left[e^{-\beta t} Q_0 + \int_0^t e^{-\beta(t-\tau)} \frac{\phi(\tau)\phi^T(\tau)}{m_s^2(\tau)} d\tau\right]^{-1}. \tag{2.21}$$

$P(t)$ is called the covariance matrix. It is guaranteed to be positive-definite for any $t \geq 0$, since $Q_0 = Q_0^T > 0$, and $\phi\phi^T \geq 0$. It is established that $\theta(t)$ and $P(t)$ in (2.20),(2.21) can be asymptotically produced on-line using the ***recursive LS (RLS) algorithm***

$$
\begin{aligned}
\dot{\theta} &= P\varepsilon\phi, \quad \theta(0) = \theta_0, \\
\dot{P} &= \beta P - P\frac{\phi\phi^T}{m_s^2}P, \quad P(0) = P_0 = Q_0^{-1}, \\
\varepsilon &= \frac{z - \theta^T\phi}{m_s^2}.
\end{aligned} \tag{2.22}
$$

If $\beta = 0$ in (2.22), algorithm becomes ***pure LS algorithm*** and given as

$$
\begin{aligned}
\dot{\theta} &= P\varepsilon\phi, \quad \theta(0) = \theta_0, \\
\dot{P} &= -P\frac{\phi\phi^T}{m_s^2}P, \quad P(0) = P_0, \\
\varepsilon &= \frac{z - \theta^T\phi}{m_s^2}.
\end{aligned} \tag{2.23}
$$

One of the disadvantages of the pure LS algorithm is that parameter convergence cannot be guaranteed to be exponential. Another disadvantage is that $P$ may be arbitrarily small and makes the adaptation slow. The reason for that is that

$$
\frac{d(P^{-1})}{dt} = \frac{\phi\phi^T}{m_s^2} \geq 0 \tag{2.24}
$$

gives a growth without bound in $P^{-1}$ which implies reduction in $P$ towards zero. This case is called *covariance wind-up* problem. In order to avoid covariance wind-up problem, we can modify ***pure LS algorithm with covariance resetting*** as follows:

$$
\begin{aligned}
\dot{\theta} &= P\varepsilon\phi, \quad \theta(0) = \theta_0, \\
\dot{P} &= -P\frac{\phi\phi^T}{m_s^2}P, \quad P(t_r^+) = P_0 = \rho_0 I, \\
m_s^2 &= 1 + n_s^2, \quad n_s^2 = \alpha\phi^T\phi, \quad \alpha > 0.
\end{aligned} \tag{2.25}
$$

$t_r^+$ is the time when $\lambda_{min}(P(t)) \leq \rho_1$ and $\rho_0 > \rho_1 > 0$ are design parameters. $P(t) \geq \rho_1 I$ because of covariance resetting. The pure LS algorithm with covariance resetting can be considered as a gradient algorithm with time-varying adaptive gain $P$. If $\beta \geq 0$, for the stability, $\frac{\phi}{m_s}$ must be PE. In this case, covariance wind-up problem does not exist. ***Modified LS algorithm with covariance resetting*** is given as

$$\dot{\theta} = P\varepsilon\phi,$$
$$\dot{P} = \begin{cases} \beta P - P\frac{\phi\phi^T}{m_s^2}P & \|P(t)\| \leq R_0, \\ 0 \quad else, \end{cases} \tag{2.26}$$

where $P(0) = P_0 = P_0^T > 0, \|P_0\| \leq R_0$ and $R_0$ is an upper bound constant for $\|P\|$.

### 2.3.3 Persistence of Excitation

A particular (measurement) signal property that constitutes a sufficient condition of parameter convergence for many parameter estimation schemes is persistence of excitation (PE), with the following formal definition:

**Definition 2.1.** ***(Persistence of Excitation (PE))*** *[61] A piecewise continuous signal vector $\phi\ : \mathcal{R}^+ \mapsto \mathcal{R}^n$ is PE in $\mathcal{R}^n$ with a level of excitation $\alpha_0 > 0$ if there exist constants $\alpha_1, T_0 > 0$ such that*

$$\alpha_1 I \geq \frac{1}{T_0}\int_t^{t+T_0} \phi(\tau)\phi^T(\tau)d\tau \geq \alpha_0 I. \tag{2.27}$$

Although the matrix $\phi(\tau)\phi^T(\tau)$ is singular for each $\tau$ for $n \geq 2$, (2.27) requires that $\phi(\tau)$ varies in such a way with time that the integral of this matrix is uniformly positive definite over any time interval $[t, t+T_0]$.

**Lemma 2.1.** *[61] If $\phi, \dot{\phi} \in \mathcal{L}_\infty$ and $\phi$ is PE, then adaptive laws (2.16) and (2.22) guarantee that $\theta(t) \to \theta^*$ exponentially fast.*

### 2.3.4 Stability and Convergence

**Stability of Gradient Based Parameter Identification:**

**Theorem 2.2.** *[60]The gradient algorithm (2.16) guarantees that*

*(i) $\varepsilon, \varepsilon m_s, \dot{\theta} \in \mathcal{L}_2 \cap \mathcal{L}_\infty$ and $\theta, P \in \mathcal{L}_\infty$.*

*(ii) If $\frac{\phi}{m_s}$ is PE, i.e., $\int_t^{t+T_0} \frac{\phi\phi^T}{m_s^2}d\tau > \alpha_0 T_0 I, \forall t \geq 0$ and for some $T_0, \alpha_0 > 0$, then $\theta(t) \to \theta^*$ exponentially fast.*

*(iii) If the plant model has stable poles and no zero-pole cancellations and the input $u$ is sufficiently rich of order $n+m+1$, i.e., it consists of at least $\frac{n+m+1}{2}$ distinct frequencies, then $\phi, \frac{\phi}{m_s}$ are PE. Furthermore, $|\theta(t)-\theta^*|, \varepsilon, \varepsilon m_s, \dot{\theta}$ converge to zero exponentially fast.*

**Stability of Recursive LS Based Parameter Identification:**

**Theorem 2.3.** *[60] If $\frac{\phi}{m_s}$ is PE, then (2.22) guarantees that $P, P^{-1} \in \mathcal{L}_\infty$ and $\theta(t) \to \theta^*$ as $t \to \infty$. When $\beta > 0$, the convergence of $\theta(t) \to \theta^*$ is exponential.*

**Stability of Pure LS Based Parameter Identification:**

**Theorem 2.4.** *[60, 61] (2.23) guarantees that*

*(i) $\varepsilon, \varepsilon m_s, \dot{\theta} \in \mathcal{L}_2 \cap \mathcal{L}_\infty$ and $\theta, P \in \mathcal{L}_\infty$.*

*(ii) $\lim_{t\to\infty} \theta(t) = \bar{\theta}$ in which $\bar{\theta}$ is a constant vector.*

*(iii) If $\frac{\phi}{m_s}$ is PE, then $\theta(t) \to \theta^*$ as $t \to \infty$.*

*(iv) If (2.9) is SPM for a SISO plant ($y = G(s)u$) with stable poles and without zero-pole cancellation, and $u$ is sufficiently rich of order $n+m+1$, i.e., contains at least $\frac{n+m+1}{2}$ distinct frequencies, then $\phi, \frac{\phi}{m_s}$ are PE; hence, $\theta(t) \to \theta^*$ as $t \to \infty$.*

**Stability of Pure LS based Parameter Identification with covariance resetting and Modified LS Based Parameter Identification:**

**Theorem 2.5.** *[60, 61] (2.25) and (2.26) guarantee that*

*(i) $\varepsilon, \varepsilon m_s, \dot{\theta} \in \mathcal{L}_2 \cap \mathcal{L}_\infty$ and $\theta, P \in \mathcal{L}_\infty$.*

*(ii) $\lim_{t\to\infty} \theta(t) = \bar{\theta}$ in which $\bar{\theta}$ is a constant vector.*

*(iii) If $\frac{\phi}{m_s}$ is PE, then $\theta(t) \to \theta^*$ as $t \to \infty$.*

*(iv) If (2.9) is SPM for a SISO plant ($y = G(s)u$) with stable poles and without zero-pole cancellation, and $u$ is sufficiently rich of order $n+m+1$, i.e., contains at least $\frac{n+m+1}{2}$ distinct frequencies, then $\phi, \frac{\phi}{m_s}$ are PE; hence, $\theta(t) \to \theta^*$ as $t \to \infty$.*

Proofs of given theorems can be found in [60, 61].

### 2.3.5 Literature on Least Squares Algorithm Properties

Based on generation time span of the parameter estimates, the parameter identification algorithms in the literature can be divided into two categories: recursive algorithms [28, 40, 58, 59, 69, 71, 106] and non-recursive algorithms [30, 31]. All algorithms in both categories aim to minimize a defined cost function. Some of the LS algorithm properties compared to the other types of update laws such as gradient, passivity-based, Lyapunov-based, are listed based on the literature outcomes.

- LS algorithm is able to adjust the adaptation rates for different parameters [71].
- RLS algorithms have faster convergence speed [40] and do not exhibit the eigenvalue spread problem [12]. Eigenvalue spread is defined as the ratio of the largest eigenvalue to the smallest eigenvalue. Larger eigenvalue spreads result in slower convergence rates.
- LS algorithms are robust to noise and give better convergence results. [87].
- RLS with forgetting factor has the ability to track time-varying parameters but there is a possibility of gain wind-up in the absence of persistent excitation. The gain wind-up problem can be overcome by employing the bounded gain forgetting technique [87].
- LS algorithms also have the convexity property [28]. Consider

$$z = \theta^{*T}\phi + d_n, \tag{2.28}$$

where $d_n$ is a noise disturbance (or considered as unmodeled dynamics, in practice, may be due to sensor noise and external sources). The average value of noise disturbance is

$$\lim_{t\to\infty} \frac{1}{t}\int_0^t d_n(\tau)d\tau = 0. \tag{2.29}$$

Let $\bar{d}_n$ be bounded by $\gamma$.

$$\begin{aligned} &\bar{d}_n^2 \le \gamma^2 \\ &(z - \theta^{*T}\phi)^2 \le \gamma^2. \end{aligned} \tag{2.30}$$

Let $S$ be a subset of $\mathcal{R}^{n+m+1}$ defined by

$$S = \left\{\theta : (z - \theta^{*T}\phi)^2 \leq \bar{d}_n^2, \theta \in \mathcal{R}^{n+m+1}\right\} \tag{2.31}$$

As a geometrical way, $S$ is a convex polytope which is algebraically defined as the set of solutions to a system of linear inequalities $mx \leq b$. Therefore, all measured values form a convex polytope in the parameter space.

- RLS algorithms have the property of continuity in parameter estimation updates. Even if a new update is provided and has no better information, the algorithm will not stop itself. In practice, this might cause the redundancies [4, 28]

- In order to guarantee the boundedness of covariance matrix $P$ and the estimates, some modifications are introduced, including dead zone, $\sigma-$modifications in adaptive laws [60].

## 2.4 Least Squares Parameter Identification Based Adaptive Control

Adaptive control has played an important role in control theory and most of the adaptive control schemes have been combined with either gradient or LS based parameter identification. To accommodate the later chapters of this thesis, we present a review of the existing works on LS based adaptive control schemes and open problems to be addressed.

### 2.4.1 Literature Review on Theory

Adaptive control schemes are classified as direct and indirect in Section 2.2.1. Analyses of adaptive controller schemes have traditionally been based on Lyapunov function. Among these controllers, especially indirect adaptive controllers, very few are based on LS parameter estimation. LS parameter estimation have been used for convergence and robustness analysis in indirect adaptive controllers [29, 56, 74, 102, 105, 112, 114].

Stability and convergence analysis of adaptive controller schemes have traditionally been based on Lyapunov stability notions and techniques [45, 60, 61, 72, 88] . Lyapunov-like functions are selected in the design of adaptive control to penalize the magnitude of the tracking or regulation error but at the same time useful in designing an adaptive law to generate the parameter estimates to feed the control law. Control designs targeting to drive the Lyapunov-like functions to zero lead to gradient based adaptive laws using a constant adaptive gains due to its convenient structure. On the other hand, it is well observed that LS algorithms have the advantage of faster convergence; hence, LS based adaptive control has potential to enhance convergence performance in direct adaptive control approaches as well [40, 51, 60, 71, 74].

Despite wide use of gradient on-line parameter based identifiers, LS adaptive algorithms with forgetting factor are developed to be capable of faster settling and/or being less sensitive to measurement noises in [40],[51]. Such properties are being justified by simulation and experiment results. LS parameter estimation have been used for convergence and robustness analysis in either indirect adaptive controllers or combination of indirect adaptive controller with direct one [24, 29, 56, 62, 63, 71, 74, 102, 105, 112, 114].

In addition to the existing LS based adaptive control theory studies, there are some publications in the recent literature on real-time applications to robotic manipulators [85, 86, 113], unmanned aerial vehicles [3, 80], and passenger vehicles [1, 10, 21, 94, 95, 101, 106].

Most of the existing studies on LS based adaptive control follow the indirect approach as opposed to direct adaptive control. One reason for this is that the analysis of direct adaptive control is complicated for producing an LS based adaptive control scheme in the Lyapunov-based design. Unlike indirect ones, in direct adaptive control schemes, the estimated parameters are those directly used in the adaptive control laws without any intermediate step.

In the literature, [60, 61] considered the possible use of LS on-line parameter identifier in direct model reference adaptive control (MRAC); however, full details of design was not provided, and Lyapunov analysis with LS parameter estimation was not mentioned. It is obvious that indirect adaptive control has been utilized with LS algorithm in the literature rather than direct one. Possible reasons of unpopularity of direct adaptive control are poor transient performance and complicated analysis of direct adaptive control with LS algorithm because of integral cost function. Most of the existing works have pointed out the necessity of LS algorithm to improve the guaranteed transient performance.

### 2.4.2 Literature Review on Applications

In addition to the studies in theory, there are some applications used with the LS algorithm. Manipulator applications of LS based adaptive control have been given in [85, 86]. They considered the trajectory tracking of a robotic manipulator driven by electro-hydraulic actuators. The controller was constructed based on the indirect adaptive control with

LS algorithm which overcame poor parameter estimation properties of the direct adaptive control based on gradient projection algorithm in [113].

[3] presented practical issues in the use of an indirect adaptive controller to control quadrotors with an emphasis on LS based estimation and the LPV controller design. [80] presented the results that quantify how velocity and attitude estimates can benefit from an improvement to the traditional quadrotor dynamic model based on LS estimator.

In automotive research area, RLS parameter estimation with forgetting factor was used in [106] for simultaneous estimation of mass and grade. They compared the performance of single and multiple forgetting RLS algorithms to prove that RLS algorithm with single forgetting factor could not estimate parameters with different rates of variation. They also formulated the reason of poor estimation performance in single forgetting. When an error is detected, the estimates of both parameters are updated without differentiating between faster changes and constant/little change. [10] used GPS readings to obtain road elevation and calculate the grade using the measured elevations. They estimated the mass with a simple LS method based on the longitudinal dynamics equation with the grade known. Some recent studies in [1, 21, 94, 95, 101] demonstrate the LS application in estimating the unknown friction models.

## 2.5 Adaptive Extremum Seeking

In this section, the classical perturbation based ES is presented in detail, then cornerstone works in ES are given.

### 2.5.1 Basics

ES is a nonmodel based real-time optimization method for dynamic problems without requiring any explicit knowledge about input output characteristic other than that it exists and has an extremum. The main objective of ES is to find the extremum and maintain the extremum value of the function.

ES is also an approach of adaptive control; however, it is not applicable to model reference and related schemes that tackle the stabilization problem of known reference trajectories or set point [6].

The increasing complexity of engineering systems has led to many optimization challenges since analytic solutions to optimization problems for multi-agent, nonlinear, and infinite-

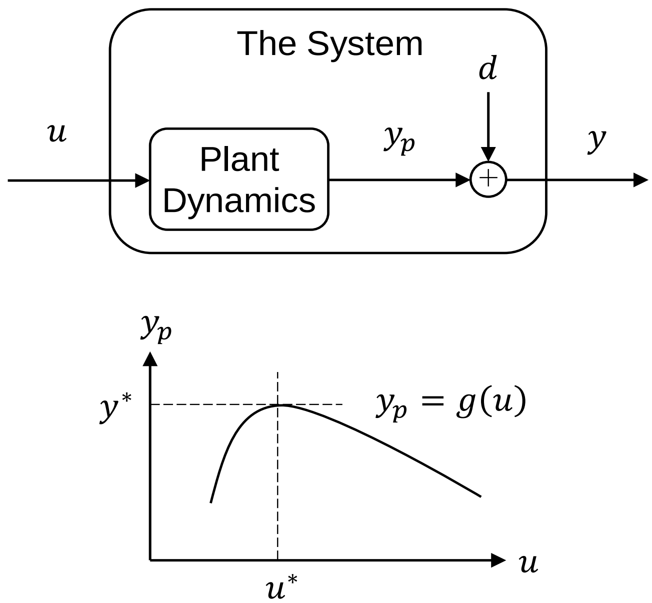


Figure 2.2: Input output system extremum seeking scheme.

dimensional systems are difficult to obtain. This difficulty arises for many reasons, including the presence of competing or adversarial goals, the high-dimensionality of the system, and the inherent system uncertainty. Moreover, if a model-based solution is obtained for those complicated optimization problems, it is likely to be conservative due to modelling deficiencies. Hence, nonmodel based ES methods are an attractive option to solve these kind of problems.

For better understanding of ES idea, a SISO system as in Fig. 2.2 can be considered. $u$ is the input to the system and $y$ is the measured output. Moreover, $y_p$ is the output of the plant and $d$ is the bounded disturbance. Input, output and disturbance are functions of time. It is assumed that the system has a well-defined steady state characteristic $(u, y_p)$ but it does not need to be a function, it could be a multi valued steady state characteristic.

It is assumed that the steady state has a local maximum $(u^*, y_p^*)$. The control purpose in ES is to complete the system in Fig. 2.2 with intent to drive input output pair $(u, y_p)$ to the extremum points $(u^*, y_p^*)$. Let the plant dynamics be modelled as

$$\dot{x} = f(x, u), \quad y_p = h(x), \quad y = y_p + d(t). \tag{2.32}$$

The functions $f, h$ are assumed to be differentiable but not strictly necessary. Also following assumptions are made to ensure the well-defined steady state notion.

**Assumption 2.1.** *There exists a differentiable function* $l : \mathbb{R} \to \mathbb{R}^n$ *such that*

$$f(x,u) = 0 \quad \textit{if and only if} \quad x = l(u). \tag{2.33}$$

**Assumption 2.2.** *For each constant* $u$*, the corresponding equilibrium* $x = l(u)$ *of the system (2.32) is globally asymptotically stable, uniformly in* $u$*.*

With Assumption 2.1, well-defined steady state characteristic and the differentiable function

$$y_p = g(u) = h\left(l(u)\right) \tag{2.34}$$

are stated. With Assumption 2.2, stable and unique steady state characteristic are ensured. If any attempts to achieve global analysis are abandoned, local results (in therms of $x$) can be simply obtained by requiring a local uniqueness and a local stability property for the equilibria $x = l(u)$.

**Assumption 2.3.** *Consider the differentiable function* $l$ *defined in Assumption 2.2. There exists a unique* $u^*$ *maximizing* $g$ *such that*

$$\begin{aligned} &Dg(u^*) = 0 \qquad D^2 g(u^*) < 0, \\ &Dg(u^* + \varrho)\varrho < 0 \qquad \forall \varrho \neq 0, \end{aligned} \tag{2.35}$$

*where* $D$ *denotes the derivative and* $D^2$ *denotes the Hessian.*

Assumption 2.3 ensures that steady state characteristic has a unique maximum. If local results are sufficient, there is no need to insist on a global maximum. Local extrema can be analysed instead. Moreover, differentiability conditions are stronger than being necessary by Assumption 2.3.

Since we have a plant (2.32) which has an extremum, the classical ES scheme can be explained. Block diagram of basic ES can be found in Fig. 2.3 [6, 70]. Design parameters in 2.3 are explained as follows: $\omega_{lp}, \omega_{hp}$ determine the cut of frequencies of low pass and high pass filters, respectively, $k$ is the gain of the integrator that determines the signal $\hat{u}$, $\omega$ is the excitation signal, and $a$ is the gain that gives the size of the dither or excitation signal. In order to have a meaningful algorithm, the dither signal $asinwt$ should belong to the pass band of both low and high pass filters, i.e., $\omega_{lp} < \frac{2\pi}{\omega} < \omega_{hp}$. The amplitude $a$ is small enough since the dither is noise signal. Furthermore, the correlation with a narrowband

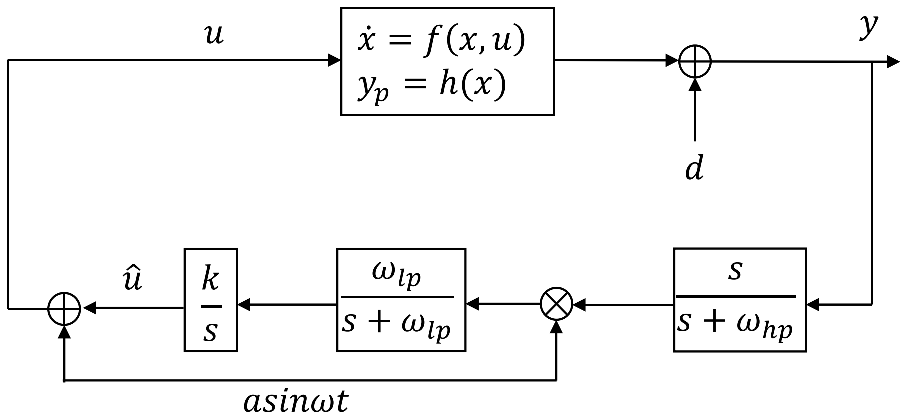


Figure 2.3: Basic Extremum Seeking Scheme.

dither signal as implemented by the multiplication operator in Fig. 2.3 followed by the integration, shows that the high and low pass filters are not main components of the ES scheme. They can be removed. However, they have the ability to reduce the oscillations in the system.

After giving necessary information about the components, we can summarize the ES scheme given in Fig. 2.3 as follows:

$$\begin{aligned} \dot{x} &= f(x, \hat{u} + a \sin \omega t), \\ \dot{\hat{u}} &= k\,(y + d)\, a \sin \omega t, \end{aligned} \tag{2.36}$$

where the filters are indeed removed. The main points of ES can be expressed as follows: the dither signal $a \sin \omega t$ explores a neighbourhood of the equilibrium manifold around the present estimate $\hat{u}, \hat{u}$ slowly develops in the direction of the gradient $Dg(\hat{u})$ to seek the maximum $u^*$. In Fig. 2.3, ES is presented as a gradient based optimization method. The following studies are given to understand the cornerstone studies in ES.

In 1922, [79] proposed a mechanism that transfers power from an electrical transmission line to a tram car using a noncontact solution. In order to have an efficient transfer [79] identified the need to adjust an inductance so as to maintain maximum power. In this study, there was an explanation on ES solution rather than an analysis. Then, the first detailed literature paper on ES analysis was given by [37]. [37] explored how to optimize an internal combustion engine to reach the maximum power output. Internal combustion engines have been very popular application area of ES since this study.

During 1950s and 1960s, ES was named differently including extremum seeking regulator, hill climbing systems, optimalizing systems [37, 91, 99]. After 1970s, [83] studied the first Lyapunov based stability analysis and [103] introduced a survey study on extremum seeking. Because of the increase in practice and applications, [8] was published and ES was titled as one of the most promising adaptive control methods.

Perturbation based ES has become the most popular class of ES approaches in recent years. Much of this success can be attributed to the work of [73]. They proved that the performance of the plant can be successfully optimized with a perturbation based ES approach if the plant satisfies certain properties. [73] also filled a gap proving the stability of ES feedback for general nonlinear dynamic systems. They used the methods of averaging developed by [65] and singular perturbation. They showed that the closed loop system converges to a small neighborhood of the extremum of the equilibrium map. The following studies are considered as cornerstones of ES and given to be insight into the thesis work.

### 2.5.2 Gradient Based SISO Extremum Seeking

[73] considered a general SISO nonlinear model as follows:

$$\begin{aligned} \dot{x} &= f(x, u), \\ y &= h(x), \end{aligned} \tag{2.37}$$

where $x \in \mathbb{R}^n$ is the state, $u \in \mathbb{R}$ is the input, $y \in \mathbb{R}$ is the output, and $f : \mathbb{R}^n \times \mathbb{R} \to \mathbb{R}^n$, $h : \mathbb{R}^n \to \mathbb{R}$ are smooth. A known smooth control law is supposed to be

$$u = \alpha(x, \theta) \tag{2.38}$$

parametrized by a scalar parameter $\theta$. $\theta$ and $y$ are taken as scalars and static state feedback control law is known, for simplicity. The closed loop system can be written as follows:

$$\dot{x} = f(x, \alpha(x, \theta)) \tag{2.39}$$

and has equilibria parametrized by $\theta$. For the closed loop system, following assumptions are made by [73]:

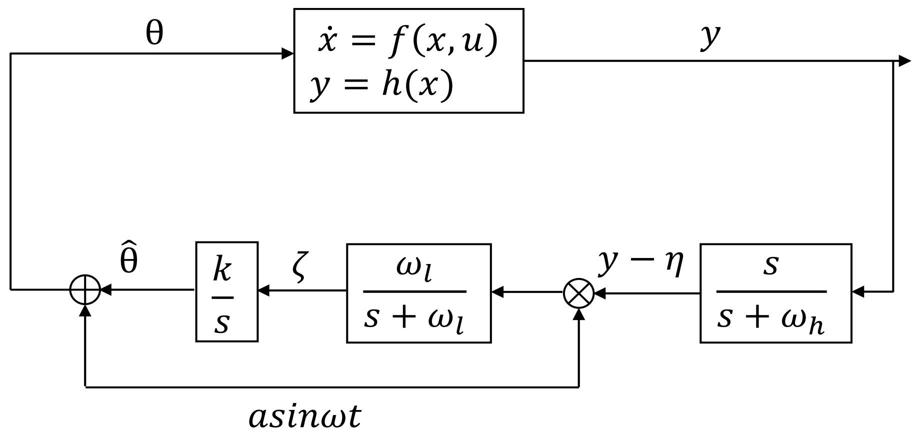


Figure 2.4: Gradient based extremum seeking for SISO dynamic systems [73].

**Assumption 2.4.** *There exists a smooth function $l : \mathbb{R} \to \mathbb{R}^n$ such that*

$$f(x, \alpha(x, \theta)) = 0 \quad \textit{if and only if} \quad x = l(\theta). \tag{2.40}$$

**Assumption 2.5.** *For each $\theta$, the equilibrium $x = l(\theta)$ of the system (2.39) is locally exponentially stable with decay and overshoot constants uniform in $\theta$.*

In the light of Assumptions 2.4 and 2.5, they assume that they have a robust control law in the sense that it exponentially stabilizes any of the equilibria that $\theta$ may produce. Assumption 2.5 is not restrictive, it means that control law is designed for local stabilization and this control law does not require the knowledge of either $f(x, u)$ or $l(\theta)$.

**Assumption 2.6.** *There exists $\theta^* \in \mathbb{R}$ such that*

$$y^{'} = 0, \quad y^{''} < 0. \tag{2.41}$$

Hence, it is assumed that $y = h(l(\theta))$ has an extremum (maximum in their case) at $\theta = \theta^*$. Therefore, main objective in [73] is to develop a feedback algorithm that maximizes the steady-state value of $y$ without the knowledge of $\theta^*, h$, or $l$.

A periodic perturbation term shown in Fig. 2.4, $asin\omega t$ is added to the signal $\hat{\theta}$ which is the best estimate of $\theta$. If the perturbation is slow, then the plant has the characteristics of a static map $y = h(l(\theta))$. Given system in Fig. 2.4 can be summarized as follows:

$$
\begin{aligned}
\dot{x} &= f(x,u), \\
u &= \alpha(x,\theta), \\
\theta &= \hat{\theta} + asin\omega t.
\end{aligned} \tag{2.42}
$$

Substituting $\theta$ into (2.39), the closed loop system equation is written as

$$
\dot{x} = f(x, \alpha(x, \hat{\theta} + asin\omega t)). \tag{2.43}
$$

The remaining part can be summarized in the following way:

$$
\begin{aligned}
\dot{\hat{\theta}} &= k\zeta, \\
\dot{\zeta} &= -\omega_l \zeta + \omega_l (y - \eta) asin\omega t, \\
\dot{\eta} &= -\omega_h \eta + \omega_h y.
\end{aligned} \tag{2.44}
$$

For further stability analysis, [73] uses the averaging and singular perturbation analysis developed by [65]. They covered the implementation of ES in singular perturbation. Conditions were very restrictive which meant that the plant had to be very fast and adaptation gain needed to be very small. Consequently, $y = h(x)$ converges exponentially to an $\mathcal{O}(\omega + a)$-neighbourhood of its maximum equilibrium value $h(l(\theta^*))$.

### 2.5.3 Gradient Based MISO Extremum Seeking

A special case of ES for MISO systems is examined in [41]. Gradient based ES is considered and the results for MISO systems are given.

Fig. 2.5 shows the block diagram of proposed algorithm in [41]. Given system can be summarized in the following way:

$$
\begin{aligned}
\dot{x} &= f(x,u), \\
u &= \alpha(x,\theta), \\
\theta &= \hat{\theta} + S(t),
\end{aligned} \tag{2.45}
$$

where $\theta = \begin{bmatrix} \theta_1 & \theta_2 & \cdots & \theta_n \end{bmatrix}^T$, and $S(t) = \begin{bmatrix} a_1 sin(\omega_1 t) & a_2 sin(\omega_2 t) & \cdots & a_n sin(\omega_n t) \end{bmatrix}^T$. It can also be written

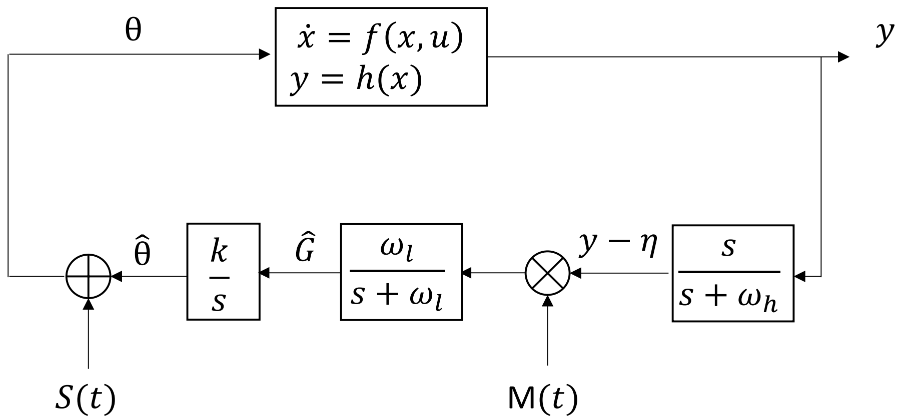


Figure 2.5: Gradient based extremum seeking for MISO dynamic systems [41].

$$
\begin{aligned}
\dot{\hat{\theta}} &= k\hat{G}, \\
\dot{\eta} &= y\omega_h - \eta\omega_h, \qquad (2.46)\\
\dot{\hat{G}} &= \omega_l M(t)(y-\eta) - G\omega_l,
\end{aligned}
$$

where $M(t) = \begin{bmatrix}\frac{2}{a_1}sin(\omega_1 t) & \frac{2}{a_2}sin(\omega_2 t) & \cdots & \frac{2}{a_n}sin(\omega_n t)\end{bmatrix}^T$. In (2.45), $x \in \mathbb{R}^m$ is the state, $u \in \mathbb{R}^n$ is the input, $y \in \mathbb{R}$ is the output, and $f : \mathbb{R}^m x \mathbb{R}^n \rightarrow \mathbb{R}^m$, $h : \mathbb{R}^m \rightarrow \mathbb{R}$ are smooth. Assumptions 2.4,2.5,4.3 in [73] are still valid.

### 2.5.4 Gradient Based Extremum Seeking for MISO Static Map

Regarding MISO gradient based ES, it is also a case to obtain gradient based ES for static maps. In [41], ES based on gradient algorithm is considered for a static map. Consider a convex static map as

$$
y = Q(\theta), \quad \theta = \begin{bmatrix}\theta_1 & \theta_1 & \ldots & \theta_n\end{bmatrix}^T \qquad (2.47)
$$

with a local maximum at $\theta^*$. The gradient based ES scheme for this multivariable static map is given in Fig. 2.6. Gradient based ES for a static map given in (2.6) is defined by

$$
\begin{aligned}
\dot{\hat{\theta}} &= kN(t)y, \\
\theta &= \hat{\theta} + M(t).
\end{aligned} \qquad (2.48)
$$

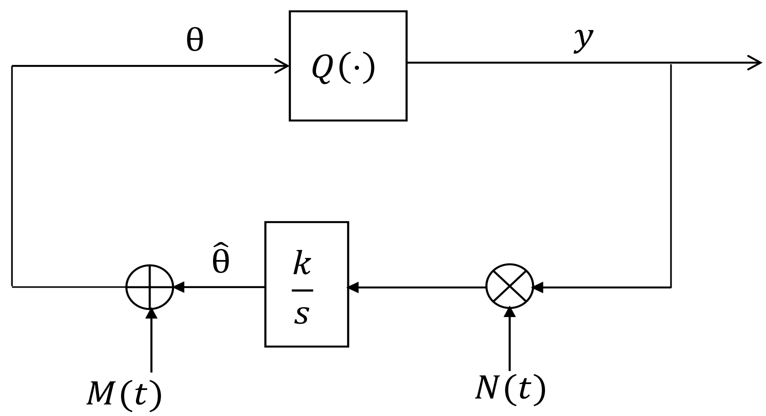

Figure 2.6: Gradient Based Extremum Seeking for a Static Map [41].

where the parameter error is $\tilde{\theta} = \hat{\theta} - \theta^*$. Together with (2.47) and (2.48), the closed loop system is given by

$$\dot{\tilde{\theta}} = kN(t)Q(\theta^* + M(t) + \tilde{\theta}), \tag{2.49}$$

where$M(t) = \begin{bmatrix} a_1 sin\omega_1 t & ... & a_n sin\omega_n t \end{bmatrix}^T$ and $N(t) = \begin{bmatrix} \frac{2}{a_1} sin\omega_1 t & ... & \frac{2}{a_n} sin\omega_n t \end{bmatrix}^T$.

Obtained averaged system based on gradient estimation algorithm needs the information of Hessian matrix which is the second derivative of the output. The convergence rate depends on that unknown Hessian matrix. Generating the estimate of Hessian matrix is very challenging in non-model based optimization algorithms. Therefore, the following study has been done to deal with unknown Hessian matrix.

### 2.5.5 Newton Based Extremum Seeking

Gradient estimation algorithm is not the only optimization algorithm used in ES. In the literature, Newton based algorithm is also examined with ES. Newton-based method has the advantage over gradient based method since Newton's method uses curvature information to take a more direct route. In addition, convergence of Newton algorithm is independent of the Hessian and can be arbitrarily assigned, while convergence rate of the gradient algorithm was governed by the unknown Hessian matrix. In this regard, it is also challenging that the estimate of the inverse of Hessian matrix which is used in Newton based ES algorithms.

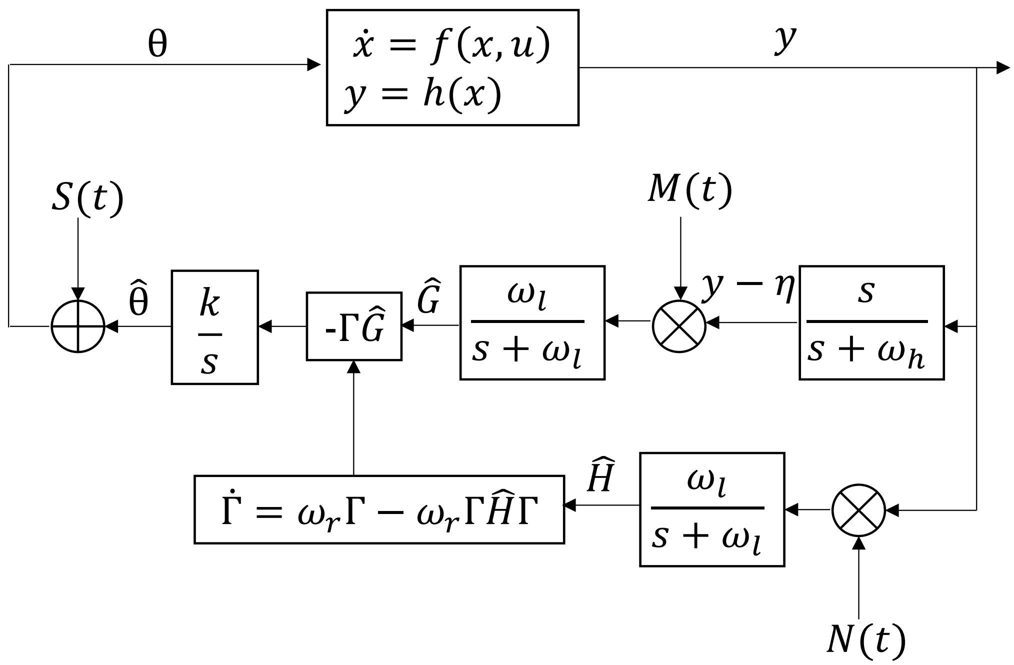


Figure 2.7: Newton based extremum seeking for MISO dynamic systems [41].

In order to deal with such problems, [41] employed a dynamic system which generates the inverse asymptotically. Added dynamic system has the form of differential Riccati equation which gives the estimate of inverse of Hessian matrix. Fig. 2.7 shows the block diagram of proposed Newton based extremum seeking algorithm. Parallel to the gradient based ES algorithm for multivariable case, [41] proposed Newton based ES algorithm in the following way :

$$\begin{aligned}\dot{\hat{\theta}} &= -k\Gamma\hat{G},\\ \dot{\hat{G}} &= \omega_l M(t)(y-\eta) - \hat{G}\omega_l,\\ \dot{\Gamma} &= \omega_r\Gamma - \omega_r\Gamma\hat{H}\Gamma.\end{aligned} \tag{2.50}$$

With Newton based algorithm, the convergence rates of both parameter and of the estimator of the Hessian inverse are independent of the unknown Hessian. It is also assigned by the user arbitrarily.

Moreover, [70] provided an analysis that they added a dynamic compensator to the integrator. They developed an algorithm and showed by an example that benefits of increasing the adaptation gain brings along the increase in sensitivity of noise. Another study regarding the ES was proposed by [22] for discrete time systems. They used the same plant model and control algorithm as in [70]. They studied the stability analysis which is rather different than that of continuous time. It was established in two steps: without perturbation and with perturbation. A mild sufficient condition which the system output exponentially converges to the neighbourhood of the extremum value was derived. They validated their algorithm by simulations. [48] and [46] considered ES approach as an estimation problem. They used a discrete time ES scheme to estimate the gradient as a time-varying parameter using least-squares like update laws.

It is clear that most of the studies on the topic of ES have been established mostly by gradient and recently by Newton based algorithms. Since we know that RLS estimation algorithm brings faster convergence rate to forefront, we focus on RLS parameter estimation based ES design in Chapter 4.

### 2.5.6 Extremum Seeking Applications

ES has been applied to many engineering domains. Application areas in the automotive industry include internal combustion engines [53, 67, 78] to minimize the fuel consumption; anti-lock braking systems [34, 36, 116] to seek the peak point of the tire force–slip curve; and transmission systems [107, 108] to maximize the efficiency.

ES has been also used to maximize the generated power of wind turbines in [26, 42] and solar arrays [43, 81]. In addition, navigation and source-seeking applications of mobile robots using ES have been investigated in [25, 35, 82, 84]. Other application areas of ES include fuel-cell power plants [27, 118], nuclear-fusion reactors [18, 19].

Applicability of the proposed ES methods are often given by simulation examples. Moreover, there are a number of applications which is given as a proof of concept by practical experiments [42, 67].

# Chapter 3

# Recursive Least Squares Based Adaptive Control

In Chapter 2, the existing studies on LS based adaptive control have been presented. Most of these existing LS based designs follow the indirect adaptive control approach as opposed to direct adaptive control. One reason for this is that the analysis of direct adaptive control, which typically starts with proposing a Lyapunov-like function that penalizes the magnitude of the tracking or regulation error but at the same time useful in designing an adaptive law to generate the parameter estimates to feed the control law, is complicated for producing an LS based adaptive control scheme in the end. On the other hand, it is well observed that LS algorithms have the advantage of faster convergence; hence, LS based adaptive control has potential to enhance convergence performance in direct adaptive control approaches as well.

This chapter builds a framework for analysis of RLS parameter estimation based adaptive control and a set of general analysis results on stability and convergence. In order to achieve this aim, RLS parameter estimation based direct adaptive control is first analysed by replacing the constant adaptation gain that is used in gradient based direct adaptive control, with a time varying covariance matrix. RLS parameter estimation based direct adaptive control is later discussed by defining a new Lyapunov function based on integral cost function instead of standard quadratic instantaneous cost function.

This chapter starts with the designs of indirect APPC and indirect MRAC as a base to test and analyse the performance of time-varying RLS parameter estimation based algorithms in indirect adaptive control, compared to the fixed gain gradient based algorithms. Later, direct MRAC with RLS parameter estimation is studied, providing details of constructive analysis, and simulation tests. Applications to active vehicle safety systems, ACC and ABS are provided to demonstrate the applicability of the proposed RLS parameter estimation based direct adaptive control.

## 3.1 Indirect Adaptive Control

In this section, the analysis of the performance of RLS based on-line parameter estimation in indirect APPC and MRAC are given based on simulation comparisons with gradient based algorithms. Firstly, a brief description is given in each section and then a simulation study including the comparison of RLS and gradient based algorithms is provided.

### 3.1.1 Indirect Adaptive Pole Placement Control

APPC schemes are applicable to both minimum phase and non-minimum phase plants. In an indirect APPC, which is composed of a PPC law and an on-line parameter identifier (PI), the on-line PI generates on-line estimates of the plant system parameters, e.g., the coefficients of the plant transfer function, which are later used to calculate the control coefficients of the PPC law by solving a certain algebraic equation that relates the plant system parameters and the ideal control coefficients.

Consider the SISO LTI plant as

$$\begin{aligned} \dot{x}_p &= A_p x_p + B_p u_p, \quad x(0) = x_0, \\ y_p &= C_p^T x_p \end{aligned} \tag{3.1}$$

where $x_p \in \mathcal{R}^n, y_p, u_p \in \mathcal{R}$ and $A_p, B_p, C_p$ have the appropriate dimensions. The transfer function of the plant is given by

$$y_p = G_p(s) u_p, \quad G_p(s) = k_p \frac{Z_p(s)}{R_p(s)}, \tag{3.2}$$

where $G_p(s)$ is proper, $Z_p(s)$ and $R_p(s)$ are monic polynomials, and $k_p$ is the high frequency gain. The PPC goal is to choose the plant input $u_p$ so that the closed loop poles are assigned to those of a given monic Hurwitz polynomial $A^*(s)$ which is referred to as the desired closed loop characteristic polynomial. Following assumptions are made to facilitate achieving the PPC goal.

**Assumption 3.1.**

*i* $R_p(s)$ *is a monic polynomial whose degree* $n$ *is known.*

*ii* $Z_p(s), R_p(s)$ *are coprime and degree of* $Z_p(s)$ *is less than* $n$.

A typical APPC task, in addition to assigning the desired closed-loop poles, also requires the output $y_p$ of the plant to track a certain reference signal $y_m$, which can be addressed following an internal model principle approach. In this approach, the reference signal $y_m \in \mathcal{L}_\infty$ is assumed to satisfy the internal model $Q_m(s)y_m = 0$ where $Q_m(s)$ is a known monic polynomial of degree $q$ and, having its roots in $\mathcal{R}[s] \leq 0$ no repeated roots on imaginary axis. Furthermore, $Q_m(s)$ is assumed to satisfy following assumption:

**Assumption 3.2.**

*iii* $Q_m(s), Z_p(s)$ *are coprime.*

For the tracking objective, the control law is considered as

$$Q_m(s)L(s)u_p = -\bar{P}(s)(y_p - y_m), \tag{3.3}$$

where $\bar{P}(s), L(s)$ are polynomials of degree $q+n-1, n-1$, respectively and chosen to satisfy following polynomial equation

$$L(s)Q_m(s)R_p(s) + \bar{P}(s)k_pZ_p(s) = A^*(s), \tag{3.4}$$

where $L(s) = s^{n-1} + l_{n-2}s^{n-2} + \cdots + l_1 s + l_0$, $\bar{P}(s) = p_{n+q-1}s^{n+q-1} + p_{n+q-2}s^{n+q-2} + \cdots + p_1 s + p_0$ and $A^*(s) = s^{2n+q-1} + a^*_{2n+q-2}s^{2n+q-2} + \cdots + a^*_1 s + a^*_0 = s^{2n+q-1} + \alpha^{*T}\alpha_{2n+q-2}(s)$. The solutions of $L(s)$ and $\bar{P}(s)$ coefficients are selected by solving an algebraic equation given in [60]. The control law in (3.3) is realized as

$$u_p = -\frac{\bar{P}(s)}{Q_m(s)L(s)}(y_p - y_m). \tag{3.5}$$

Since we have $L(s)$ in the denominator that is not necessarily Hurwitz, we may have poles in the right half complex plane, which is not desirable. (3.5) can be rewritten as

$$u_p = \frac{\Lambda(s) - Q_m(s)L(s)}{\Lambda(s)}u_p - \frac{\bar{P}(s)}{\Lambda(s)}(y_p - y_m) \tag{3.6}$$

with any monic Hurwitz polynomial $\Lambda(s)$ of degree $n+q-1$. Since the coefficients of $G_p(s)$ are unknown, adaptive control is used to estimate the plant polynomials.

Using (3.2), the following parametric model can be derived:

$$z = \theta_p^{*T}\phi, \tag{3.7}$$

where

$$\begin{aligned} &z = \frac{s^n}{\Lambda_p(s)}y_p, \quad \theta_p^* = \begin{bmatrix}\theta_b^{*T} & \theta_a^{*T}\end{bmatrix}^T, \quad \phi = \begin{bmatrix}\frac{\alpha_{n-1}^T(s)}{\Lambda_p(s)}u_p & -\frac{\alpha_{n-1}^T(s)}{\Lambda_p(s)}y_p\end{bmatrix}^T, \\ &\alpha_{n-1}(s) = [s^{n-1}, \cdots, s, 1]^T, \quad \theta_b^{*T} = [b_{n-1}, \cdots, b_0]^T, \quad \theta_a^{*T} = [a_{n-1}, \cdots, a_0]^T. \end{aligned} \tag{3.8}$$

In order to estimate $\theta_p^*$, unknown plant parameters, gradient (2.14) and RLS (2.22) estimation algorithms can be used. Thus, the estimated plant parameters are given as

$$\theta_p = \begin{bmatrix}\theta_b^T & \theta_a^T\end{bmatrix}^T, \quad \theta_b^T = \begin{bmatrix}\hat{b}_{n-1}, \cdots, \hat{b}_0\end{bmatrix}^T, \theta_a^T = \begin{bmatrix}\hat{a}_{n-1}, \cdots, \hat{a}_0\end{bmatrix}^T. \tag{3.9}$$

Using the estimated plant parameters, the adaptive control law is obtained by replacing the unknown polynomials $L(s), P(s)$ in (3.6) with their on-line estimates $\hat{L}(s,t), \hat{P}(s,t)$ as

$$u_p = \frac{\Lambda(s) - Q_m(s)\hat{L}(s,t)}{\Lambda(s)}u_p - \frac{\hat{\hat{P}}((s,t)}{\Lambda(s)}(y_p - y_m). \tag{3.10}$$

The existence and uniqueness of $\hat{L}(s,t), \hat{\hat{P}}(s,t)$ are guaranteed, provided that $\hat{R}_p(s,t)Q_m(s)$, $\hat{Z}_p(s)$ are coprime at each time $t$. In order to compare the gradient and RLS on-line estimation algorithms in indirect adaptive control, the following plant model is examined.

**Example 3.1.** *In order to demonstrate the performance of LS based parameter estimation algorithm in indirect adaptive control, a simulation application is provided. Consider the plant given by*

$$y = \frac{1}{s(s-p_1)(s-p_2)}u, \tag{3.11}$$

*with unknown parameters $p_1, p_2$. (3.11) can be rewritten as follows:*

$$y = \frac{1}{s^3 + a_2 s^2 + a_1 s} u, \tag{3.12}$$

*with* $a_1 = p_1 p_2$ *and* $a_2 = -(p_1 + p_2)$*. In order to design an APPC, the closed loop system is assumed to be stable with a pole at* $-1$*.*

*By following the PPC algorithm, we have APPC law as follows:*

$$u = \frac{\Lambda - sL}{\Lambda} u - \frac{\bar{P}}{\Lambda}(y - y_m), \tag{3.13}$$

*where* $L = s^2 + l_1 s + l_0,\ \bar{P} = p_3 s^3 + p_2 s^2 + p_1 s + p_0,\ \Lambda = (s+2)^3,\ l_1 = 6 - a_2, l_0 = 15 - l_1 a_2 - a_1, p_3 = 20 - l_0 a_2 - l_1 a_1, p_2 = 15 - l_0 a_1, p_1 = 6, p_0 = 1.$

*In order to compare the transient performance, RLS and gradient parameter estimation based adaptive control laws are implemented. Parameter model is written as*

$$z = \theta_p^{*T} \phi \tag{3.14}$$

*where*

$$\phi = \begin{bmatrix} -\frac{s^2}{\Lambda} y, & -\frac{s}{\Lambda} y \end{bmatrix}^T, \quad \theta_p^* = \begin{bmatrix} a_2, & a_1 \end{bmatrix}^T. \tag{3.15}$$

*Next the estimation model and estimation error are written as follows:*

$$\begin{aligned} \hat{z} &= {\theta_p}^T \phi, \quad \theta_p = \begin{bmatrix} \hat{a}_2 & \hat{a}_1 \end{bmatrix}^T, \\ \varepsilon &= \frac{z - \hat{z}}{m_s^2}. \end{aligned} \tag{3.16}$$

*And lastly, adaptive law with RLS estimation is given by*

$$\dot{\theta}_p = P \varepsilon \phi, \qquad \dot{P} = \beta P - P \frac{\phi \phi^T}{m_s^2} P, \tag{3.17}$$

*with* $\beta$ *forgetting factor and* $P$ *covariance matrix. Adaptive law with gradient estimation to compare the performance is given by*

$$\dot{\theta}_p = \gamma \varepsilon \phi, \tag{3.18}$$

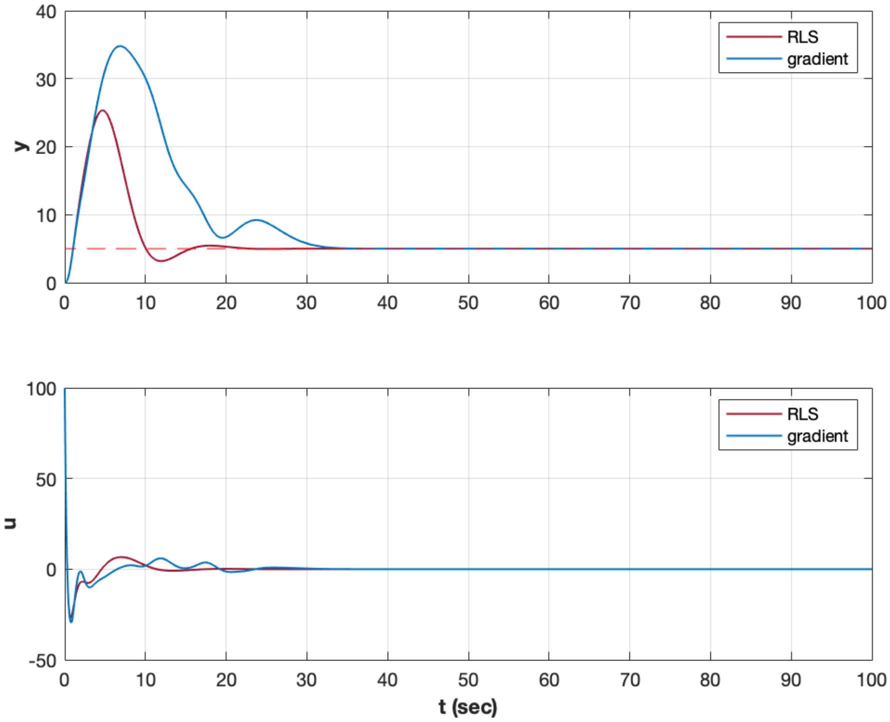


Figure 3.1: Plant results with respect to gradient and RLS for indirect APPC.

*where $\gamma$ is constant adaptive gain.*

*Simulation results for indirect APPC are given in Figs. 3.1 and 3.2. Fig.3.1 shows applied inputs and plant results, and Fig.3.2 demonstrates the parameter estimates for both gradient and RLS based indirect APPC. $\beta = 0.9$ for RLS algorithm and $\gamma = 100$ for gradient algorithm are used in the simulation. Estimation results verifies that RLS based indirect APPC has better convergence performance than gradient one.*

### 3.1.2 Indirect Model Reference Adaptive Control

APPC is considered as the most general class of adaptive control schemes due to its flexibility in choosing the controller design methodology and adaptive law. Indirect MRAC is a special case where some of the poles of the controller are assigned to be equal to the zeros of the plant to facilitate the required zero-pole cancellation for transfer function matching.

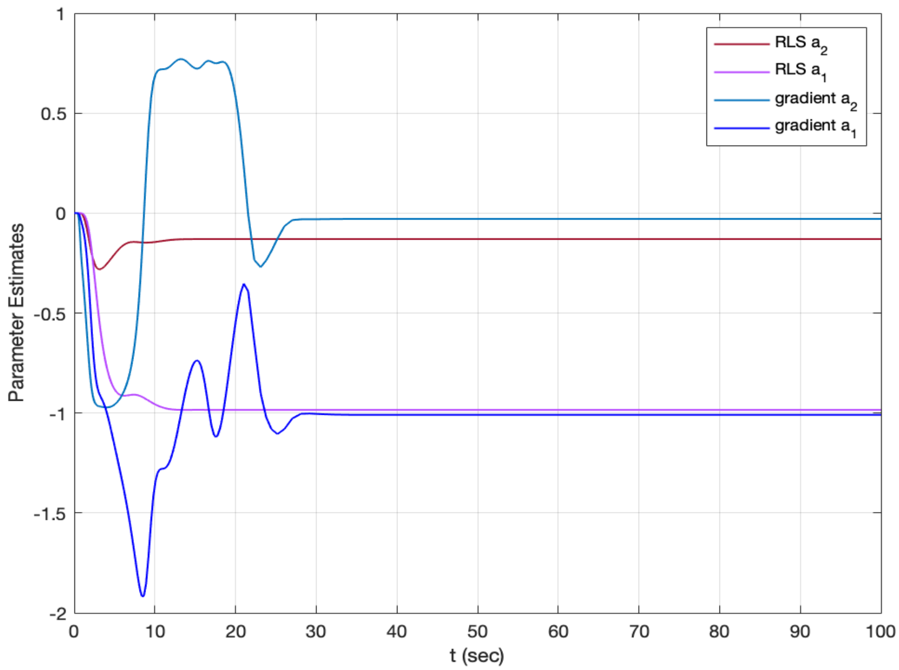


Figure 3.2: Parameter estimates with respect to gradient and RLS for indirect APPC.

The details of MRAC scheme will be given broadly in the next section, the idea of MRAC in indirect adaptive control will be explained with a scalar example from [61].

Consider the plant

$$\dot{x} = ax + bu, \tag{3.19}$$

where $a, b$ are unknown constants and $sgn(b)$ is known.It is desired to choose $u$ such that all signals in the closed loop plant are bounded and the plant state $x$ follows the reference model state $x_m$

$$\dot{x}_m = -a_m x_m + b_m r, \tag{3.20}$$

where $a_m > 0$, $b_m$ and the reference input signal $r$ are chosen so that $x_m(t)$ shows the desired state response of the plant. If the plant parameters $a, b$ are known, then the control law

$$u = -k^* x + l^* r, \tag{3.21}$$

with

$$k^* = \frac{a_m + a}{b}, \quad l^* = \frac{b_m}{b} \tag{3.22}$$

are one way to meet the control objective. For unknown plant parameters, the control law becomes

$$u = -k(t)x + l(t)r, \tag{3.23}$$

where $k(t), l(t)$ are the online estimates of $k^*, l^*$ at time $t$, respectively. In indirect adaptive control, $k$ and $l$ are evaluated by the relationship of (3.24) and the estimates $\hat{a}, \hat{b}$ of the unknown parameters $a, b$ as follows:

$$k = \frac{a_m + \hat{a}(t)}{\hat{b}(t)}, \quad l = \frac{b_m}{\hat{b}(t)}. \tag{3.24}$$

Rewriting the (3.19) as

$$x = \frac{1}{s + a_m} \left[ (a + a_m)x + bu \right], \tag{3.25}$$

and the estimate of $x$ becomes

$$\hat{x} = \frac{1}{s + a_m} \left[ (\hat{a} + a_m)\hat{x} + \hat{b}u \right] = x_m. \tag{3.26}$$

The tracking error is written as

$$e_1 = x - x_m, \tag{3.27}$$

that satisfies the following differential equation

$$\begin{aligned} \dot{e}_1 &= -a_m e_1 - \tilde{a}x - \tilde{b}u \\ \tilde{a} &= \hat{a} - a, \quad \tilde{b} = \hat{b} - b. \end{aligned} \tag{3.28}$$

A Lyapunov function is chosen as

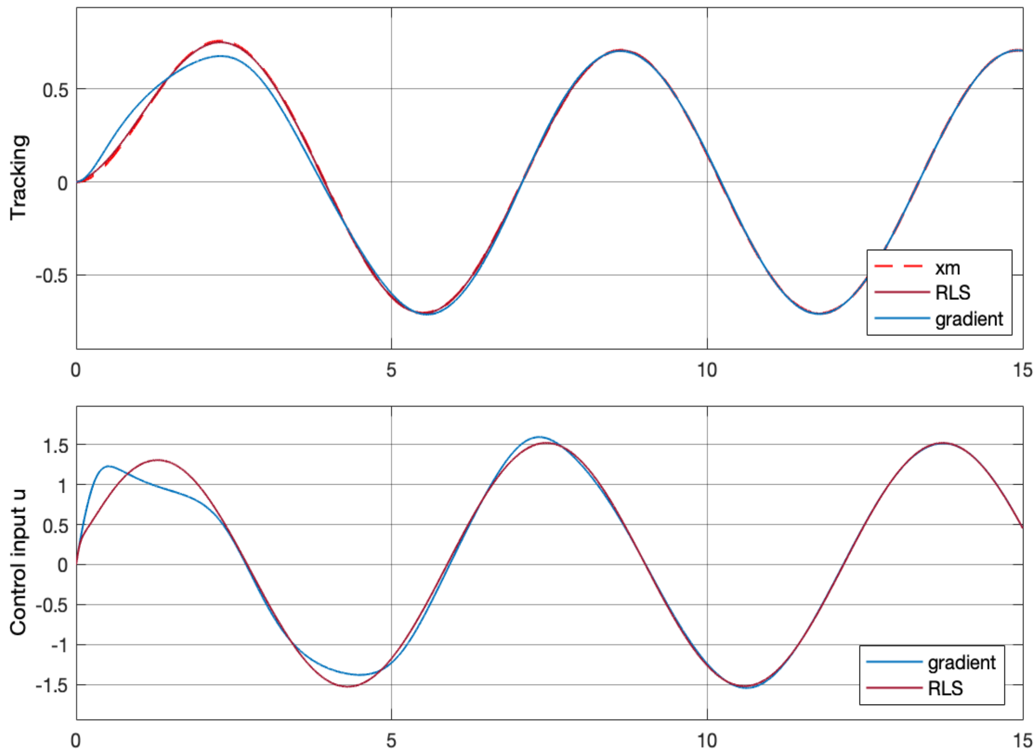


Figure 3.3: Tracking results and applied control inputs with respect to gradient and RLS for indirect MRAC.

$$V = \frac{1}{2}\left(e_1^2 + \frac{\tilde{a}^2}{\gamma_1} + \frac{\tilde{b}^2}{\gamma_2}\right), \tag{3.29}$$

where $\gamma_1, \gamma_2 > 0$. The time derivative of $V$ is given by

$$\dot{V} = -a_m e_1^2 - \tilde{a} x e_1 - \tilde{b} u e_1 + \frac{\tilde{a}\dot{\tilde{a}}}{\gamma_1} + \frac{\tilde{b}\dot{\tilde{b}}}{\gamma_2}. \tag{3.30}$$

For the selections of

$$\dot{\tilde{a}} = \dot{\hat{a}} = \gamma_1 e_1 x, \quad \dot{\tilde{b}} = \dot{\hat{b}} = \gamma_2 e_1 u, \tag{3.31}$$

(3.30) becomes

$$\dot{V} = -a_m e_1^2 \leq 0, \tag{3.32}$$

which implies that $e_1, \hat{a}, \hat{b}, x_m, x \in \mathcal{L}_\infty$, and $e_1 \in \mathcal{L}_2$. The boundedness proof of $u$ can be found by showing the boundedness of $k(t)$ and $l(t)$ as in [61]. Replacing the constant adaptive gains $\gamma_1, \gamma_2$ with time varying covariance matrix $P$, the adaptive law is written based on LS parameter estimation as follows:

$$\begin{aligned}
&\dot{\theta} = PE_1\phi \\
&\theta = [\hat{a}, \hat{b}]^T, \quad E_1 = e_1 I_2 \quad \phi = [x, u]^T, \\
&\dot{P} = \beta P - P\phi\phi^T P.
\end{aligned} \tag{3.33}$$

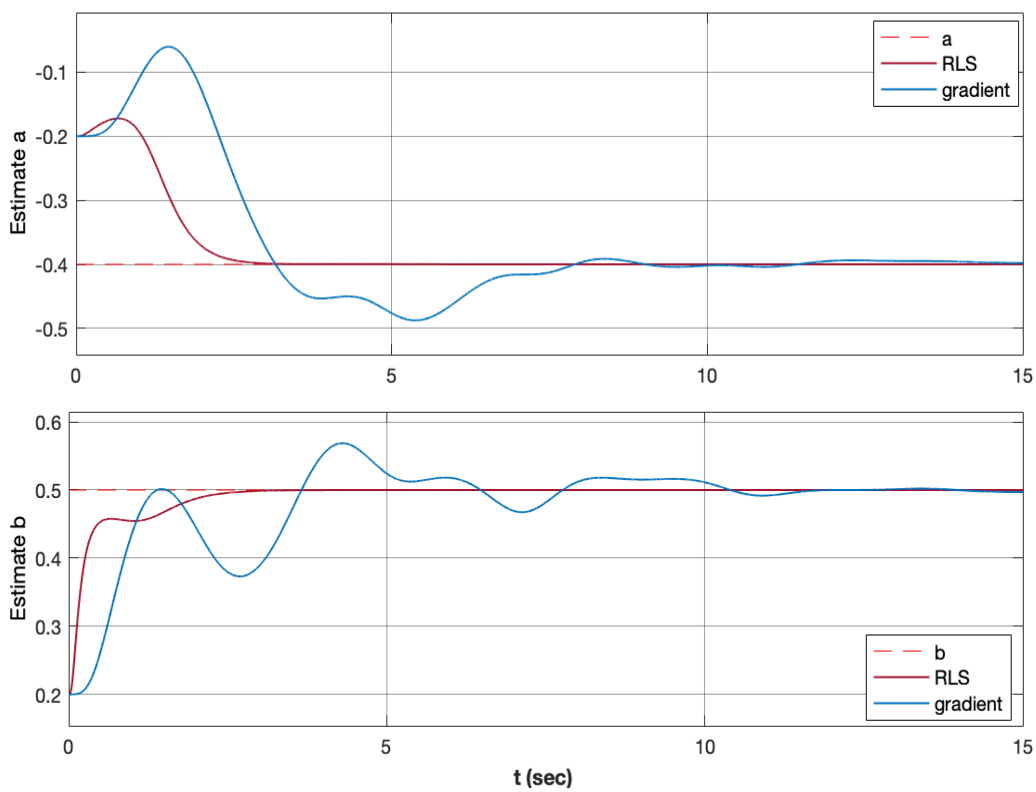


Figure 3.4: Estimation results with respect to gradient and RLS for indirect MRAC.

Simulation results for indirect MRAC are given in Figs. 3.3 and 3.4. Reference signal is given as $sint$. System and reference model parameters are given as $a = -0.4, b = 0.5, x_0 = 0, x_{m0} = 0, a_m = 1, b_m = 1$. Initial estimates are defined as $\hat{a}_0 = -0.2, \hat{b}_0 = 0.2$. Adaptive gains for gradient algorithm is given as $[\gamma_1, \gamma_2] = [5, 3]$. Covariance matrix for RLS algorithm is $P_0 = 50I_2$. Tracking results for applied inputs in Fig. 3.3 and estimation results of $\hat{a}, \hat{b}$ in Fig. 3.4 demonstrate that RLS parameter estimation based indirect MRAC is significantly better than gradient one in terms of convergence rate.

## 3.2 Direct Model Reference Adaptive Control

In this section, the direct adaptive control problem is revisited by selecting a suitable Lyapunov function to design the adaptive law. In the literature, the Lyapunov-like functions are typically selected to penalize the tracking error and parameter estimation error together, since the dynamics of these errors are coupled, and control designs targeting to drive this Lyapunov-like function to zero leads to gradient based adaptive laws using a constant adaptive gains.

In this section, the aim is to construct a similar Lyapunov analysis framework with an appropriate Lyapunov-like function resulting in an adaptive law with a time-varying gain matrix $P$, instead of a constant gain $\Gamma$, with time variations corresponding to RLS based parameter estimation. The key motivation is the aforementioned superior characteristics of RLS based online parameter estimation observed in comparative simulations and experimental tests, and to further investigate the reasons of the observed superiorities in Lyapunov function and see the effect of RLS in the analysis.

### 3.2.1 Adaptive Control Scheme

In MRAC, desired plant behaviour is described by a reference model which can be described by a transfer function and driven by a reference input. Then, a control law is developed so that the closed loop plant has a transfer function equal to the reference model. Unlike APPC, in MRAC, the plant has to be minimum phase, i.e, all zeros have to be stable.

Consider the plant given in (3.1) and the transfer function in (3.2). The reference model is described by

$$\begin{aligned} \dot{x}_m &= A_m x_m + B_m u_m, \quad x_m(0) = x_{m0}, \\ y_m &= C_m^T x_m \end{aligned} \tag{3.34}$$

The transfer function of the reference model (3.34) is given by

$$y_m = W_m(s)r, \quad W_m(s) = k_m \frac{Z_m(s)}{R_m(s)}, \tag{3.35}$$

with constant design parameter $k_m$. The control purpose is to find the plant input $u_p$ so that all signals are bounded and the plant output $y_p$ follows the reference model output $y_m$ with given reference input $r(t)$. The following assumptions are made for MRAC:

**Assumption 3.3.** ***Plant Assumptions***

*i* *$Z_p(s)$ is a monic Hurwitz polynomial.*

*ii* *Upper bound $n$ of the degree $n_p$ of $R_p(s)$ is known.*

*iii* *Relative degree $n^* = n_p - m_p$ of $G_p(s)$ is known and $m_p$ is the degree of $Z_p(s)$.*

*iv* *The sign of $k_p$ is known.*

**Assumption 3.4.** ***Reference Model Assumptions***

*i* *$Z_m(s), R_m(s)$ are monic Hurwitz polynomials of the degree of $q_m, p_m$, respectively.*

*ii* *Relative degree $n_m = p_m - q_m$ of $W_m(s)$ is the same as that of $G_p(s)$, i.e, $n^* = n_m^*$.*

Consider the following feedback control law

$$u_p = \theta_1^{*T} \frac{\alpha(s)}{\Lambda(s)} u_p + \theta_2^{*T} \frac{\alpha(s)}{\Lambda(s)} y_p + \theta_3^* y_p + c_0^* r, \tag{3.36}$$

where

$$\begin{aligned} & c_0^* = \frac{k_m}{k_p}, \\ & \alpha(s) \triangleq \alpha_{n-2}(s) = [s^{n-2}, s^{n-3}, \cdots, s, 1]^T \qquad \text{for} \quad n \geq 2, \\ & \alpha(s) \triangleq 0 \qquad \text{for} \quad n = 1. \end{aligned} \tag{3.37}$$

$\Lambda(s)$ is an arbitrary monic Hurwitz polynomial of degree $n-1$ containing $Z_m(s)$ as a factor, i.e.,

$$\Lambda(s) = \Lambda_0(s) Z_m(s)$$

implying that $\Lambda_0(s)$ is monic and Hurwitz. The controller parameter vector $\theta^* = \begin{bmatrix} \theta_1^{*T} & \theta_2^{*T} & \theta_3^* & c_0^* \end{bmatrix}^T$ is chosen so that the transfer function from $r$ to $y_p$ is equal to $W_m(s)$.

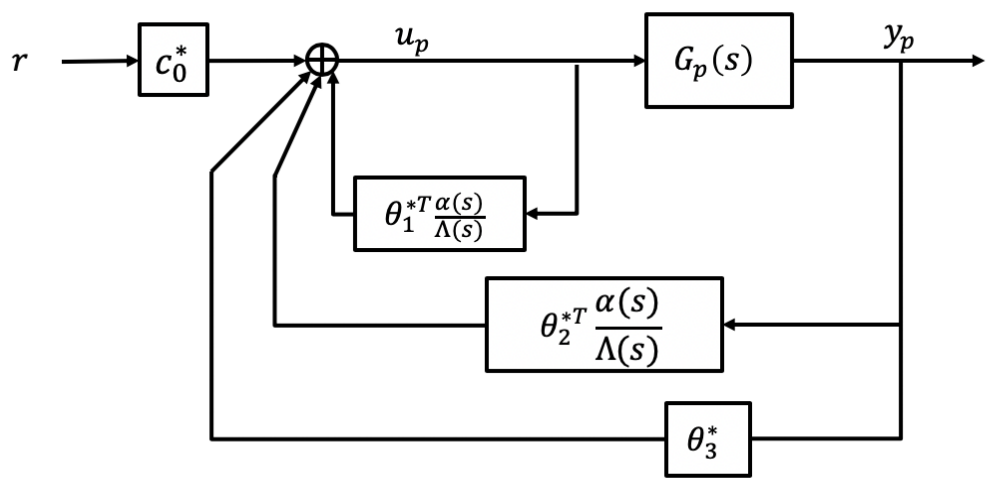


Figure 3.5: Structure of MRAC.

The structure of the closed-loop MRAC scheme is shown in Fig. 3.5 and has the reference to output relation

$$y_p = G_c(s) r \tag{3.38}$$

where

$$G_c(s) = \frac{c_0^* k_p Z_p(s) \Lambda^2(s)}{\Lambda(s)(\Lambda(s) - \theta_1^{*T}(\alpha(s)) R_p(s) - k_p Z_p(s)[\theta_2^{*T} \alpha(s) + \theta_3^* \Lambda(s)]}. \tag{3.39}$$

The control objective is to select the controller parameter $\theta^*$ so that the closed-loop poles are stable and the closed-loop transfer function satisfies $G_c(s) = W_m(s)$, i.e.,

$$\frac{c_0^* k_p Z_p(s) \Lambda^2(s)}{\Lambda(s)(\Lambda(s) - \theta_1^{*T}(\alpha(s)) R_p(s) - k_p Z_p(s)[\theta_2^{*T} \alpha(s) + \theta_3^* \Lambda(s)]} = k_m \frac{Z_m(s)}{R_m(s)} \qquad \forall s \in \mathcal{C}. \tag{3.40}$$

Since $Z_p(s)$ is Hurwitz by assumption and $\Lambda(s) = \Lambda_0(s)Z_m(s)$ is designed to be Hurwitz, all zeros of $G_c(s)$ are stable and hence any zero-pole cancellation can occur only in $\mathcal{C}^-$. Nonzero intial conditions will affect the transient response of $y_p(t)$.

A state-space realization of the control law (3.36) is given by

$$
\begin{aligned}
\dot{\omega}_1 &= F\omega_1 + gu_p, \quad \omega_1(0) = 0, \\
\dot{\omega}_2 &= F\omega_2 + gy_p, \quad \omega_2(0) = 0, \\
u_p &= \theta^{*T}\omega,
\end{aligned}
\tag{3.41}
$$

where $\omega_1, \omega_2 \in \mathcal{R}^{n-1}$,

$$
\begin{aligned}
&\theta^* = \begin{bmatrix}\theta_1^{*T} & \theta_2^{*T} & \theta_3^* & c_0^*\end{bmatrix}^T, \quad \omega = \begin{bmatrix}\omega_1 & \omega_2 & y_p & r\end{bmatrix}^T, \\
&F = \begin{bmatrix} -\lambda_{n-2} & -\lambda_{n-3} & -\lambda_{n-4} & \cdots & -\lambda_0 \\ 1 & 0 & 0 & \cdots & 0 \\ 0 & 1 & 0 & \cdot & 0 \\ \vdots & \vdots & \ddots & \ddots & \vdots \\ 0 & 0 & \cdots & 1 & 0 \end{bmatrix}, \\
&\Lambda(s) = s^{n-1} + \lambda_{n-2}s^{n-2} + \cdots + \lambda_1 s + \lambda_0 = det(sI - F), \\
&g = \begin{bmatrix}1 & 0 & \cdots & 0\end{bmatrix}^T.
\end{aligned}
\tag{3.42}
$$

Since the plant parameters are unknown, the desired controller parameter vector $\theta^*$ cannot be calculated from the matching equation. Following the certainty equivalence approach the following equation is used instead of (3.41):

$$
\begin{aligned}
\dot{\omega}_1 &= F\omega_1 + gu_p, \quad \omega_1(0) = 0, \\
\dot{\omega}_2 &= F\omega_2 + gy_p, \quad \omega_2(0) = 0, \\
u_p &= \theta^{T}\omega,
\end{aligned}
\tag{3.43}
$$

where $\theta(t)$ is the online estimate of the unknown control parameter vector $\theta^*$. In order to find the adaptive law generating $\theta(t)$, first a composite state space representation of the plant and controller is considered [60] as follows:

$$
\begin{aligned}
\dot{Y}_c &= A_0 Y_c + B_c u_p, \\
y_p &= C_c^T Y_c, \\
u_p &= \theta^T\omega,
\end{aligned}
\tag{3.44}
$$

where $Y_c = [x_P^T, \omega_1^T, \omega_2^T]^T$,

$$A_0 = \begin{bmatrix} A_p & 0 & 0 \\ 0 & F & 0 \\ gC_p^T & 0 & F \end{bmatrix}, \quad B_c = \begin{bmatrix} B_p \\ g \\ 0 \end{bmatrix}, \quad C_c^T = \begin{bmatrix} C_p^T, & 0, & 0 \end{bmatrix}. \tag{3.45}$$

When we add and subtract the desired input, we obtain

$$\dot{Y}_c = A_0 Y_c + B_c \theta^{*T}\omega + B_c(u_p - \theta^{*T}\omega) \tag{3.46}$$

and absorbing the desired input term into the homogeneous part of the above equation, we have

$$\begin{aligned} \dot{Y}_c &= A_c Y_c + B_c c_0^* r + B_c(u_p - \theta^{*T}\omega), \quad Y_c(0) = Y_0 \\ y_p &= C_c^T Y_c, \end{aligned} \tag{3.47}$$

where

$$A_c = \begin{bmatrix} A_p + B_p\theta^* C_p^T & B_p\theta_1^{*T} & B_p\theta_2^{*T} \\ g\theta_3^* C_p^T & F + g\theta_1^{*T} & g\theta_2^{*T} \\ gC_p^T & 0 & F \end{bmatrix}. \tag{3.48}$$

Let the state error be

$$e = Y_c - Y_m, \tag{3.49}$$

and output tracking error be

$$e_1 = y_p - y_m. \tag{3.50}$$

Error equation is written using (3.49) and (3.50) as follows:

$$\begin{aligned} \dot{e} &= A_c e + B_c(u_p - \theta^{*T}\omega), \quad e(0) = e_0, \\ e_1 &= C_c^T e, \end{aligned} \tag{3.51}$$

where $A_c, B_c, C_c$ represent the parameter matrices of the plant in state space realization. We have

$$W_m(s) = C_c^T(sI - A_c)^{-1}B_c c_0^*, \tag{3.52}$$

then $e_1$ becomes

$$e_1 = W_m(s)\rho^*(u_p - \theta^{*T}\omega). \tag{3.53}$$

where $\rho^* = 1/c_0^*$. The estimate $\hat{e}_1$ of $e_1$ is given as

$$\hat{e}_1 = W_m(s)\rho(u_p - \theta^T\omega), \tag{3.54}$$

where $\rho$ is the estimate of $\rho^*$. Since the control input is

$$u_p = \theta^T(t)\omega, \tag{3.55}$$

the estimate $\hat{e}_1$ and the estimation error $\epsilon_1$ becomes

$$\hat{e}_1 = 0, \quad \epsilon_1 = e_1 - \hat{e}_1 = e_1. \tag{3.56}$$

Substitute (3.56) into (3.51), we obtain

$$\begin{aligned} \dot{e} &= A_c e + B_c\tilde{\theta}^T\omega, \\ e_1 &= C_c^T e, \end{aligned} \tag{3.57}$$

where

$$\tilde{\theta} = \theta(t) - \theta^*. \tag{3.58}$$

### 3.2.2 Lyapunov-Like Function Composition and Analysis

In the typical direct adaptive control designs of the literature, which are gradient adaptive law based, the Lyapunov-like function is chosen as

$$V(\tilde{\theta}, e) = \frac{e^T P_c e}{2} + \frac{\tilde{\theta}^T\Gamma^{-1}\tilde{\theta}}{2}|\rho^*|, \tag{3.59}$$

where $\tilde{\theta} = \theta - \theta^*$, $\theta^*$ is the desired controller parameter vector, and $P_c = P_c^T > 0$ satisfying certain conditions to be detailed in the sequel and $\Gamma = \Gamma^T > 0$ is a constant positive definite the algebraic equations

$$\begin{aligned} P_c A_c + A_c^T P_c &= -qq^T - \nu_c L_c, \\ P_c B_c c_0^* &= C_c, \end{aligned} \tag{3.60}$$

where $q$ is a vector, $L_c = L_c^T > 0$, and $\nu_c > 0$ is small constant. The time derivative $\dot{V}$ of $V$ along the solution of (3.59) is

$$\dot{V} = -\frac{e^T qq^T e}{2} - \frac{\nu_c}{2} e^T L_c e + e^T P_c B_c c_0^* \rho^* \tilde{\theta}^T \omega + \tilde{\theta}^T \Gamma^{-1} \dot{\tilde{\theta}} |\rho^*|. \tag{3.61}$$

Since $e^T P_c B_c c_0^* = e^T C_c = e_1$ and $\rho^* = |\rho^*| sgn(\rho^*)$, $\dot{V} \leq 0$ is established by choosing

$$\dot{\tilde{\theta}} = \dot{\theta} = -\Gamma e_1 \omega sgn(\rho^*), \tag{3.62}$$

which leads to

$$\dot{V} = -\frac{e^T qq^T e}{2} - \frac{\nu_c}{2} e^T L_c e. \tag{3.63}$$

(3.59) and (3.63) imply that $V, e, \tilde{\theta} \in \mathcal{L}_\infty$. Since $e = Y_c - Y_m$ and $Y_m \in \mathcal{L}_\infty$, $Y_c \in \mathcal{L}_\infty$ that gives use $x_p, y_p, \omega_1, \omega_2 \in \mathcal{L}_\infty$. We also know that $u_p = \theta^T \omega$ and $\theta, \omega \in \mathcal{L}_\infty$; therefore, $u_p \in \mathcal{L}_\infty$. All the signals in the closed-loop plant are bounded. Hence, the tracking error $e_1 = y_p - y_m$ goes to zero as time goes to infinity.

(3.62) is given based on gradient algorithm and considers a constant $\Gamma$ gain in the Lyapunov function. Fast adaptation is referred to the implementation of adaptive control with a large adaptive gain to reduce the tracking error rapidly. However, a large adaptive gain can lead to high-frequency oscillations which can adversely affect robustness of the adaptive control law. As adaptive gain increases, time delay for a standard MRAC decreases causing loss of robustness. Unlike $\Gamma$, $P$ is adjusted based on identification error during estimation process, i.e, it allows an initial large adaptive gain to be set arbitrarily and provides the ability to drive the adaptive gain to a lower value as the adaptation has achieved sufficiently the desired tracking performance.

An RLS based direct adaptive control design would start with an alternative Lyapunov-like function to replace (3.59) and end up with a control law that is either the same as or similar to (3.55) together with and adaptive law that is the RLS based alternative of (3.62).

Here we start with a reverse process of this analysis, starting with the following RLS based alternative of the adaptive law. We define $\dot{\theta}$ in terms of RLS algorithm by replacing constant $\Gamma$ term with time-varying $P(t)$ matrix. In this regard, we write Lyapunov-like function in (3.59) as follows:

$$V(\tilde{\theta}, e) = \frac{e^T P_c e}{2} + \frac{\tilde{\theta}^T P^{-1} \tilde{\theta}}{2} |\rho^*|, \tag{3.64}$$

The time derivative $\dot{V}$ of $V$ along the solution of (3.64) is expressed by

$$\dot{V} = -\frac{e^T q q^T e}{2} - \frac{\nu_c}{2} e^T L_c e + e^T P_c B_c c_0^* \rho^* \tilde{\theta}^T \omega + \frac{1}{2} \tilde{\theta}^T \frac{d(P^{-1})}{dt} \tilde{\theta} |\rho^*| + \tilde{\theta}^T P^{-1} \dot{\tilde{\theta}} |\rho^*|. \tag{3.65}$$

where

$$\frac{d(P^{-1})}{dt} = -P^{-1} \dot{P} P^{-1}. \tag{3.66}$$

If $P(t)$ is updated according to the RLS adaptive law (3.17) with forgetting factor, i.e.,

$$\dot{P} = \beta P - P \omega \omega^T P, \tag{3.67}$$

(3.66) becomes

$$\frac{d(P^{-1})}{dt} = -\beta P^{-1} + \omega \omega^T. \tag{3.68}$$

Substituting (3.68) into (3.65), we have

$$\dot{V} = -\frac{e^T q q^T e}{2} - \frac{\nu_c}{2} e^T L_c e + e_1 \rho^* \tilde{\theta}^T \omega - \frac{\beta}{2} \tilde{\theta}^T P^{-1} \tilde{\theta} |\rho^*| + \tilde{\theta}^T P^{-1} \dot{\tilde{\theta}} |\rho^*| + \frac{\epsilon^2}{2} |\rho^*|, \tag{3.69}$$

where

$$\epsilon = \tilde{\theta}^T \omega. \tag{3.70}$$

$\dot{V} \leq 0$ can be established by choosing

$$\dot{\tilde{\theta}} = \dot{\theta} = -Pe_1 \omega sgn(\rho^*) + \frac{1}{2} P \epsilon \omega. \tag{3.71}$$

A new adaptive law based on RLS parameter estimation with time-varying covariance matrix $P$ is defined in (3.71),(3.67). Substituting these equations into (3.69), (3.65) becomes

$$\dot{V} = -\frac{e^T q q^T e}{2} - \frac{\nu_c}{2} e^T L_c e \leq 0. \tag{3.72}$$

**Theorem 3.1.** *The RLS parameter estimation based MRAC scheme* (3.43),(3.67),(3.71) *has the following properties:*

*i. All signals in the closed-loop are bounded and tracking error converges to zero in time for any reference input $r \in \mathcal{L}_\infty$.*

*ii. If the reference input $r$ is sufficiently rich of order $2n$, $\dot{r} \in \mathcal{L}_\infty$, and $Z_p(s), R_p(s)$ are relatively coprime, then $\omega$ is persistently exciting (PE) given in Definition 2.1, which implies that $P, P^{-1} \in \mathcal{L}_\infty$ and $\theta(t) \to \theta^*$ as $t \to \infty$. When $\beta > 0$, the parameter error $\| \tilde{\theta} \| = \| \theta - \theta^* \|$ and the tracking error $e_1$ converges to zero exponentially fast.*

*Proof.* i. $e \in \mathcal{L}_2$, $\theta, \omega, \in \mathcal{L}_\infty$, and $\dot{e} \in \mathcal{L}_\infty$. Therefore, all signals in the closed loop plant are bounded. In order to complete the design, we need to show tracking error $e_1$ converges to the zero asymptotically with time. Using (3.64), (3.72), we know that $e, e_1 \in \mathcal{L}_2$. Using, $\theta, \omega, e \in \mathcal{L}_\infty$ in (3.57), we have $\dot{e}, \dot{e}_1 \in \mathcal{L}_\infty$. Since $\dot{e}, \dot{e}_1 \in \mathcal{L}_\infty$ and $e_1 \in \mathcal{L}_2$, the tracking error $e_1$ goes to zero as $t$ goes to infinity.

ii. By Theorem 3.4.3 of [60], if $r$ is sufficiently rich of order $2n$ then the $2n$ dimensional regressor vector $\omega$ is PE. Let $Q = P^{-1}$ and (3.68) can be rewritten as

$$\dot{Q} = -\beta Q + \omega \omega^T. \tag{3.73}$$

and taking the integral of both sides, we obtain

$$Q(t) = e^{-\beta t} Q_0 + \int_0^t e^{-\beta(t-\tau)} \omega(\tau) \omega^T(\tau) d\tau. \tag{3.74}$$

Since $\omega(t)$ is PE,

$$
\begin{aligned}
Q(t) &\geq \int_{T_0}^{t} e^{-\beta(t-\tau)}\omega(\tau)\omega^T(\tau)d\tau \\
&\geq \bar{\alpha}_0 e^{-\beta T_0}\int_{T_0}^{t} e^{-\beta(t-\tau)}\omega(\tau)\omega^T(\tau)d\tau \\
&\geq \beta_1 e^{-\beta T_0} I, \qquad \forall t \geq T_0,
\end{aligned}
\tag{3.75}
$$

where $\beta_1 = \bar{\alpha}_0\alpha_0 T_0$, and $\alpha_0, \bar{\alpha}_0, T_0 > 0$ are design constants, given in (2.27). For $t \leq T_0$,

$$
Q(t) \geq e^{-\beta T_0}Q_0 \geq \lambda_{min}(Q_0)e^{-\beta T_0}I \geq \gamma_1 I \quad \forall t \geq 0, \tag{3.76}
$$

where $\gamma_1 = min\{\frac{\alpha_0 T_0}{\beta}, \lambda_{min}(Q_0)\}e^{-\beta T_0}$. Since $\omega$ is PE,

$$
Q(t) \leq Q_0 + \beta_2 \int_0^t e^{-\beta(t-\tau)}d\tau I \leq \gamma_2 I, \quad \beta_2 > 0. \tag{3.77}
$$

where $\gamma_2 = \lambda_{max}(Q_0) + \frac{\beta_2}{\beta} > 0$. Using (3.76) and (3.77), we obtain

$$
\gamma_2^{-1} I \leq P(t) = Q((t) \leq \gamma_1^{-1} I. \tag{3.78}
$$

Therefore, $P(t), Q(t) \in \mathcal{L}_\infty$. Exponential convergence is established following steps similar to those in [60].

□

Comparing two adaptive laws in (3.62) and (3.71), we can clearly see the effect of time varying covariance matrix reflected as an additional term to the similar part of (3.62). Now, we reverse the process and consider defining a new Lyapunov function based on integral cost function instead of standard quadratic instantaneous cost function.

Consider(3.73) and its solution (3.74). For simplicity, instead of (3.64), we consider the Lyapunov function as follows:

$$
V = \tilde{\theta}^T Q \tilde{\theta}, \tag{3.79}
$$

Substitute (3.74) into (3.79), we obtain

$$
\begin{aligned}
V &= e^{-\beta t}\tilde{\theta}^T(t)Q_0\tilde{\theta}(t) + \int_0^t e^{-\beta(t-\tau)}\tilde{\theta}^T(t)\omega(\tau)\omega^T(\tau)\tilde{\theta}(t)d\tau, \\
&= e^{-\beta t}\tilde{\theta}^T(t)Q_0\tilde{\theta}(t) + \int_0^t e^{-\beta(t-\tau)}\epsilon(t,\tau)\epsilon^T(t,\tau))d\tau, \\
&= e^{-\beta t}\tilde{\theta}^T(t)Q_0\tilde{\theta}(t) + \int_0^t e^{-\beta(t-\tau)}\epsilon^2(t,\tau)d\tau.
\end{aligned}
\tag{3.80}
$$

In literature, e.g. [60], the integral part of (3.80) is called integral cost function for gradient adaptive law. The additional term in RLS based Lyapunov function penalizes the initial estimate error.

The time derivative of (3.80) is written as

$$
\dot{V} = -\beta\left[-e^{-\beta t}\tilde{\theta}^T Q_0\tilde{\theta}\right] + 2e^{-\beta t}\tilde{\theta}^T Q_0\dot{\tilde{\theta}} + \left(-\beta + \beta e^{-\beta t}\right)\epsilon^2. \tag{3.81}
$$

$$
\dot{V} = -\beta e^{-\beta t}\tilde{\theta}^T Q_0\tilde{\theta} + 2e^{-\beta t}\tilde{\theta}^T Q_0\dot{\tilde{\theta}} - \beta\epsilon^2 + \beta e^{-\beta t}\epsilon^2. \tag{3.82}
$$

Choosing the adaptive law as

$$
\begin{aligned}
\dot{\tilde{\theta}} &= \frac{\beta}{2}\epsilon^2 Q_0^{-1}(\tilde{\theta})^{-1} \\
&= -\frac{\beta}{2}P_0\epsilon\omega,
\end{aligned}
\tag{3.83}
$$

we obtain

$$
\dot{V} = -\beta e^{-\beta t}\tilde{\theta}^T Q_0\tilde{\theta} - \beta\epsilon^2 < 0. \tag{3.84}
$$

The abovementioned stability properties applies to this design as well.

**Example 3.2.** *Consider the plant given in (3.11). We design direct MRAC for matching with the reference model*

$$
R_m(s) = \frac{1}{(s+1)^3} \tag{3.85}
$$

*We have the followings:*

$$y = k_p \frac{Z_p(s)}{R_p(s)} u = \frac{1}{s^3 + a_2 s^2 + a_1 s} u, \quad a_1 = p_1 p_2, \quad a_2 = -(p_1 + p_2), \quad k_p = 1, \tag{3.86}$$

*where $n = 3, m = 0$. By following the MRAC algorithm, the control structure can be obtained as follows:*

$$\begin{aligned} n = 3, \quad \alpha(s) &= \begin{bmatrix} s \\ 1 \end{bmatrix}, \quad \Lambda = (s+1)^2, \\ u = \theta_1^{*T} \frac{\alpha(s)}{\Lambda(s)} u &+ \theta_2^{*T} \frac{\alpha(s)}{\Lambda(s)} y + \theta_3^* y + c_0^* r. \end{aligned} \tag{3.87}$$

*with*

$$\theta_1^* = \left[a_2 - 3, a_1 + 5a_2 - a_2^2 - 9\right]^T$$

$$\theta_2^* = \left[10a_1 - a_1^2 - 5a_1 a_2 + a_1 a_2^2 - 5 - 2\theta_3^*, -1 - \theta_3^*\right]^T$$

$$\theta_3^* = 5a_1 + 10a_2 - 2a_1 a_2 - 5a_2^2 + a_2^3 - 10.$$

*For the implementation, we use*

$$\begin{aligned} \dot{\omega}_1 &= \begin{bmatrix} -2 & -1 \\ 1 & 0 \end{bmatrix} \omega_1 + \begin{bmatrix} 1 \\ 0 \end{bmatrix} u, \quad \dot{\omega}_2 = \begin{bmatrix} -2 & -1 \\ 1 & 0 \end{bmatrix} \omega_2 + \begin{bmatrix} 1 \\ 0 \end{bmatrix} y, \\ u &= \theta^{*T} \omega, \quad \theta^* = \begin{bmatrix} \theta_1^* \\ \theta_2^* \\ \theta_3^* \\ c_0^* \end{bmatrix}, \quad \omega = \begin{bmatrix} \omega_1 \\ \omega_2 \\ y \\ r \end{bmatrix}. \end{aligned} \tag{3.88}$$

*Parametric model is obtained as*

$$\begin{aligned} z &= \rho^*(\theta^{*T} \phi + z_0), \quad \theta^* = \begin{bmatrix} \theta_1^* \\ \theta_2^* \\ \theta_3^* \\ c_0^* \end{bmatrix} = \begin{bmatrix} \theta_1^* \\ \theta_2^* \\ \theta_3^* \\ 1 \end{bmatrix}, \quad c_0^* = 1, \quad \rho^* = \frac{1}{c_0^*} = 1, \\ z &= y - R_m u, \quad \phi = -R_m(s) \omega, \quad z_0 = R_m(s) u, \quad \omega = \begin{bmatrix} \omega_1 \\ \omega_2 \\ y \\ r \end{bmatrix} = \begin{bmatrix} \frac{\alpha(s)}{\Lambda(s)} u \\ \frac{\alpha(s)}{\Lambda(s)} y \\ y \\ r \end{bmatrix}. \end{aligned} \tag{3.89}$$

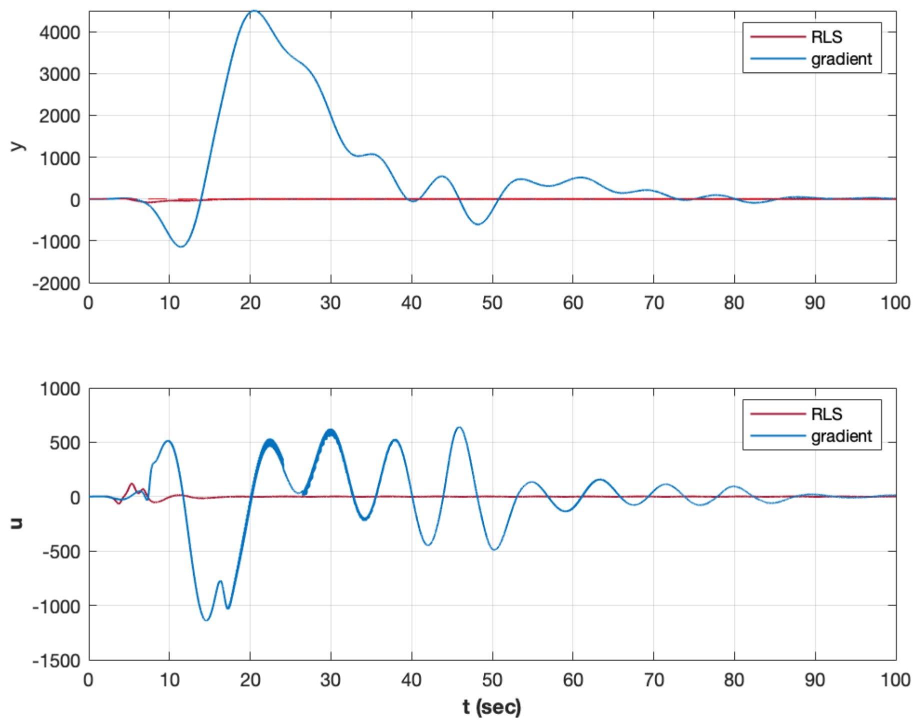


Figure 3.6: Input-output signals with gradient and RLS parameter estimation based direct MRAC.

*Since we know $c_0^*$ and $\rho^*$, parametric model becomes*

$$\bar{z} = \bar{\theta}^{*T}\bar{\phi}, \quad \bar{z} = e + y_m - z_0 = y - R_m(s)u, \quad \bar{\phi} = -R_m(s)\bar{\omega}, \quad \bar{\omega} = \begin{bmatrix}\omega_1 & \omega_2 & y\end{bmatrix}^T. \tag{3.90}$$

*Therefore, the estimation model is*

$$\begin{aligned} \hat{\bar{z}} &= \bar{\theta}^T\bar{\phi}, \quad \bar{\theta} = \begin{bmatrix}\theta_1^T & \theta_2^T & \theta_3\end{bmatrix}^T, \\ \varepsilon &= \frac{\bar{z} - \hat{\bar{z}}}{m_s^2} \end{aligned} \tag{3.91}$$

*Adaptive law with gradient estimation is given by*

$$\dot{\bar{\theta}} = \gamma\varepsilon\bar{\phi}, \tag{3.92}$$

*and adaptive law with gradient estimation is given by*

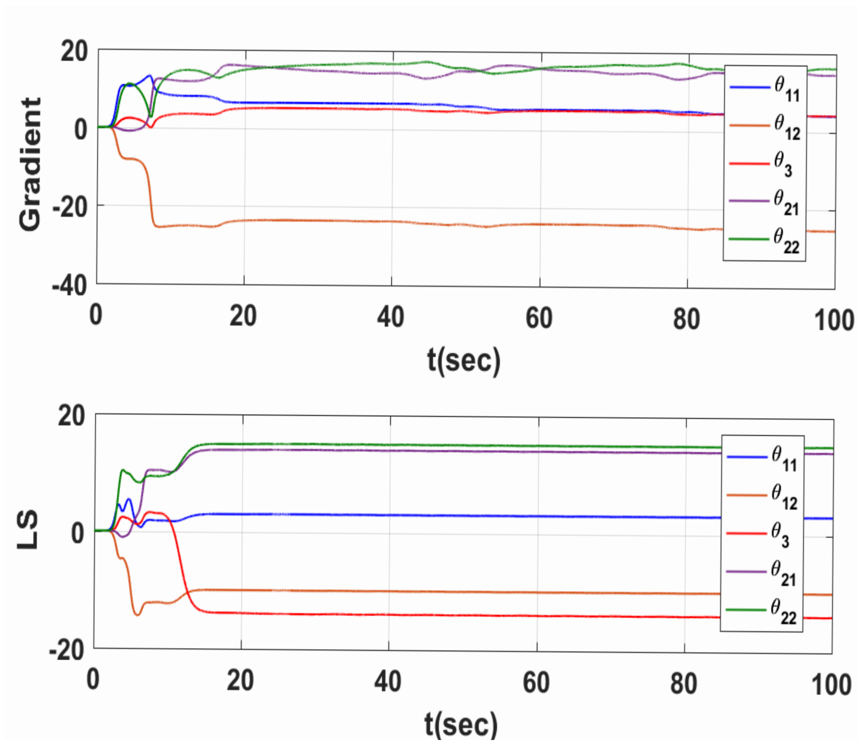


Figure 3.7: Parameter estimates in gradient and RLS parameter estimation based direct MRAC.

$$\begin{aligned}
\dot{\bar{\theta}} &= \bar{P}\varepsilon\phi \\
\dot{\bar{P}} &= \beta\bar{P} - \bar{P}\frac{\phi\phi^T}{m_s^2}\bar{P}.
\end{aligned} \tag{3.93}$$

*The parameters for the simulation are given as follows:* $\theta^* = \left[-3, -10, 14, 14, -15\right]^T$, $\gamma = 100I$ *and* $\beta = 0.9$.

*The results shown in Fig. 3.6 verify the effectiveness of RLS parameter estimation over gradient one in direct adaptive control. In the gradient based parameter estimation, convergence is reached after 80 seconds, whereas RLS algorithm provides faster convergence in*

*20 seconds. Fig. 3.7 also shows the parameter estimates obtained using gradient and RLS based estimation algorithms.*

## 3.3 Application to Adaptive Cruise Control

Adaptive Cruise Control (ACC) is a crucial part of the self-driving cars. ACC is an advanced driver assistance system aiming at enhancing the safety and decreasing the number of people killed or injured in road accidents which has been deteriorated due to the increasing number of the vehicles on the road. ACC needs to track the car in front but also cars in adjacent lanes in case a lane change becomes inevitable. ACC is an intelligent form of cruise control that slows down and speeds up automatically to keep desired spacing with the car in front of you.

The driver sets the desired spacing from leading vehicle in the same lane and ACC system takes over the control of brake and gas pedals and keep the desired spacing. The driver is responsible for keeping the vehicle in the center of the lane by managing the steering wheel. A sensor mounted in the front of the vehicle measures the distance from the front of the vehicle to the rear of the vehicle in front in the same lane. It also measures the relative speed between two vehicles. A basic ACC scheme can be seen in Fig. 3.8. ACC regulates the following vehicle's speed $v$ towards the leading vehicle's speed $v_l$ and keeps the distance between vehicles $x_r$ close to desired spacing $s_d$.

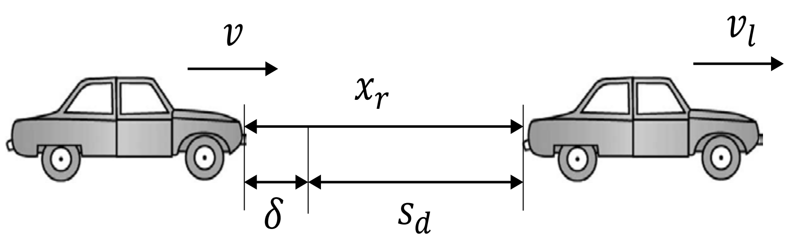


Figure 3.8: Leading and following vehicles.

The control objective in ACC is to make the speed error close to zero as time increases. This objective can be expressed as

$$v_r \to 0, \quad \delta \to 0, \quad t \to \infty, \tag{3.94}$$

where $v_r = v_l - v$ which is defined as the speed error or sometimes relative speed, $\delta = x_r - s_d$ is the spacing error. The desired spacing is proportional to the speed since the desired spacing between vehicles is given as

$$s_d = s_0 + hv \tag{3.95}$$

where $s_0$ is the fixed spacing for safety so that the vehicles are not touching each other at zero speed and $h$ is constant time headway. Moreover, the control objective should satisfies the followings:

$a_{min} \leq \dot{v} \leq a_{max}$,
$|\ddot{v}|$ should be small.

First constraint restricts ACC vehicle generating high acceleration and the second one is given for the driver's comfort. For ACC system longitudinal nonlinear model is used. However, we consider a simple model approximating the actual vehicle longitudinal model without considering nonlinear dynamics which is given by

$$\dot{v} = -av + bu + d, \tag{3.96}$$

where $v$ is the longitudinal speed, $u$ is the throttle/brake command, $d$ is the modeling uncertainty, $a$ and $b$ are positive constant parameters. We assume that $d, \dot{d}v_l, \dot{v}_l$ are all bounded. Model reference adaptive control is considered so that the throttle/brake command $u$ forces the vehicle speed to follow the output of the reference model

$$v_m = \frac{a_m}{s + a_m}(v_l + k\delta), \tag{3.97}$$

where $a_m$ and $k$ are positive design parameters.We first assume that $a, b$, and $d$ are known and consider the control law as follows:

$$u = k_1^* v_r + k_2^* \delta + k_3^*, \tag{3.98}$$

where

$$k_1^* = \frac{a_m - a}{b}, \quad k_2^* = \frac{a_m k}{b}, \quad k_3^* = \frac{a v_l - d}{b}. \tag{3.99}$$

Since $a, b$, and $d$ are unknown, we change the control law as

$$u = k_1 v_r + k_2 \delta + k_3, \tag{3.100}$$

where $k_i$ is the estimate of $k_i^*$ to be generated by the adaptive law so that the closed-loop stability is guaranteed. The tracking error is given as

$$e = v - v_m, \tag{3.101}$$

which satisfies

$$e = \frac{b}{s + a_m}(k_1^* v_r + k_2^* \delta + k_3^* + u). \tag{3.102}$$

(3.102) is in the form of B-DPM. Substituting the control law in (3.100) into (3.102), we obtain

$$e = \frac{b}{s + a_m}(\tilde{k}_1 v_r + \tilde{k}_2 \delta + \tilde{k}_3), \tag{3.103}$$

where $\tilde{k}_i = k_i - k_i^*$ for $i = 1, 2, 3$. In order to find the adaptive law, consider the Lyapunov function [60] as

$$V = \frac{e^2}{2} + \sum_{i=1}^{3} \frac{b}{2\gamma_i}\tilde{k}_i^2 \quad \gamma_i > 0, b > 0. \tag{3.104}$$

Then, its time derivative is

$$\dot{V} = -a_m e^2 + be(\tilde{k}_1 v_r + \tilde{k}_2 \delta + \tilde{k}_3) + \sum_{i=1}^{3} \frac{b}{2\gamma_i}\tilde{k}_i \dot{\tilde{k}}_i. \tag{3.105}$$

Therefore, the following gradient based adaptive laws are applied to ACC

$$\begin{aligned} \dot{k}_1 &= Pr\{-\gamma_1 e v_r\}, \\ \dot{k}_2 &= Pr\{-\gamma_2 e \delta\}, \\ \dot{k}_3 &= Pr\{-\gamma_3 e\}, \end{aligned} \tag{3.106}$$

where the projection operator keeps $k_i$ within the lower and upper intervals and $\gamma_i$ are the positive constant adaptive gains. These adaptive laws lead to

$$\dot{V} = -a_m e^2 - \frac{b}{\gamma_i}\tilde{k}_i \dot{k}_3^*, \tag{3.107}$$

where $\dot{k}_3^* = \frac{a\dot{\nu}_l - \dot{d}}{b}$. By projection operator, estimated parameters are guaranteed to be bounded by forcing them to remain inside the bounded sets, $\dot{V}$ implies that $e \in \mathcal{L}_\infty$, in

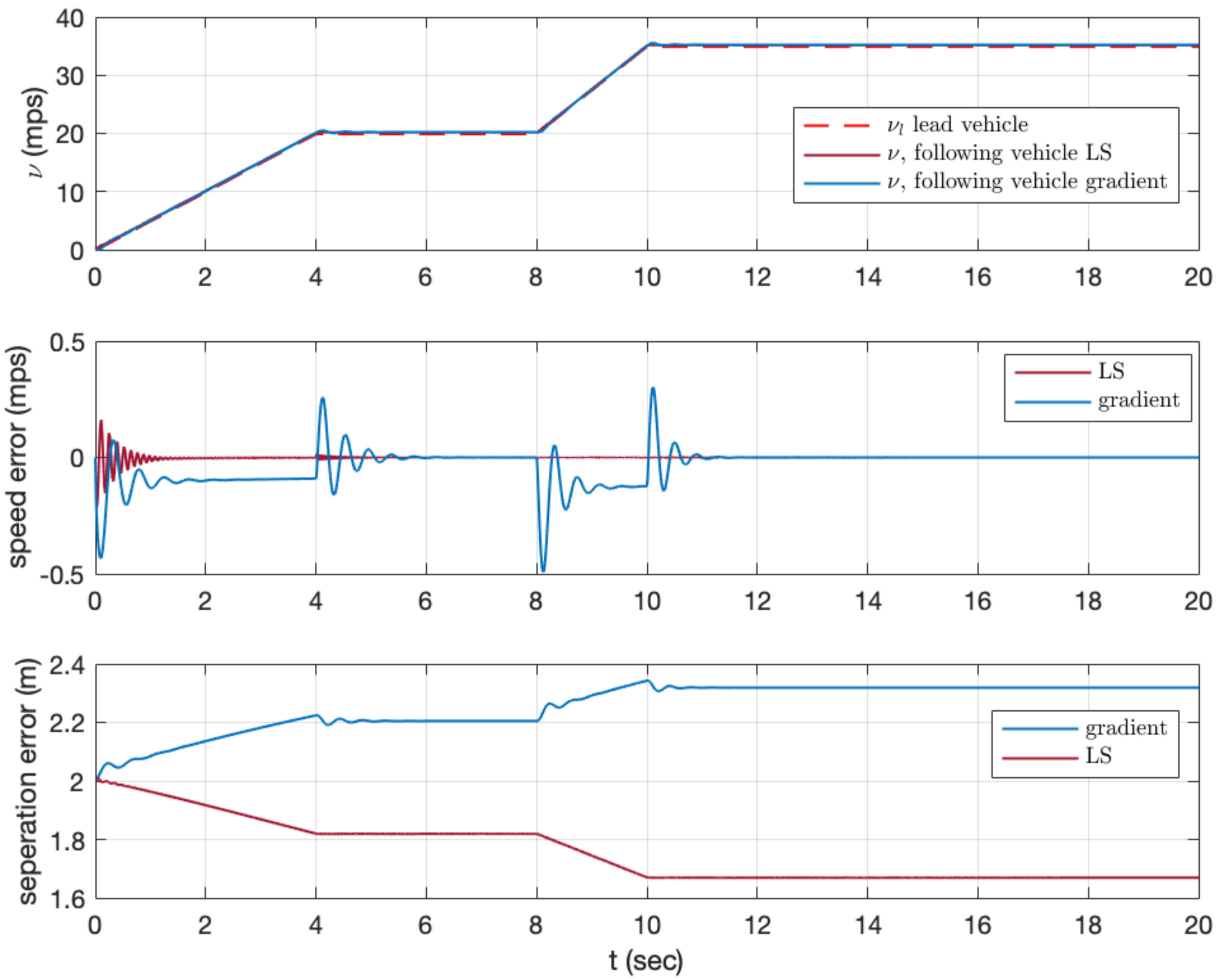


Figure 3.9: ACC comparison results in Matlab/Simulink.

turn all other signals in the closed loop are bounded. For the purpose of this chapter, we apply RLS based adaptive law to (3.104) and obtain following equations to be used in simulations

$$\begin{aligned} \dot{\hat{\theta}} &= Pr\{P_{ii} e \phi\} \\ \dot{P} &= \beta P - P\phi\phi^T P, \quad P(0) = I_{3\times 3}, \end{aligned} \tag{3.108}$$

where $e = v - v_m$, $\theta = \begin{bmatrix} k_1, & k_2, & k_3 \end{bmatrix}^T$, $\phi = \begin{bmatrix} \frac{v_r}{s+a_m}, & \frac{\delta}{s+a_m}, & \frac{1}{s+a_m} \end{bmatrix}^T$, and $P_{ii}$ are the diagonal elements of $P$ covariance matrix, i=1,2,3.

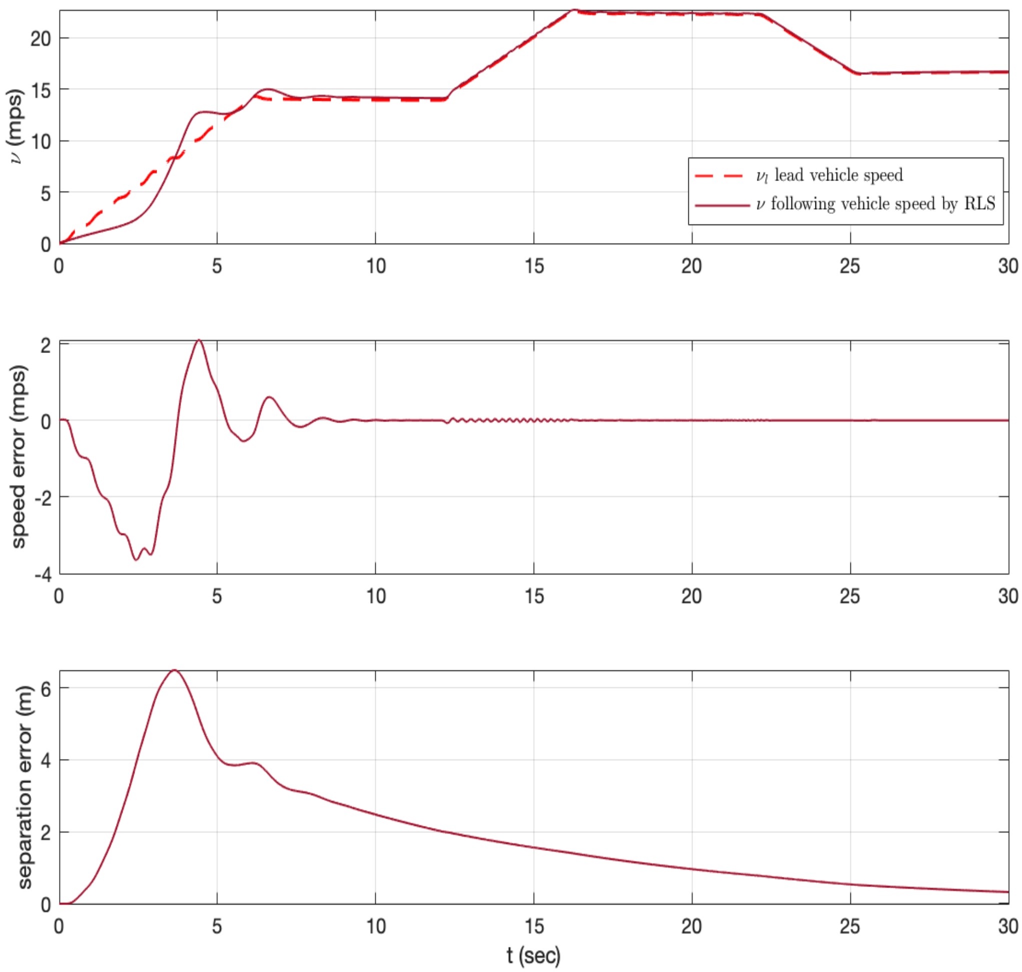


Figure 3.10: ACC results in CarSim.

### 3.3.1 Simulation Results

Since the throttle and brake cannot be applied at the same time, in this application, throttle subsystem is simulated. For gradient based algorithm, $\gamma_1 = 50I, \gamma_2 = 30I, \gamma_3 = 40I$ constant gains are given. For RLS based algorithm $\beta = 0.95$ and $P(0) = 100I_3$ are given. Simulation results from Matlab/Simulink for throttle subsystem are given in Fig. 3.9. Fig.

3.9 shows the vehicle following for both gradient and RLS based adaptive laws. The speed error in velocity tracking shows the better performance for RLS adaptive law. The results give the idea that RLS based adaptive control can be used with this form.

We also implemented RLS based adaptive control algorithm in (3.108) to CarSim for more realistic results. CarSim is one of the most widely used vehicle dynamics simulation packages in industry. Adopting the CarSim vehicle model, we can simulate its real operation condition and reflect the system dynamic characteristic and balance model accuracy, making the simulation results better consistent with the real scene. The vehicle parameters used in CarSim are as follows: $m = 567.75\ kg$, $R = 0.3\ m$, $I = 1.7\ kgm^2$, $B = 0.01\ kg/s$. The adaptive gains for both gradient and RLS are used the same as in Matlab/Simulink. CarSim results for RLS based ACC can be found in Fig. 3.10. Results demonstrate the ability of the following vehicle equipped with RLS based adaptive law on dry road by adjusting the speed and the distance between the leading vehicle and itself.

## 3.4 Application to Vehicle Braking System

As vehicle safety oriented control systems become more advanced, their dependence on accurate information on the vehicle state increases. Performance of driver-assistance technologies such as braking and traction systems is greatly influenced by the characteristics of the tire-road friction force.

In this section, we consider the vehicle longitudinal dynamics and an MRAC for braking system is designed. Block diagram of the overall design is given in Fig. 3.11. For the purpose of our control problem, we first start with the modelling of vehicle longitudinal dynamics.

In this application, we consider the single wheel model. The wheel characteristic is given by

$$I\dot{\omega} = -B\omega - NR\mu + \tau, \tag{3.109}$$

where

$$N\mu = m\dot{\nu}. \tag{3.110}$$

$v, \omega, m, N, R, I$ are linear velocity, angular velocity, the mass, the weight, radius, and the moment of inertia of the wheel, respectively. $B\omega$ is the bearing friction torque, $\tau$ is the braking torque, $\mu$ is the friction force coefficient.

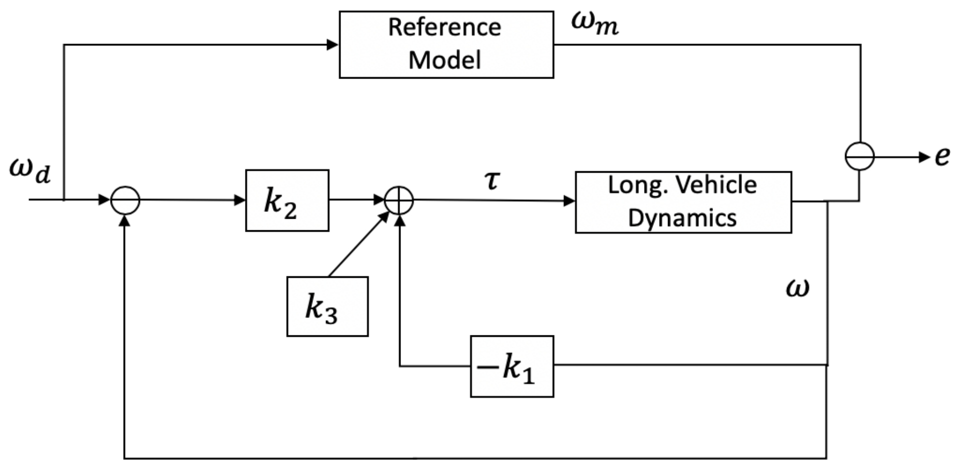


Figure 3.11: Block diagram of MRAC structure.

Substitute (3.110) into (3.109), the wheel dynamics is written as

$$\dot{\omega} = -\frac{B}{I}\omega - \frac{mR}{I}\dot{\nu} + \frac{1}{I}\tau. \tag{3.111}$$

The objective of the control design is to make the vehicle wheel velocity $\omega$ follow the response of the reference model $\omega_m$

$$\omega_m = \frac{a_m}{s + a_m}\omega_d, \tag{3.112}$$

where $\omega_d$ is the desired wheel velocity to be tracked. The reference model is used to smooth the trajectory of the desired velocity $\omega_d$. To achieve the control objective, we use the similar way as in Section 3.3 to design MRAC.

The control input is given in 3.11 as follows:

$$\tau = -k_1\omega + k_2(\omega_d - \omega) + k_3, \tag{3.113}$$

where $k_i$ is the estimate of $k_i^*$ to be generated by the adaptive law so that the closed-loop stability is guaranteed. The tracking error is given as

$$e = \omega - \omega_m. \tag{3.114}$$

Using the similar steps as in (3.102)-(3.104) and substituting (3.109), we obtain

$$\dot{e} = -a_m e + b(-\tilde{k}_1\omega + \tilde{k}_2(\omega_d - \omega) + \tilde{k}_3). \tag{3.115}$$

In order to find the adaptive laws, we define the Lyapunov function as

$$V = \frac{e^2}{2} + \sum_{i=1}^{3} \frac{b}{2\Gamma_i}\tilde{k}_i^2 \quad \Gamma_i > 0, b > 0. \tag{3.116}$$

The time derivative of (3.116) is given as follows:

$$\dot{V} = -a_m e^2 + be(-\tilde{k}_1\omega + \tilde{k}_2(\omega_d - \omega) + \tilde{k}_3) + \sum_{i=1}^{3} \frac{b}{\Gamma_i}\tilde{k}_i\dot{\tilde{k}}_i. \tag{3.117}$$

The following gradient based adaptive laws are obtained to satisfy $\dot{V} < 0$.

$$\begin{aligned} \dot{k}_1 &= \Gamma_1 \; e \; \omega, \\ \dot{k}_2 &= -\Gamma_2 \; e \; (\omega_d - \omega), \\ \dot{k}_3 &= -\Gamma_3 \; e, \end{aligned} \tag{3.118}$$

where $\Gamma_i > 0$. With (3.118), we have

$$\dot{V} = -a_m e^2 < 0. \tag{3.119}$$

To define RLS based adaptive laws, we use Lyapunov function in a similar way as follows

$$V = \frac{e^2}{2} + \sum_{i=1}^{3} \frac{b}{2P_i}\tilde{k}_i^2. \tag{3.120}$$

The time derivative of (3.120) is given as follows:

$$\dot{V} = -a_m e^2 + be(-\tilde{k}_1\omega + \tilde{k}_2(\omega_d - \omega) + \tilde{k}_3) + \sum_{i=1}^{3} \frac{b}{P_i}\tilde{k}_i\dot{\tilde{k}}_i - \frac{b\beta}{2P_i} - \frac{b}{2}\frac{P_i\phi_i\phi_i^T P_i}{Pi^2}\tilde{k}^2, \tag{3.121}$$

where $\dot{P}_i = \beta P_i - P_i \phi_i \phi_i^T P_i$. Choosing RLS based adaptive laws as

$$\begin{aligned} \dot{\hat{\theta}} &= P_{ii} \; e \; \phi \\ \dot{P} &= \beta P - P \phi \phi^T P, \quad P(0) = I_{3\times 3}, \end{aligned} \tag{3.122}$$

where

$$\begin{aligned} \theta &= \begin{bmatrix} k_1, & k_2, & k_3 \end{bmatrix}^T \\ \phi &= \begin{bmatrix} \omega, & (\omega_d - \omega), & 1 \end{bmatrix}^T, \end{aligned} \tag{3.123}$$

and $P_{ii}$ are the diagonal elements of $P_{3\times 3}$ covariance matrix, $i = 1, 2, 3$.

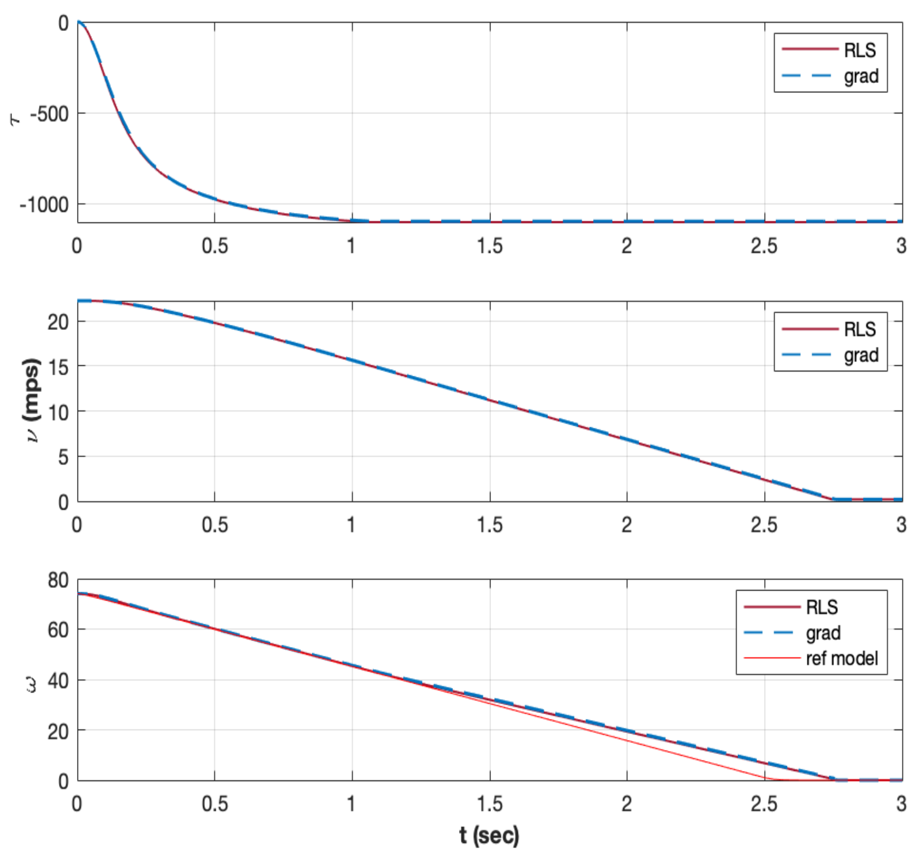


Figure 3.12: Braking torque and velocity results of MRAC in Simulink.

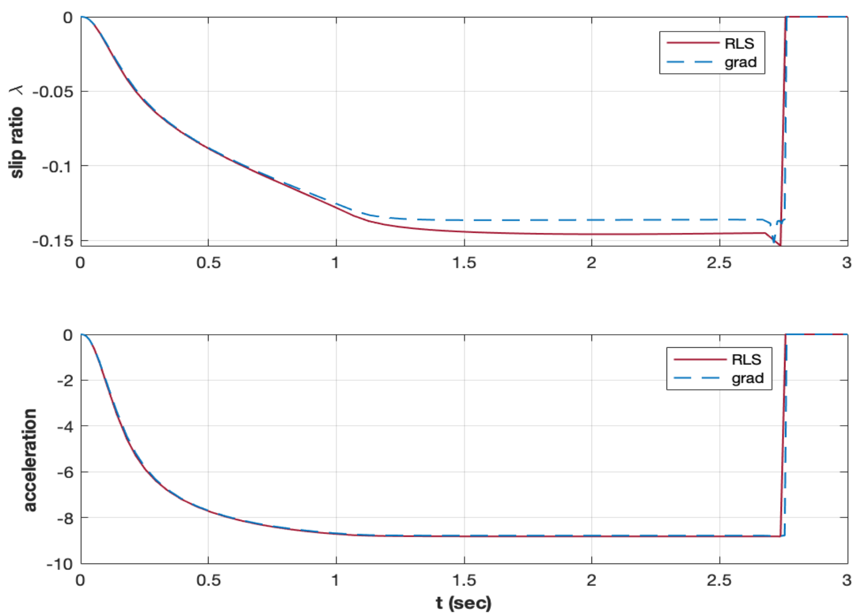


Figure 3.13: Deceleration and slip ratio results in Simulink.

### 3.4.1 Simulation Results

We tested RLS based MRAC algorithm for vehicle braking system and compared the performance with gradient based MRAC algorithm in Matlab/Simulink. The vehicle parameters are given as follows: $m = 400kg$, $R = 0.3m$, $I = 1.7kgm^2$, $B = 0.01kg/s$. Forgetting factor for RLS $\beta = 0.9$. The simulation is performed under the Gaussian noise ($\sigma = 0.01$).

Simulation results with given reference model velocity and velocity results from both gradient and RLS designs are given in Fig. 3.12 and Fig. 3.13. The proposed algorithm is first tested in Matlab/Simulink. Road condition is chosen as dry road. Results show the ability of designed MRAC to follow the reference model with small errors for both gradient and RLS based adaptive laws. Note that simulation time is given based on a realistic time range to stop the vehicle with an initial speed of $80kph$ on a dry road. The results show that the tracking of a reference model $\omega_m$ can be tracked by a small error near the stopping time. The vehicle equipped with both gradient and RLS based MRAC stops around 2.7 second, and achieved slip ratios and acceleration can be found in Fig. 3.13.

For CarSim application, vehicle parameters are used the same as in Matlab/Simulink. Adaptive gains for gradient algorithm are given as $\Gamma_i = [10,\ 20,\ 10]$ and covariance matrix is used as $P_i = 10I_3$. Forgetting factor is $\beta = 0.95$.

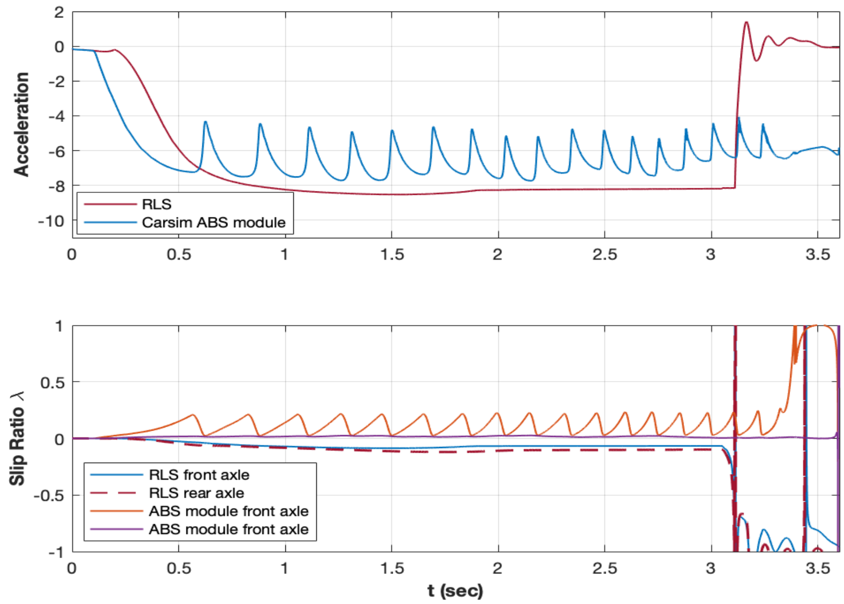


Figure 3.14: Deceleration and slip ratios with CarSim.

Fig. 3.14 and Fig. 3.15 show the results from CarSim. RLS based MRAC is compared with ABS module in CarSim. Generated torques is applied to front and rear axle. The vehicle with RLS based MRAC stops the vehicle in a shorter time while the vehicle follows the reference wheel velocity.

## 3.5 Summary

In this chapter, RLS based adaptive control was examined under two structures: indirect adaptive control and direct adaptive control. As an introductory study, indirect adaptive control was studied utilizing APPC and MRAC with numerical simulation examples. Performance comparisons verified that RLS parameter estimation based adaptive control provides faster convergence compared to the gradient based adaptive control.

Direct MRAC was analysed by replacing the constant adaptation gain that was used in gradient based direct adaptive control, with a time varying covariance matrix for a constructive Lyapunov analysis. RLS parameter estimation based direct adaptive control was later studied by defining a new Lyapunov function based on integral cost function instead of standard quadratic instantaneous cost function.

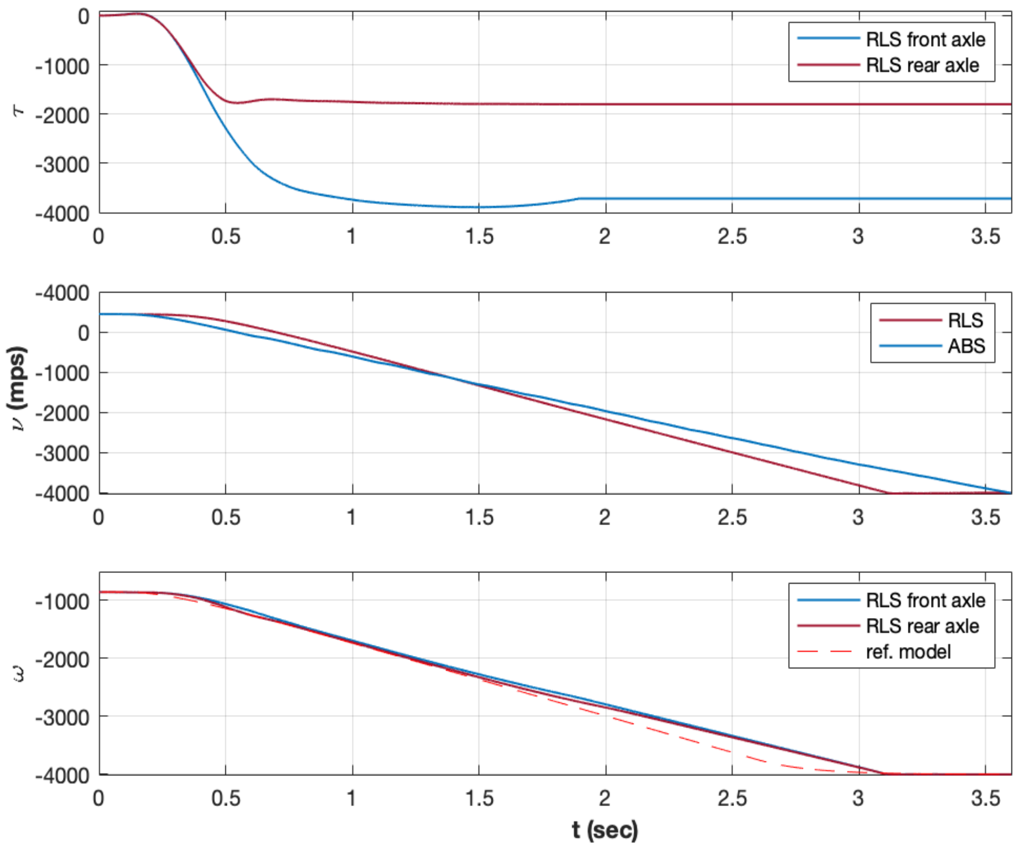


Figure 3.15: Braking results of MRAC in CarSim.

For application of RLS based adaptive control, ABS and ACC were considered. Matlab/Simulink results were provided giving the comparison results of RLS and gradient based adaptive laws. CarSim simulations were also performed for high-fidelity simulation results.

# Chapter 4

# Recursive Least Squares Based Extremum Seeking

ES is a well established approach for on-line optimization and optimal control of unknown dynamic systems. However, convergence rate of conventional ES approaches is a limiting factor in many applications. LS based on-line parameter estimation has significant potential in relaxing this limitation and improving accuracy and robustness to measurement noises, based on the characteristics discussed in previous chapters.

In this chapter, the integration of ES of static maps and dynamic systems with RLS based on-line estimation is examined, noting that the existing ES works in the literature have utilized gradient/Newton-based estimation algorithms.

The formal problem definition for ES of static maps and dynamics systems, each, is given in Section 4.1. In Section 4.2, RLS based ES system redesign is studied, utilizing high-pass and low pass filters based on the work of [73]. An alternative approach that does not involve bandpass filtering and considering ES as an estimation problem is introduced in Section 4.3. In Section 4.4, the proposed LS based ES schemes are applied to vehicle safety systems, ABS and TCS with their application to Matlab/Simulink and CarSim.

## 4.1 Problem Statement

The ES problem of interest is defined for static map systems and dynamic systems separately in the following subsections to be the base of our designs.

### 4.1.1 Static Maps

Consider a concave static map system

$$y = h_s(u) = \bar{h}_s(\theta^*, u), \quad \theta^* = \begin{bmatrix} \theta_1^* & \cdots & \theta_N^* \end{bmatrix}^T, \tag{4.1}$$

where $\theta^* \in \mathbb{R}^N$ is a fixed unknown parameter vector, $u \in \mathbb{R}^m$ is the input and $y \in \mathbb{R}$ is the output of the system. Assume that the control input signal $u$ is generated by a smooth control law

$$u = \alpha(\theta) \tag{4.2}$$

parametrized by a control parameter vector $\theta \in \mathbb{R}^N$.

**Assumption 4.1.** *The static map $\bar{h}_s(\theta^*, u)$ is smoothly differentiable.*

**Assumption 4.2.** *$h_s(u) = \bar{h}_s(\theta^*, u)$ has a single extremum (maximum) $y^*$ at $u = \alpha(\theta^*)$.*

The control objective is to maximize the steady-state value of $y$ but without requiring the knowledge of $\theta^*$ or the system function $h_s$.

### 4.1.2 Dynamic Systems

Consider a general multi-input-single-output (MISO) nonlinear system

$$\dot{x} = f(x, u) = \bar{f}(\theta^*, x, u), \tag{4.3}$$

$$y = h_d(x) = \bar{h}_d(\theta^*, \theta) = h(\theta), \tag{4.4}$$

$$\theta = \pi(x) \tag{4.5}$$

where $x \in \mathbb{R}^n$ is the state, $u \in \mathbb{R}^m$ is the input, $y \in \mathbb{R}$ is the output, all measurable, and $f : \mathbb{R}^n \times \mathbb{R}^m \to \mathbb{R}^n$ and $h_d = h \circ \pi$ are smooth functions. Assume that the control input signal $u$ is in the form (4.2), the control parameter $\theta \in \mathbb{R}^N$ is dependant on $x$ through a map $\pi(.) : \mathbb{R}^n \to \mathbb{R}^N$.

The closed loop system can be written as follows:

$$\dot{x} = f(x, \alpha(\theta)) = f(x, \alpha(\pi(x))). \tag{4.6}$$

The equilibria of (4.6) can be parameterized by $\theta$. The following assumptions about the closed loop system (4.3) are made, similarly to [73].

**Assumption 4.3.** *There exists a smooth function $l : \mathbb{R}^N \to \mathbb{R}^m$ such that*

$$f(x, \alpha(x, \theta)) = 0 \quad \textit{if and only if} \quad x = l(\theta), \tag{4.7}$$

*for any $(x, \theta) \in \mathbb{R}^m \times \mathbb{R}^N$. For each $\theta \in \mathbb{R}^N$, the equilibrium $x_e = l(\theta)$ of the system (4.6) is locally exponentially stable with decay and overshoot constants uniformly dependent on $\theta$.*

**Assumption 4.4.** *There exists $\theta^* \in \mathbb{R}^N$ such that for all admissible $x$ values, $h_d(x)$ has its unique maximum at $x = x^* = l(\theta^*)$,*

$$y'(x^*) = \frac{\partial h}{\partial x}\Big|_{x=x^*} = 0, \tag{4.8}$$

*and the $m \times m$ Hessian matrix $y''(x^*) = \frac{\partial^2 h}{\partial x^2}\Big|_{x=x^*}$ is negative definite.*

The control objective is to maximize the steady-state value of $y$ but without requiring the knowledge of $\theta^*$ or the system functions $h_d, f$. This objective could be perfectly performed if $\theta^*$ was known and substituted in (4.2).

## 4.2 Redesign of ES with respect to RLS

In this section, RLS based ES is introduced as alternative to the designs of [73],[70] involving bandpass filtering and perturbation signals. The gradient estimation is replaced with RLS estimation in the following subsection for scalar and vector parameter systems.

### 4.2.1 RLS based ES for Scalar Parameter Systems

We first consider scalar parameter case, $m = 1$. As in Section 4.1, static maps and dynamic systems will be focused on separately.

#### Static Maps

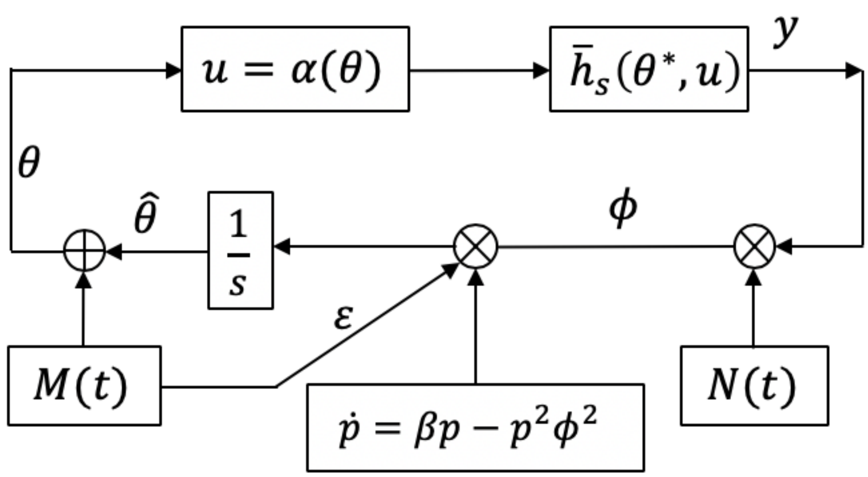


Figure 4.1: RLS estimation based ES redesign for scalar parameter static maps.

Consider RLS based ES scheme for static map defined in (4.1). Proposed scheme is given in Fig. 4.1. In this algorithm, there are three important parts: one generates the covariance matrix, $P$, one generates estimation error, $\varepsilon$, one generates regressor signal, $\phi$.

A parameter error variable for the static map is given by

$$\theta = M(t) + \hat{\theta}. \tag{4.9}$$

RLS based ES scheme for a static map is defined as follows:

$$\begin{aligned} \dot{\hat{\theta}} &= p\varepsilon\phi, \\ \dot{p} &= \beta p - p^2\phi^2, \\ \phi &= N(t)y = N(t)\bar{h}_s(\theta^*, u), \end{aligned} \tag{4.10}$$

$$
\begin{aligned}
M(t) &= a\sin(\omega t), \\
N(t) &= \frac{a^2}{16}\sin^2(\omega t).
\end{aligned} \tag{4.11}
$$

where estimation error, $\varepsilon = \theta - \hat{\theta}$. In this design, perturbation signals $M(t)$ generating $u$, and $N(t)$ generating $\phi$, and forgetting factor $\beta$ have important places and they are arbitrarily chosen so that parameter convergence can be achieved. This design has design parameters including $\beta, a, \omega$ that need to be tuned during the application.

### Dynamic Systems

In this section, ES scheme is considered for dynamic systems. Consider the defined nonlinear system (4.3) with its input (4.2), state (4.6), and assumptions (4.3-4.4).

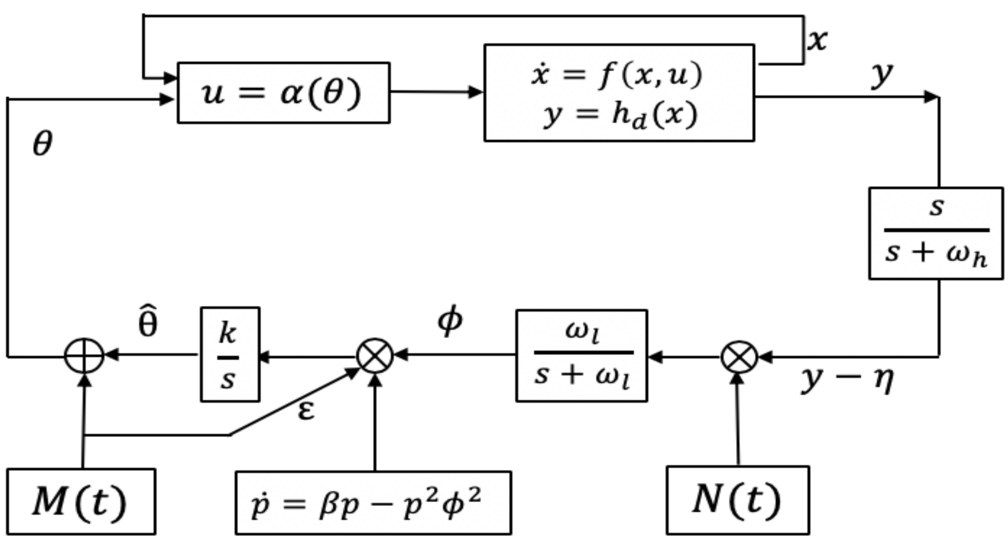


Figure 4.2: RLS estimation based ES redesign for scalar parameter dynamic systems.

The proposed algorithm is given in Fig. 4.2 to maximize the steady state value of $y$ without requiring the knowledge of either $\theta^*$ or the function of h. RLS based ES scheme can be derived as follows:

$$
\begin{aligned}
\dot{\hat{\theta}} &= P\varepsilon\phi \\
\dot{p} &= \beta p - p^2\phi^2 \\
\dot{\phi} &= \omega_l N(t)(y-\zeta) - \phi\omega_l, \\
\dot{\zeta} &= \zeta\omega_h + y\omega_h,
\end{aligned}
\tag{4.12}
$$

where

$$
\begin{aligned}
\varepsilon &= M(t) = \theta - \hat{\theta}, \\
M(t) &= a\sin(\omega t), \\
N(t) &= \frac{a^2}{16}\sin^2(\omega t).
\end{aligned}
\tag{4.13}
$$

By appropriate choices of $\beta$, $M(t)$ and $N(t)$, convergence will be satisfied. One disadvantage of this scheme is that it has multiple design parameters including $\beta, a, \omega, \omega_h, \omega_l$ that need to be tuned accordingly during the application and that makes the scheme very sensitive to any changes in the design parameters.

### 4.2.2 RLS based ES for Vector Parameter Systems

In this section, the redesign process is considered for vector parameter systems in scalar maps and dynamic systems, respectively.

#### Static Maps

Consider RLS based ES scheme for static map defined in (4.1). Proposed scheme is given in Fig. 4.1. In this algorithm, there are three important parts: one generates the covariance matrix, $P$, one generates estimation error, $\varepsilon$, one generates regressor signal, $\phi$.

A parameter error variable for the static map is given by

$$
\theta = M(t) + \hat{\theta}. \tag{4.14}
$$

RLS based ES scheme for a static map is defined as follows:

$$
\begin{aligned}
\dot{\hat{\theta}} &= P\varepsilon\phi, \\
\dot{P} &= \beta P - P\phi\phi^T P, \\
\phi &= N(t)y = N(t)h_s(\theta^*, u),
\end{aligned}
\tag{4.15}
$$

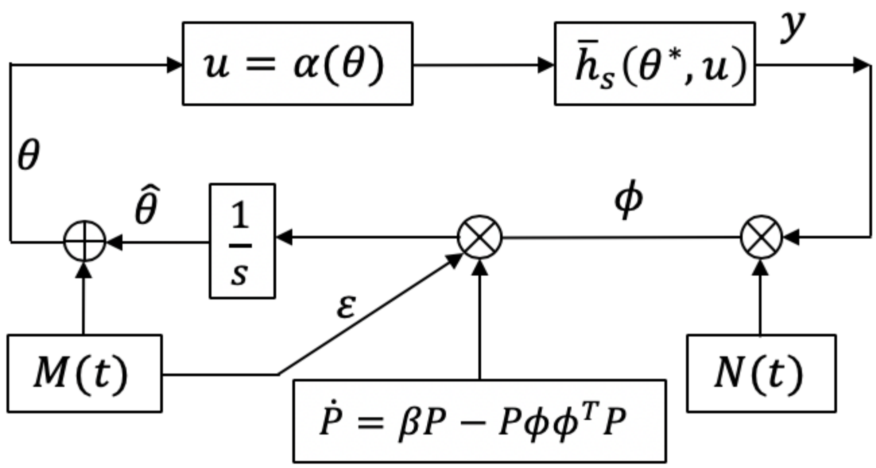


Figure 4.3: RLS estimation based ES redesign for vector parameter static maps.

where estimation error, $\varepsilon = \theta - \hat{\theta}$. In this design, perturbation signals $M(t)$, which generates $u$, and $N(t)$, which generates $\phi$, and forgetting factor $\beta$ have important places and they are chosen so that parameter convergence can be achieved.

### Dynamic Systems

In this section, ES scheme is considered for dynamic systems. Consider the defined nonlinear system (4.3) with its input (4.2), state (4.6), and assumptions (2.4-4.3).

The proposed algorithm is given in Fig. 4.4 to maximize the steady state value of $y$ without requiring the knowledge of either $\theta^*$ or the function of h. LS based ES scheme can be derived as follows:

$$\begin{aligned} \dot{\hat{\theta}} &= P\varepsilon\phi \\ \dot{P} &= \beta P - P\phi\phi^T P \\ \dot{\phi} &= \omega_l N(t)(y - \zeta) - \phi\omega_l, \\ \dot{\zeta} &= \zeta\omega_h + y\omega_h, \end{aligned} \tag{4.16}$$

where

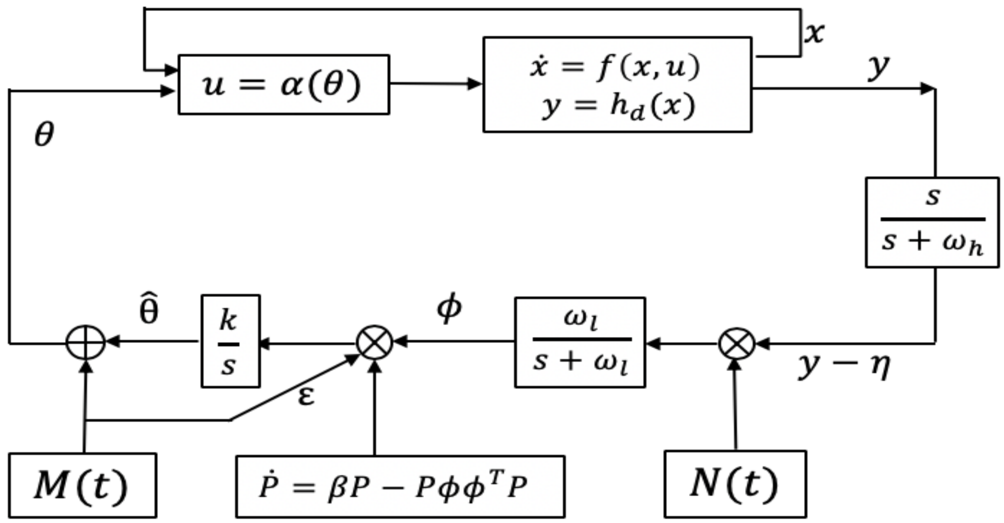


Figure 4.4: RLS estimation based ES redesign for vector parameter dynamic systems.

$$\begin{aligned}
&\varepsilon = \theta - \hat{\theta}, \\
&M(t) = \left[a_1 \sin(\omega_1 t), \cdots, a_n(\sin \omega_n t)\right]^T, \\
&N(t) = \left[\tfrac{a_1^2}{16} \sin^2(\omega_1 t), \cdots, \tfrac{a_n^2}{16} \sin^2(\omega_n t)\right]^T.
\end{aligned} \tag{4.17}$$

By appropriate choices of $\beta$, $M(t)$ and $N(t)$, convergence will be satisfied. However, the same discussion on the number of design parameters are applied here.

## 4.3 Adaptive ES design

In absence of the knowledge of $\theta^*$, a series of control/optimization schemes have been proposed in the literature utilizing certain ES tools such as switching methods ([15]), signal perturbation for persistence excitation, and band pass filtering ([15],[70],[73],[89]). In the previous section, we considered the work of [73] and replace the gradient part with RLS estimation algorithm. However, the high efforts on design and tuning process leads us to a new design. In this section, we propose following the certainty equivalence approach [60], producing an estimate $\hat{\theta}^*$ of $\theta^*$ and substituting in place of $\theta^*$ in (4.2) using RLS with forgetting factor.

The control parameter vector estimation can be done in different ways, leading to different ES schemes, even for the fixed control structure (4.2). The assumption that $h$ has a maximum is without loss of generality, considering a maximum seeking task. Minimum seeking case would be treated identically, replacing $y$ with $-y$ in the subsequent feedback design.

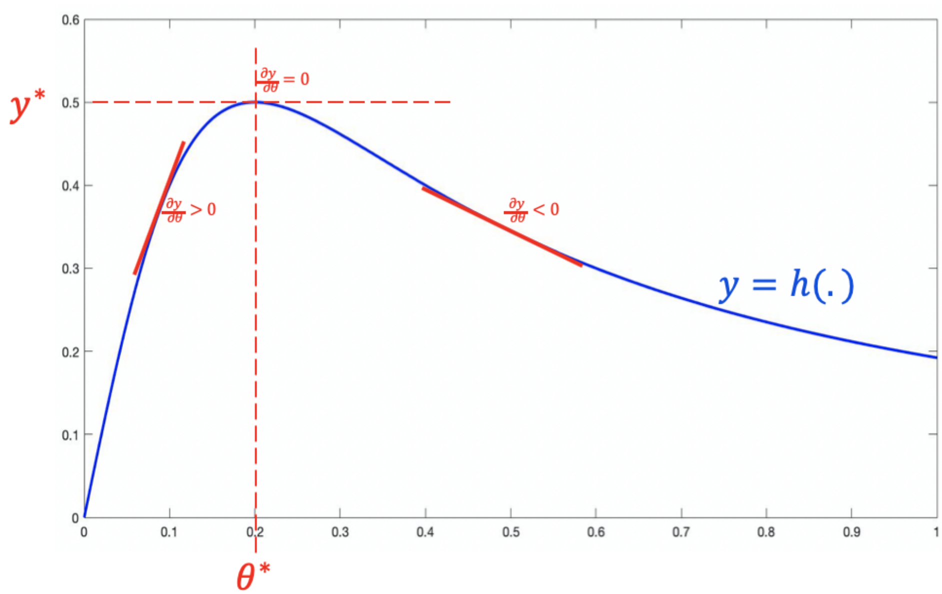


Figure 4.5: The idea of ES derivation.

The general idea of ES is derived from Fig. 4.5. The idea is to find the gradient of the output with respect to the input which is basically the direction to the extremum point, and add or subtract it, depending on the direction from previous value of the output, to get closer to the extremum. Once we reach the extremum point, the gradient will be zero and the algorithm will stop updating and maintain its extremum value. In this design in the absence of bandpass filtering, we consider scalar parameter and vector parameter cases separately. The reason behind this consideration is the need of perturbation signal in vector parameter case. For scalar parameter case, we will not need to use perturbation signal; however, for vector parameter case, we need to identify the system inputs by given them enough excitation.

Our proposed RLS estimation based adaptive ES scheme will be separately developed for two cases: for scalar parameter ($N = 1$) systems and for vector parameter ($N > 1$) systems, respectively.

### 4.3.1 RLS based ES Design for Scalar Parameter Systems

#### Static Maps

Consider the static map (4.1) and the control law (4.2) for scalar case, $N = 1$, under Assumptions 4.1 and 4.2 about the closed-loop system. The proposed scheme is depicted in Fig. 4.6. RLS estimation based ES block shown in Fig. 4.6 consists of two parts: an RLS based adaptive parameter identifier estimating the gradient $h_\theta = \frac{\partial y}{\partial \theta}$ and a control law to be fed by this estimate.

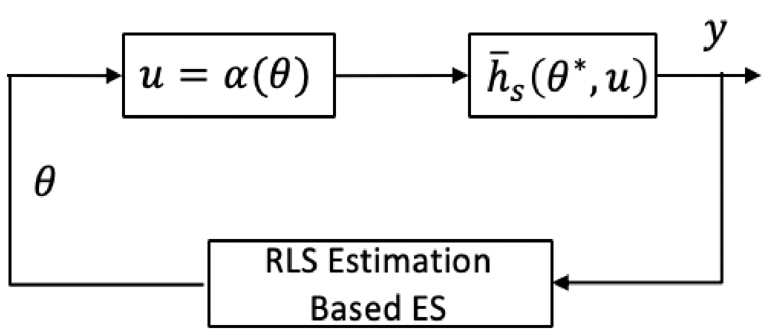


Figure 4.6: RLS based ES scheme for scalar parameter static maps.

Consider the static map equation (4.1). In this equation, the time derivative of the output $y$ is given by

$$\dot{y} = h_\theta \dot{\theta}. \tag{4.18}$$

Design of the RLS based estimator to generate $\hat{h}_\theta$ considers the relation (4.18) that is in the linear parametric model form.

$$z = h_\theta \phi. \tag{4.19}$$

where

$$z = \dot{y}, \quad \phi = \dot{\theta}. \tag{4.20}$$

If $\dot{y}$ is not available for measurement, then the regressor signals can be generated as

$$z = \frac{s}{s+\omega_l}[y], \quad \phi = \frac{1}{s+\omega_l}[\dot{\theta}], \tag{4.21}$$

i.e.,

$$\dot{z} = -\omega_l z + \dot{y}, \quad \dot{\phi} = -\phi\omega_l + \dot{\theta}, \tag{4.22}$$

where $\omega_l > 0$ is a constant design parameter. The control law generating $\theta$ is proposed to be

$$\dot{\theta} = k\hat{h}_\theta, \quad k > 0. \tag{4.23}$$

Assuming that the time variation of $h_\theta$ is sufficiently slow, we design an RLS estimator for the parametric model (4.19) as follows:

$$\dot{\hat{h}}_\theta = p\epsilon\phi, \tag{4.24}$$

$$\dot{p} = \beta p - p^2\phi^2, \tag{4.25}$$

$$\epsilon = z - \hat{h}_\theta \phi, \tag{4.26}$$

where $\beta > 0$ is forgetting factor and $p$ is the covariance term. The overall ES scheme producing $\theta(t)$ can be summarized by (4.23), (4.24), (4.25), and (4.26).

### Dynamic Systems

The RLS estimation based ES control scheme (4.23)-(4.26) applies to the dynamic system (4.3)-(4.5) for $N = 1$ with the control law (4.2) under Assumptions 4.3 and 4.4. The proposed ES scheme is depicted in Fig. 4.7.

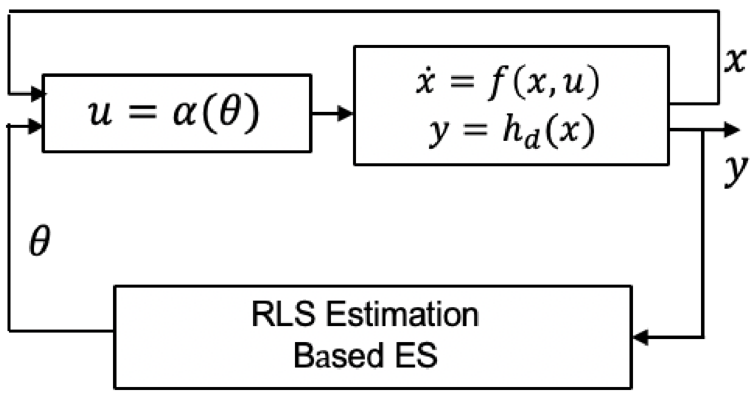


Figure 4.7: RLS based ES scheme for scalar parameter dynamic systems.

### Stability Analysis

In this section, stability proof of the proposed schemes in Sections 4.1 and 4.2 will be presented. We know that $\theta^*$ is the equilibrium point and the estimated gradient will be $h_\theta = 0$ at the equilibrium point $\theta = \theta^*$. We can write our stability result as follows:

**Theorem 4.1.** *Consider the RLS estimation based ES scheme given in Figs. 4.6, 4.7 and defined in (4.23) - (4.26) with $z$ and $\phi$ as given in* (4.20) *or (4.21), and Assumptions 4.1 - 4.4. For any initial condition $\hat{\theta}(0) \in \mathbb{R}^N$ and adaptation gain $k$, $\theta(t)$ asymptotically converges to small neighborhood of extremum parameter $\theta^*$.*

*Proof.* We consider the Lyapunov function as

$$V(\theta(t)) = \frac{1}{2}\left(\theta(t) - \theta^*\right)^2 = \frac{1}{2}\tilde{\theta}^2. \tag{4.27}$$

We write the time derivative of $V$ along the solutions of (4.23) as

$$\dot{V} = \dot{\theta}\left(\theta(t) - \theta^*\right) = \dot{\theta}\tilde{\theta}. \tag{4.28}$$

Substitutung (4.23) into (4.28), we obtain

$$\dot{V} = k\hat{h}_\theta\tilde{\theta}. \tag{4.29}$$

For the maximum case, $k > 0$. Negative definiteness of (4.29) depends on the initial condition $\theta_0$ that determines the signs of $\hat{h}_\theta$ and $\tilde{\theta}$. If $\theta(0) < \theta^*$, then $\hat{h}_\theta > 0$ and $\tilde{\theta} < 0$. On the other hand, if $\theta(0) > \theta^*$, then $\hat{h}_\theta < 0$ and $\tilde{\theta} > 0$. Hence, for both cases $\dot{V} < 0$. We also need to examine the forgetting factor $\beta$ and the persistent excitation (PE) of $\phi$. If $\phi$ is PE, then (4.23) guarantees that $p \in \mathcal{L}_\infty$ and $\theta(t) \to \theta^*$ as $t \to \infty$. When $\beta > 0$, the convergence of $\theta(t) \to \theta^*$ is exponential ([60]).

□

### 4.3.2 RLS based ES Design for Vector Parameter Systems

In this section, the proposed RLS estimation based ES scheme is extended to the systems with vector parameters ($N > 1$). Similar to the classical gradient based analysis, small sinusoidal perturbation signals with different frequencies ($\omega_1, \cdots, \omega_N$) are added to the control signals to provide sufficiently rich excitation.

#### Static Maps

Consider the block diagram in Fig. 4.8 for the static map in (4.1). The time derivative of (4.1) is given by

$$\dot{y} = h_\theta^T\dot{\theta}, \tag{4.30}$$

which, similarly to (4.19), can be written in the linear parametric form

$$z = h_\theta^T\phi, \tag{4.31}$$

where $z$ and $\phi$ are again defined by either (4.20) or (4.21). The control law (4.23) is used for updating $\theta$ in the vector case as well.

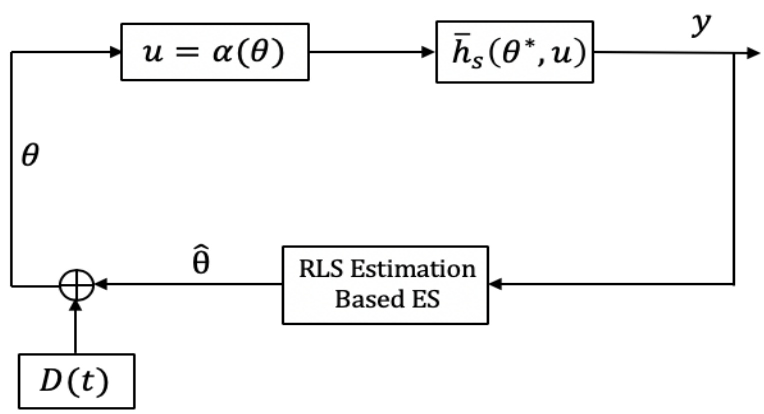


Figure 4.8: RLS based ES scheme for vector parameter static maps.

The design of the RLS estimator to produce $\hat{h}_\theta$ is based on the parametric model (4.31) and is given as follows ([60]):

$$\dot{\hat{h}}_\theta = P\epsilon\phi, \tag{4.32}$$

$$\dot{P} = \beta P - P\phi\phi^T P, \tag{4.33}$$

$$\epsilon = z - \hat{h}_\theta^T \phi, \tag{4.34}$$

where $\beta$ is the forgetting factor and $P$ is the covariance matrix of the RLS algorithm. The control law generating $\theta$ is proposed to be

$$\dot{\hat{\theta}} = k\hat{h}_\theta, \quad k > 0. \tag{4.35}$$

$$\theta(t) = \hat{\theta}(t) + D(t), \tag{4.36}$$

where

$$D(t) = [a_1 sin(\omega_1 t) \;\; \cdots \;\; a_N sin(\omega_N t)]^T.$$

$a_N$ are dither signals' amplitudes and $\omega_N$ are dither signals' frequencies.

Different from scalar parameter systems, we use perturbation signals, $D(t)$. The need to use of dither signals in vector parameter systems is that dither signals with different frequencies can be implemented on each input signal to achieve overall PE.

### Dynamic Systems

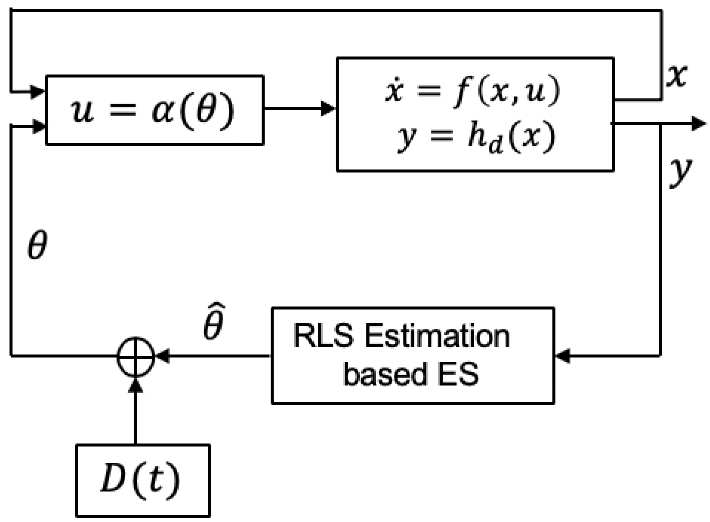


Figure 4.9: RLS based ES scheme for vector parameter dynamic systems.

The RLS estimation based ES scheme (4.32) - (4.35) applies to the dynamic system (4.3)-(4.5) with control law (4.2) under Assumptions 4.3 and 4.4 for vector parameter systems. Block diagram of the proposed ES scheme is given in Fig.4.9.

### Stability Analysis

The intuition in (4.36) is to satisfy persistence of excitation for $N$-dimensional $\phi$ by introducing at least one distinct dither frequency for each input, following the standard perturbation based ES control approaches mentioned in Section 3. Similar to the analysis in Section 4.3, consider the Lyapunov function as

$$V(\tilde{\theta}(t)) = \frac{1}{2}\tilde{\theta}^T\tilde{\theta}. \tag{4.37}$$

We write the time derivative of $V$ along the solutions of (4.35) as

$$\dot{V} = \tilde{\theta}^T\dot{\tilde{\theta}} = \tilde{\theta}^T\dot{\theta}. \tag{4.38}$$

Substitutung (4.36) into (4.38), we obtain

$$\dot{V} = \tilde{\theta}^T (k\hat{h}_\theta + \dot{D}). \tag{4.39}$$

The relationship between $\tilde{\theta}$ and $\hat{h}_\theta$ in Section 4.3 applies to vector parameter case. The stability again depends on $k$, initial condition $\theta(0)$, forgetting factor $\beta$, and PE of $\phi$, that is guaranteed by addition of dither signals in (4.36). Hence, $P \in \mathcal{L}_\infty$ and $\theta(t) \to \theta^*$ as $t \to \infty$.

**Example 4.1.** *Consider the following model for scalar parameter case*

$$\begin{aligned} y &= 10m(u), \\ m(u) &= k_1 \left(1 - e^{-k_2 u}\right) - k_3 u \\ u &= \theta, \end{aligned} \tag{4.40}$$

*where $\theta^* = 0.3$. $\theta_0 = 0.01$ is chosen as initial value for both schemes. $k_1 = 1.05, k_2 = 23, k_3 = 0.52$ are given. For RLS estimation based ES scheme, the following parameters are used: $k_{ls} = 0.01$, $p_0 = 10^3$, and $\beta = 0.98$ are given. For classical ES scheme, the following parameters are given: $k = 0.08$, $\omega_h = 0.6$, $\omega_l = 0.8$, $S(t) = 0.01 \sin 3t$, and $M(t) = sin3t$.*

*We apply RLS estimation based ES scheme in Fig.4.7. The results for this example is given in Fig.4.10. It is obvious that proposed scheme can reach very smal neighborhood of the extremum point $\theta^* = 0.3$ at $y^* = 8.85$ less than 2 second while classical ES finds the extremum point very late and cannot maintain that extremum point under measurement noise.*

**Example 4.2.** *Consider the following model for vector parameter case*

$$\begin{aligned} y &= y_1 + y_2, \\ y_1 &= am(u_1),\ m(u_1) = (2m_1^* u_1^* u_1)/(u_1^{*2} + u_1^2), \\ y_2 &= am(u_2),\ m(u_2) = (2m_2^* u_2^* u_2)/(u_2^{*2} + u_2^2), \\ u &= [u_1,\ u_2] = [\theta_1,\ \theta_2]. \end{aligned} \tag{4.41}$$

*where $[\theta_1^*,\ \theta_2^*] = [0.2,\ 0.3]$. For both schemes, initial values are given as $u_0 = [0.1,\ 0.1]$. We aim to reach $y_1^*(\theta_1^*) = 5$ and $y_2^*(\theta_2^*) = 9$. For RLS estimation based ES scheme, the following parameters are used: $k = [0.01,\ 0.01]$, $P_0 = 10^4$, $\beta = 0.98$, and $D(t) = [0.01 \sin 7t,\ 0.01 \sin 10t]$ are given. For classical ES scheme, the following parameters are*

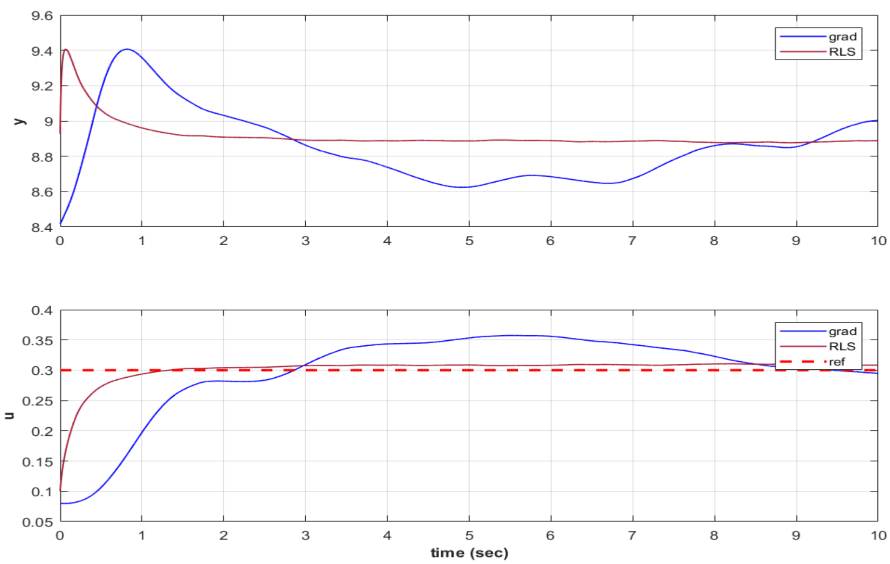


Figure 4.10: RLS estimation based ES result for $y$.

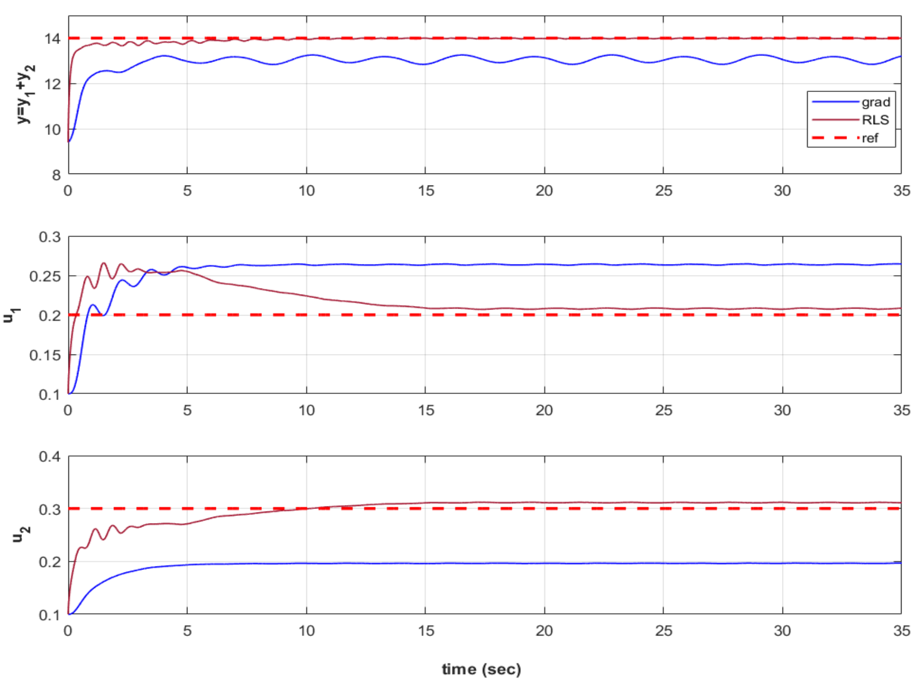


Figure 4.11: RLS estimation based ES results.

*given:* $k = [0.02,\ 0.01]$, $\omega_h = [0.6,\ 0.6]$, $\omega_l = [0.8,\ 0.8]$, $S(t) = [0.01 \sin t,\ 0.01 \sin 2t]$, *and* $M(t) = [4.5 \sin 5t,\ 11 \sin 5t]$.

*Simulation results are given in Fig.4.11 for both RLS estimation based and classical ES schemes. It is clear that the results taken with RLS can converge the extremum point and find the maximized output* $y^*$ *while classical ES scheme has difficulty to reach the extremum point. One reason for this difficulty is that in classical ES scheme has many tuning parameters that must be tuned accordingly.*

*For vector case, we also emphasize the need to apply perturbation terms to the scheme in order to observe multiple input channels separately. When there is no perturbation signal applied, the inputs cannot be distinguished and converge to an average value that caused to reach a value near the maximum. Similar to scalar case, RLS estimation based ES scheme outweighs classical ES scheme in terms of reaching extremum.*

## 4.4 Application to Vehicle ABS and TCS

Tire-road friction characteristics affect in all vehicle dynamics control systems, especially, vehicle safety systems like ABS and TCS [44, 110]. Finding maximum friction force between the tire and the road is a challenging task for such systems, where the road friction coefficient is mostly unknown and difficult to estimate on-line.

ABS in passenger vehicles increases safety by preventing wheel lock-up, reducing vehicle stopping distance and enhancing steerability on low friction surfaces like wet and icy roads during braking. On the other hand, TCS assures optimal friction coefficient during acceleration. In ABS and TCS applications, wheel lock-up and excessive slip significantly decreases the friction coefficient between the road and the tires.

[68] developed a gradient estimation based ES which uses classical band pass filtering to find the maximum friction force on ABS. In this classical approach, ES has a low pass filter, high pass filter and a multiplier to estimate the optimum slip ratio to obtain maximum deceleration at the same time. Developed gradient estimation based ES was only used for ABS and was simulated in Matlab/Simulink for a specific road condition with high effort of tuning design parameters.

Since RLS based estimation algorithm has the advantage of fast convergence under measurement noises, we develop RLS parameter estimation based ES to find the optimum slip ratio for ABS to obtain maximum deceleration during emergency braking and also for TCS to obtain maximum acceleration during driving. Its stability analysis is provided.

Developed scheme is tested in Matlab/Simulink and compared to [68] for ABS. We also apply gradient based algorithm to TCS to compare developed RLS estimation based ES. Moreover, we show the results and effectiveness of our developed algorithm for different road scenarios and compare it with gradient estimation based ES algorithm. We use CarSim simulation environment to provide high-fidelity results for proposed scheme and give comparative results with CarSim ABS module itself.

### 4.4.1 System Modelling

A single wheel tire friction model is considered, as illustrated in Fig.4.12, for both braking and traction control cases. The wheel characteristics are modelled by the equations

$$\begin{aligned} \dot{x} &= f(\lambda^*, x, \tau) = \begin{bmatrix} 0 & 0 \\ 0 & -\frac{B}{I} \end{bmatrix} x + \begin{bmatrix} g \\ \frac{NR}{I} \end{bmatrix} h(\lambda^*, x) + \begin{bmatrix} 0 \\ \tau \end{bmatrix}, \\ y &= \mu = h(\lambda^*, x) = h_\lambda(\lambda^*, \lambda(x)), \end{aligned} \tag{4.42}$$

where $x = \begin{bmatrix} \nu, \omega \end{bmatrix}^T$; $N = mg$; $\nu, \omega, m, N, R, I$ are the linear velocity, angular velocity, mass, weight, radius, and the moment of inertia of the wheel, respectively. $B\omega$ is the bearing friction torque. $\tau$ is the input torque which will be specified in the sequel as $\tau_B$ for braking torque, and $\tau_D$ for driving torque. $\mu(\lambda)$ is the friction force coefficient.

$\lambda$ is the wheel slip defined as

$$\lambda(x) = \frac{R\omega - \nu}{\max\{\nu, \omega R\}}. \tag{4.43}$$

According to (4.43), $\lambda$ is negative during braking and positive during traction. It can be seen from (4.43) that by increasing braking action, slip value $\lambda$ decreases from 0 to -1. $\lambda = -1$ denotes that the wheel is locked ($\omega = 0$).

The relationship between friction force coefficient, $\mu$, and wheel slip, $\lambda$, can be described in different ways including Magic formula, Dahl's model, LuGre model, Burckhardt model, and Pacejka model [98]. The friction relation is further described by various parametric models in the literature [17].

The Burckhardt model considers a mapping $h_\lambda(\lambda^*, \lambda(x))$ whose typical shape for different road conditions is shown in Fig.4.13 and whose approximation is given by [68]

$$\mu = h_\lambda(\lambda^*, \lambda(x)) = 2\mu_m \frac{\lambda^* \lambda}{\lambda^{*2} + \lambda^2}. \tag{4.44}$$

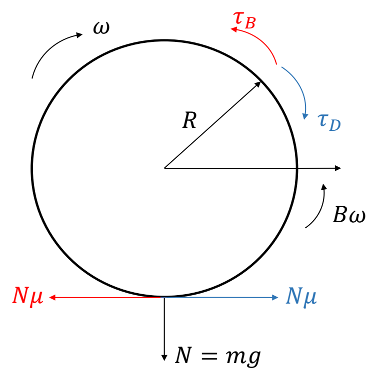


Figure 4.12: Single wheel model.

Note from Fig.4.13 that each friction curve has a single maximum friction force coefficient $\mu_m$ at a particular wheel slip value $\lambda^*$.

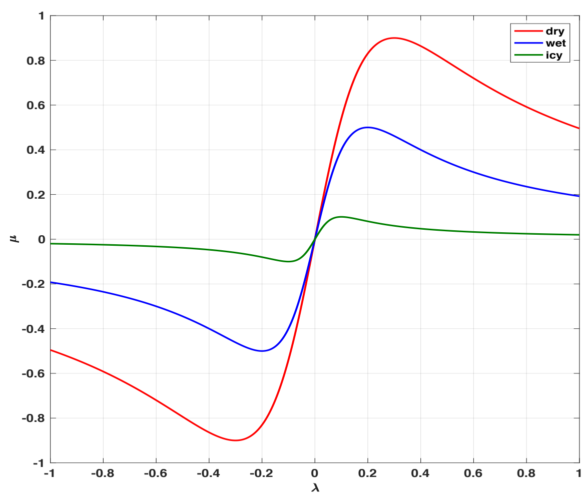


Figure 4.13: Relationship between force coefficient and wheel slip.

### 4.4.2 Control and Optimization Task

Our control task is to find the optimum wheel slip in order to maximize the force by measuring velocity and acceleration. We introduce an unknown constant $\lambda_0$, which is the optimum slip value to generate the maximum force. We will examine two cases, braking and traction, to derive torque controllers to generate appropriate torques.

### Braking Case

In braking case, $v > \omega R$; hence, the wheel slip (4.43) becomes

$$\lambda(x) = \frac{R\omega - \nu}{v}. \tag{4.45}$$

We differentiate (4.45) and obtain

$$\dot{\lambda} = \frac{(R\dot{\omega} - \dot{\nu})\nu - \dot{\nu}(R\omega - \nu)}{\nu^2}. \tag{4.46}$$

Substituting (4.42) into (4.46), for $\tilde{\lambda}(t) = \lambda(t) - \lambda_0$, we obtain

$$\dot{\tilde{\lambda}} = \dot{\lambda} = -\left(\frac{R\omega}{\nu^2} + \frac{mR^2}{I\nu}\right)\dot{\nu} - \frac{RB}{I\nu}\omega + \frac{R}{I\nu}\tau. \tag{4.47}$$

We assume that longitudinal and angular velocities are available for measurement, i.e., $\dot{v}$ is measurable. The wheel model given in [68] is written as follows:

$$\dot{\lambda} = -c(\lambda - \hat{\lambda}_0). \tag{4.48}$$

where $c$ is a positive constant which makes equilibrium $\lambda_0$ of the system exponentially stable ($\dot{\tilde{\lambda}} = -c\tilde{\lambda}$). Substituting (4.48) into (4.47), we obtain our torque controller for braking case as follows:

$$\tau = \tau_B = -\frac{cI\nu}{R}(\lambda - \hat{\lambda}_0) + B\omega + \left(\frac{I\omega}{\nu} + mR\right)\dot{\nu}. \tag{4.49}$$

### Traction Case

In traction case, $v < \omega R$; hence, the wheel slip (4.43) becomes

$$\lambda(x) = \frac{R\omega - \nu}{R\omega}. \tag{4.50}$$

We differentiate (4.50) and obtain

$$\dot{\lambda} = \frac{(\dot{R\omega} - \dot{\nu})R\omega - R\dot{\omega}(R\omega - \nu)}{R^2\omega^2}. \tag{4.51}$$

Substituting (4.42) into (4.51), we obtain

$$\dot{\hat{\lambda}} = \dot{\lambda} = -\left(\frac{\nu m}{I\omega^2} + \frac{1}{R\omega}\right)\dot{\nu} - \frac{B}{R\omega}\nu + \frac{\nu}{RI\omega^2}\tau. \tag{4.52}$$

Substituting (4.48) into (4.52), we obtain the torque controller for driving case as

$$\tau = \tau_D = -\frac{cRI\omega^2}{v}(\lambda - \hat{\lambda}_0) + B\omega + \left(mR + \frac{I\omega}{v}\right)\dot{v}. \tag{4.53}$$

In order to maximize the force $\mu N$, we should maximize $\mu(\lambda)$. In our design, estimation algorithm updates the optimum wheel slip that corresponds to the maximum friction or traction coefficient.

Note that existing ES scheme [68] is designed only for ABS case. We will design our RLS based ES scheme for both ABS and TCS control. In simulation part, we will apply existing algorithm to both ABS and TCS and compare them with proposed RLS algorithm.

### 4.4.3 RLS Based ES Design

In this section, we present the proposed RLS estimation based ES scheme, where the RLS estimator will be used to estimate the partial derivative of the acceleration with respect to the slip. In this way, we will check the slope of the curve and the algorithm will search for the maximum. Block diagram of the proposed scheme is shown in Fig.4.14. Within the proposed scheme, the RLS based ES scheme is designed based on the parametric model [60]

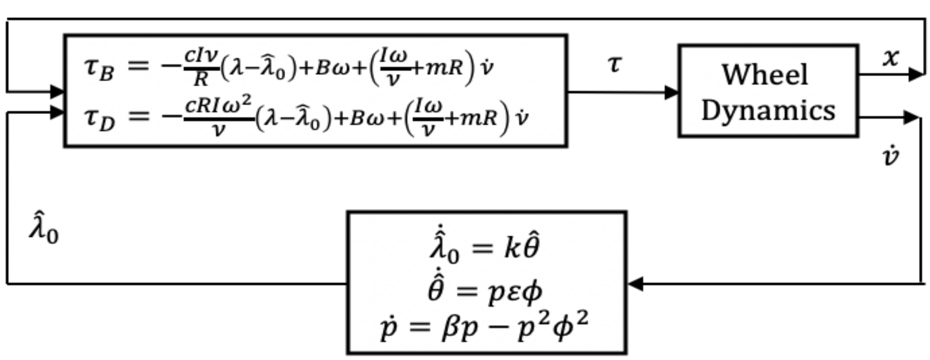


Figure 4.14: RLS parameter estimation based ES scheme.

$$z = \theta^* \phi \tag{4.54}$$

where $z = \ddot{\nu}$, $\phi = \dot{\lambda}$ and $\theta^* = \frac{\partial \dot{v}}{\partial \lambda}$ . Note here that $\theta^*$ corresponds to the slope of the curve in Fig. 4.13 multiplied by the factor $g$. Hence, $\theta^*$ has the same sign as $\lambda^* - \lambda$, for any $\lambda$. Treating the time variation of $\theta^*$ to be negligible for parameter estimation purposes. Based on the parametric model (13), $\theta^*$ is estimated using the following RLS adaptive law with forgetting factor $\beta$:

$$\begin{aligned} \dot{\hat{\theta}} &= p\epsilon\phi, \\ \dot{p} &= \beta p - p^2\phi^2, \\ \epsilon &= z - \hat{\theta}\phi, \end{aligned} \tag{4.55}$$

where $p$ is the time varying adaptive gain, named as the covariance term in the literature [60]. The estimate $\hat{\theta}$ of $\theta^*$ is then used to steer the estimate $\hat{\lambda}_0$ towards the optimal value $\lambda_0$ via

$$\dot{\hat{\lambda}}_0 = k\hat{\theta}, \tag{4.56}$$

where $k$ is a positive gain coefficient. The reasoning of the selection of the RLS based ES scheme laws as above will be more clear in the following section on stability and convergence analysis. The proposed scheme is modular to any initial conditions, initial speeds and noises.

### 4.4.4 Simulation Results

#### Matlab/Simulink Results

In this section, we present the results of the simulation tests of the proposed RLS based ES algorithm (4.54), (4.56), (4.55) for both ABS and TCS cases using Matlab/Simulink. Then, we compare their performances with the gradient based ES scheme developed in [68]. Note that in the literature simulation results are not presented for TCS.

The vehicle parameters are assumed to be as follows: $m = 567.75$ $(2271/4)$ $kg$, $R = 0.3$ $m$, $I = 1.7$ $kgm^2$, $B = 0.01$ $kg/s$. Controller parameter is selected as $c = 5$ for both the proposed RLS and the benchmark gradient-based schemes. RLS estimation algorithm parameters are selected as $\beta = 0.95, k = \pm 0.006, p_0 = 10^4$. Gradient estimation parameters are used as $a = 0.035$, $\omega = 5$, high pass, low pass and regulation gain are selected as $\omega_h = 0.6$, $\omega_l = 0.8$, $k = \pm 1.5$.

The simulations for both the gradient and RLS based schemes are performed assuming a Gaussian noise ($\sigma = 0.05$) in longitudinal acceleration measurement, $\dot{v}$. Initial conditions of the slip and vehicle speed estimates are set the same for both schemes for a fair comparison, $\lambda_{00} = \pm 0.01$, $\nu_0 = 120$ for ABS and $\nu_0 = 1$ for TCS, respectively . [68] uses an approximate friction model to match with the original friction model in the form

$$\mu(\lambda) = 2\mu_{max}\frac{\lambda^*\lambda}{\lambda^{*2} + \lambda^2}, \tag{4.57}$$

having a maximum $\mu(\lambda^*) = \mu_m$ at $\lambda = \lambda^*$. We use this model in MATLAB/Simulink simulations to see the effect of the algorithm.

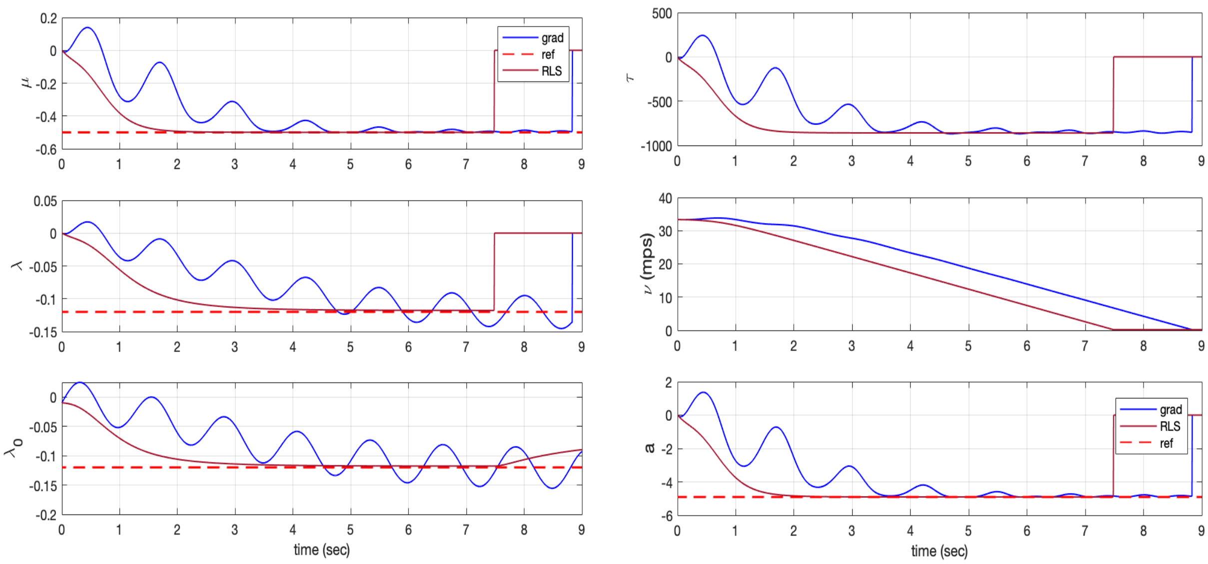


(a) Friction force coefficient and estimated slip results for ABS.

(b) Braking torque, velocity and deceleration results for ABS.

Figure 4.15: Wet road comparison results for ABS.

Simulation results of ABS/TCS in a wet road for gradient/RLS based ES scheme comparison are given in Figs. (4.15a), (4.15b), (4.16b), and (4.16a). We select wet road scenario to evaluate the convergence characteristics, because it is safety critical. Results demonstrate that with gradient based ABS the vehicle stops almost 1.5 sec longer than with the RLS based ABS. Similar to the ABS results, the vehicle with gradient algorithm reaches optimal slip in longer time compared to the RLS one. Similar results can be seen for TCS on wet road. The time to reach optimal slip and maximum acceleration is shorter than the one with gradient.

We also show the results for different road conditions in Figs. (4.17a), (4.17b), (4.18a), and (4.18b). Road condition is changed from wet to icy. As can be seen from the figures for

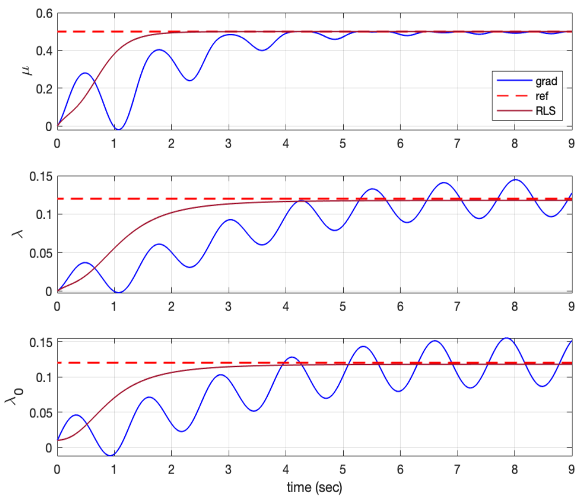


(a) Traction force coefficient and estimated slip results for TCS.

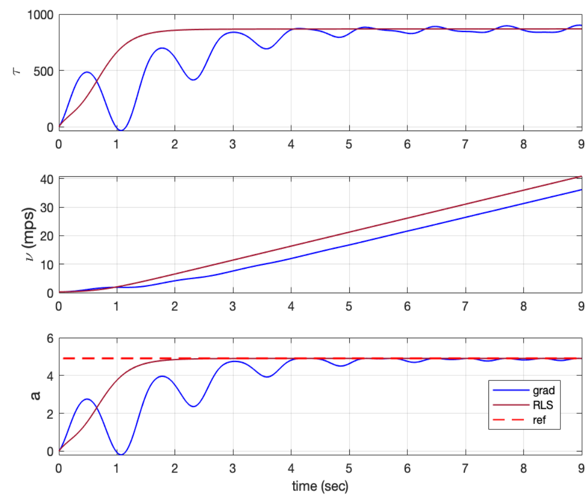


(b) Driving torque, velocity and acceleration results for TCS.

Figure 4.16: Wet road comparison results for TCS.

both ABS and TCS, the gradient based scheme is not robust to road change unlike the RLS based scheme. Once the road is different, it is hard for the gradient based scheme to adapt itself. There is a very small discrepancy in slip estimation of the RLS based scheme for icy road. The reason for this is that if we approach the maximum value from left or right in Fig. 4.13, the gradient values in the small neighborhood of the maximum are very close to each other. Results in Matlab/Simulink show how fast the algorithm adapts itself to new road condition and find optimal slips to reach the maximum deceleration/acceleration.

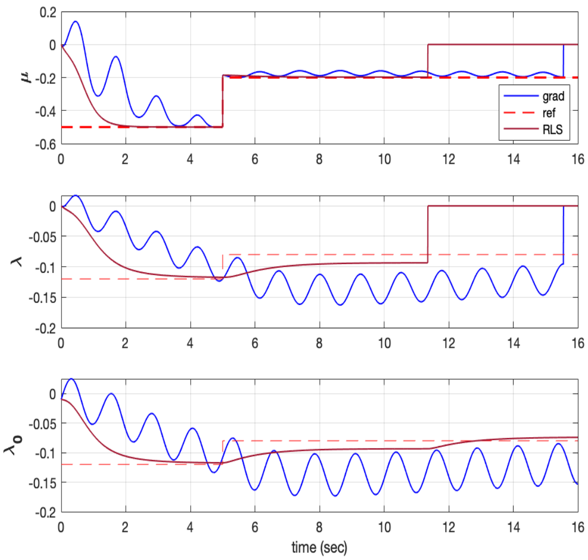


(a) Friction force coefficient and estimated slip results for ABS in wet-icy road change condition.

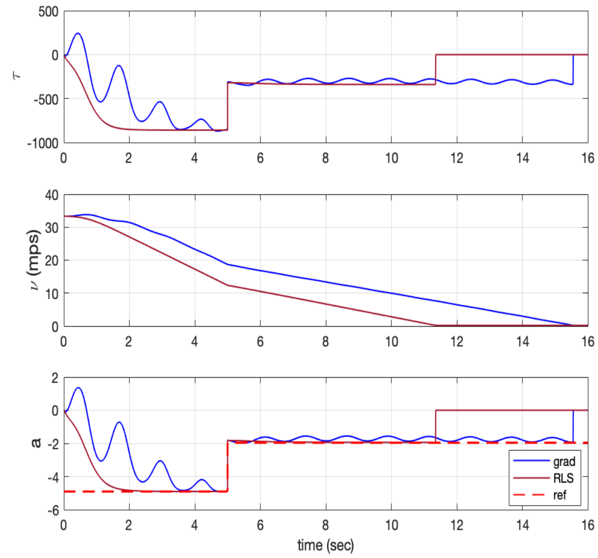


(b) Braking torque, velocity and deceleration results for ABS in wet-icy road change condition.

Figure 4.17: ABS application results in different road conditions.

### Carsim Results

In this section, Carsim is used to present more realistic results for ABS. Since CarSim has an ABS module itself, ABS is only considered to show the comparison of RLS estimation based ES scheme performance with ABS module.

The vehicle is selected as E-class Sedan and the vehicle parameters are given as follows: $m = (1650 + 90 * 2)/4\ kg$ (sprung and unsprung mass for each wheel), $R = 0.353\ m$, $I = 1.7\ kgm^2$, $B = 0.01\ kg/s$. The same vehicle parameters are used in ABS module for a fair comparison. Controller parameter is selected as $c = 15$. RLS estimation algorithm parameters are selected as $\beta = 0.95, k = -0.006, p_0 = 10^4$.

For wet road, the results of vehicle speeds and accelerations in CarSim are given in Fig. (4.19a). As can be seen from the results, the vehicle with RLS scheme has the advantage of stopping in shorter distance and time. The reason for this can be seen in Fig. (4.19b). Since ABS by its nature is applying pulses to stop the vehicle in any emergency situations, RLS estimation based ES can find the optimum slip and/or maximum deceleration and try to maintain these values to stop the vehicle in shorter time. Estimated slips and measured

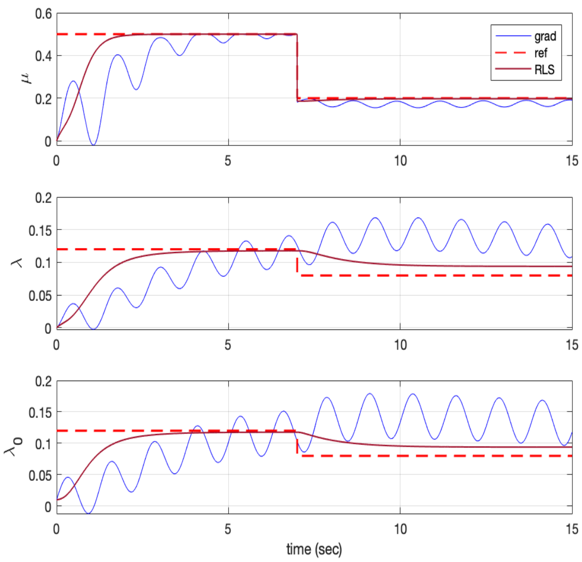


(a) Friction force coefficient and estimated slip results for TCS in wet-icy road change condition.

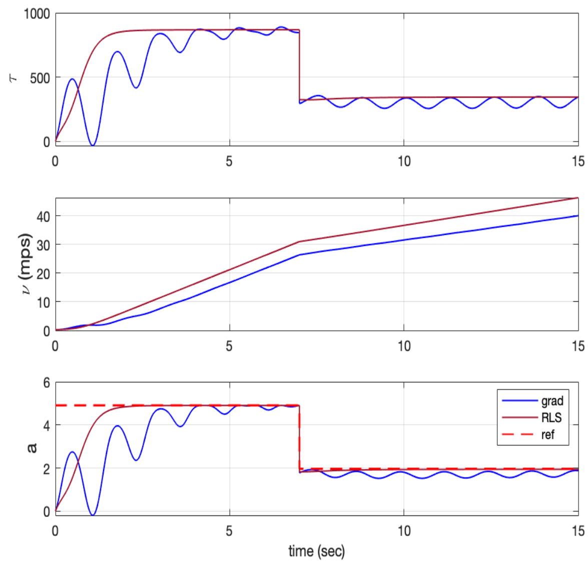


(b) Driving torque, velocity and acceleration results for TCS in wet-icy road change condition.

Figure 4.18: TCS application results in different road conditions.

slips are given for the RLS scheme in Fig. (4.20a), and measured slips are given for the CarSim module in Fig. (4.20b).

### ABS Control with Redesigned ES scheme

In this section, proposed RLS based ES redesigned in Section 4.2 is considered. One can use this redesign; however, tuning parameters should be selected wisely.

$$\begin{aligned} \text{Estimation error:} \quad & \epsilon = \lambda - \hat{\lambda}_0, \\ \text{Regressor Signal:} \quad & \dot{\phi} = \omega_l N(t)(\dot{v} - \eta) - \phi\omega_l, \\ & \dot{\eta} = \omega_h \dot{\nu} - \omega_h \eta \\ \text{LS Estimation Algorithm} \quad & \dot{\hat{\lambda}}_0 = P\epsilon\phi, \\ & \dot{P} = \beta P - \frac{P^2\phi^2}{m_s^2}, \end{aligned} \tag{4.58}$$

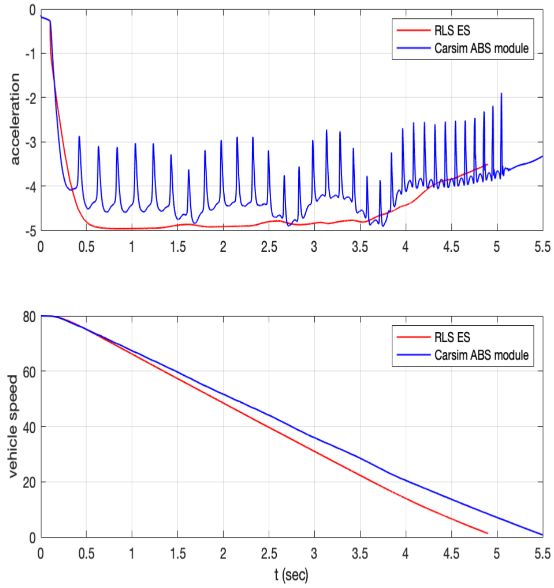


(a) Acceleration and longitudinal velocity.

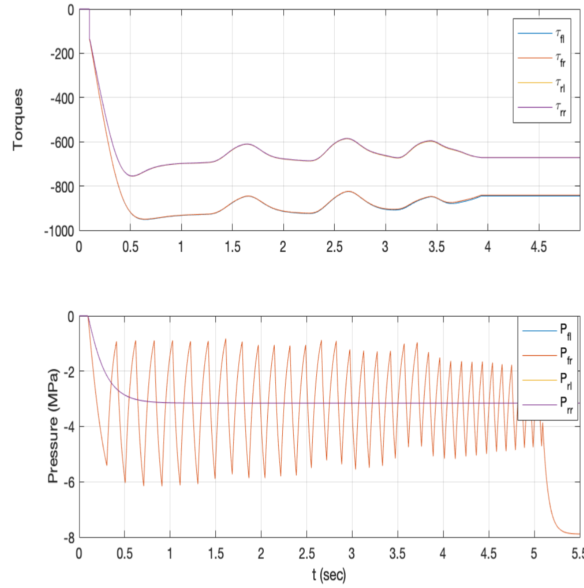


(b) Applied torques and pressures.

Figure 4.19: CarSim results of RLS based ES and ABS module for wet road.

where $M(t) = a \sin \omega t$ and $N(t) = \frac{a^2}{16^2} \sin^2 \omega t - \frac{1}{2}$.

The parameters are given as follows: $k = 1.5$, $a = 0.013$, $\omega = 3$, $\omega_h = 0.6$, $\omega_l = 0.8$, $\lambda^* = 0.25$. The simulation is performed under the Gaussian noise ($\sigma = 0.1$) in longitudinal acceleration measurement, $\dot{v}$.

Gradient based ES proposed by [68] and proposed RLS based ES are simulated using MATLAB/Simulink. Simulation results for $\lambda_0$ estimation for both gradient and RLS designs are given in Fig.4.21a. Results show that the system cannot reach the optimal wheel slip $\lambda^*$ within the time the vehicle stops. However, in RLS based design, the system reaches the optimal wheel slip within a short period of time.

Fig. 4.21b shows applied braking torque to the wheel and velocity of the wheel for gradient and RLS based designs. It is clear that RLS based algorithm has an advantage of convergence rate over gradient based one since the vehicle with RLS algorithm stops less than with gradient one. ES scheme reached the maximum friction force coefficient is shown in Fig. 4.22. The maximum friction force coefficient is reached in less than a second with RLS algorithm. The gradient algorithm cannot reach the maximum friction

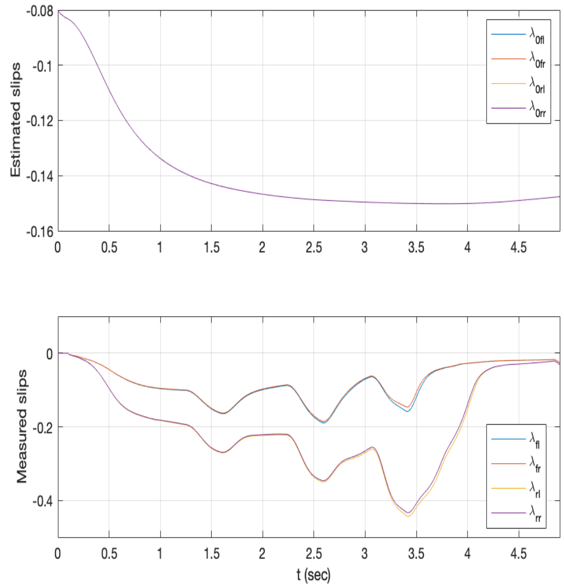


(a) Estimated and measured slips for RLS based ES scheme.

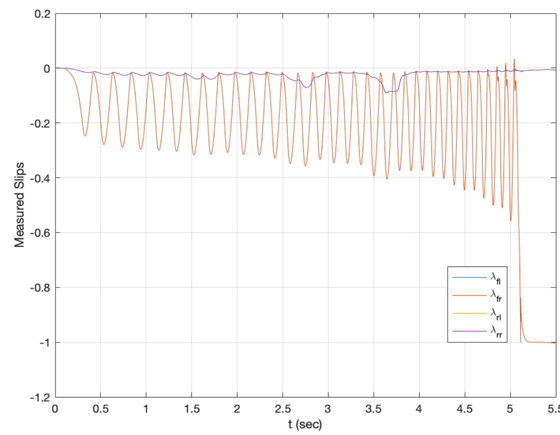


(b) Measured slips for ABS module.

Figure 4.20: CarSim slip results for RLS based ES and ABS module.

force coefficient within the stopping time. Similar to ABS, TCS is also performed with Matlab/Simulink in dry road and simulation results can be found in Fig. 4.23 and Fig. 4.24. The results show the performance improvement and effectiveness of RLS estimation algorithm over gradient.

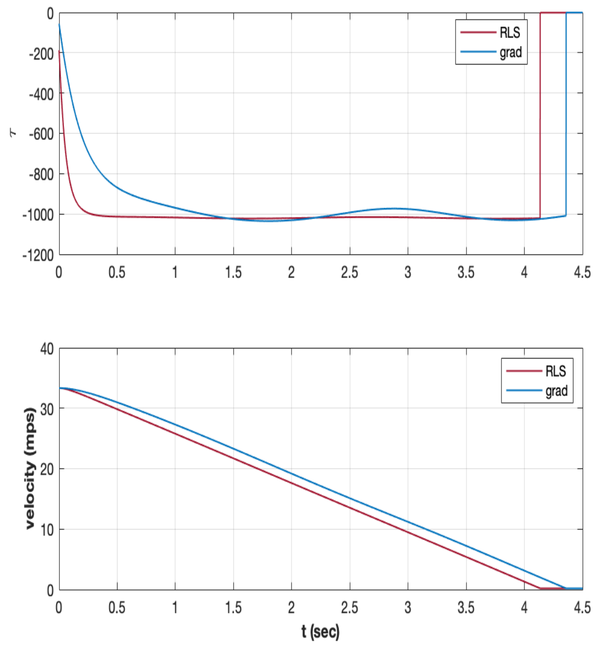


(a) Braking torque and speed results for gradient and RLS based ES.

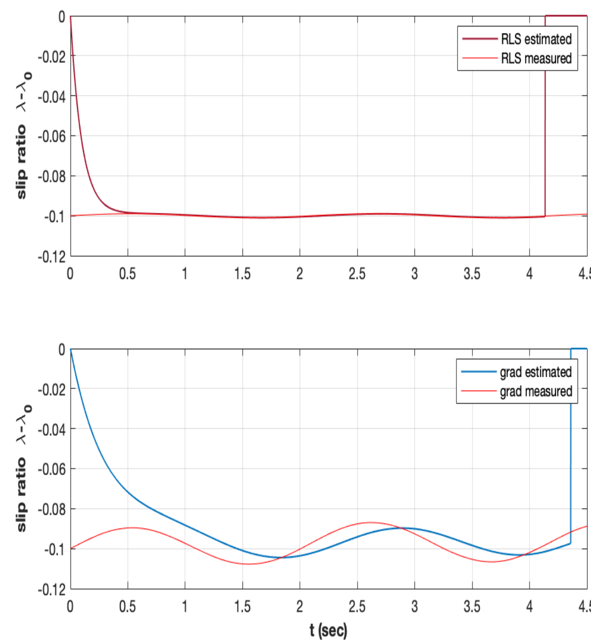


(b) $\lambda - \lambda_0$ results for gradient and RLS based ES.

Figure 4.21: RLS based redesigned ES results for ABS.

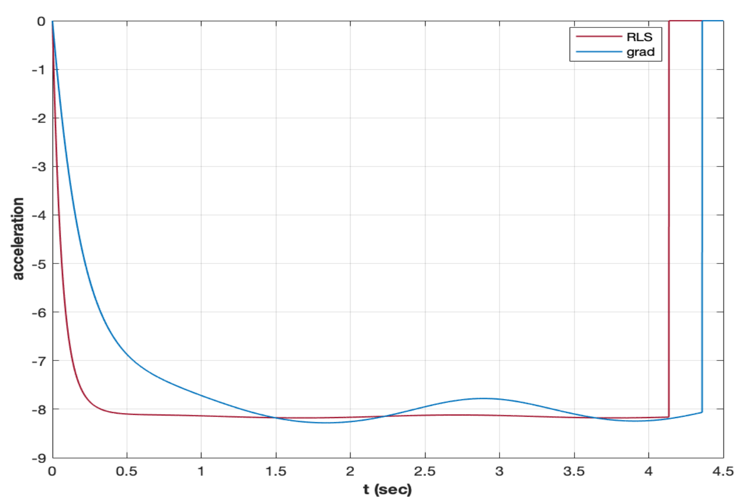


Figure 4.22: Acceleration results for gradient and RLS based ES.

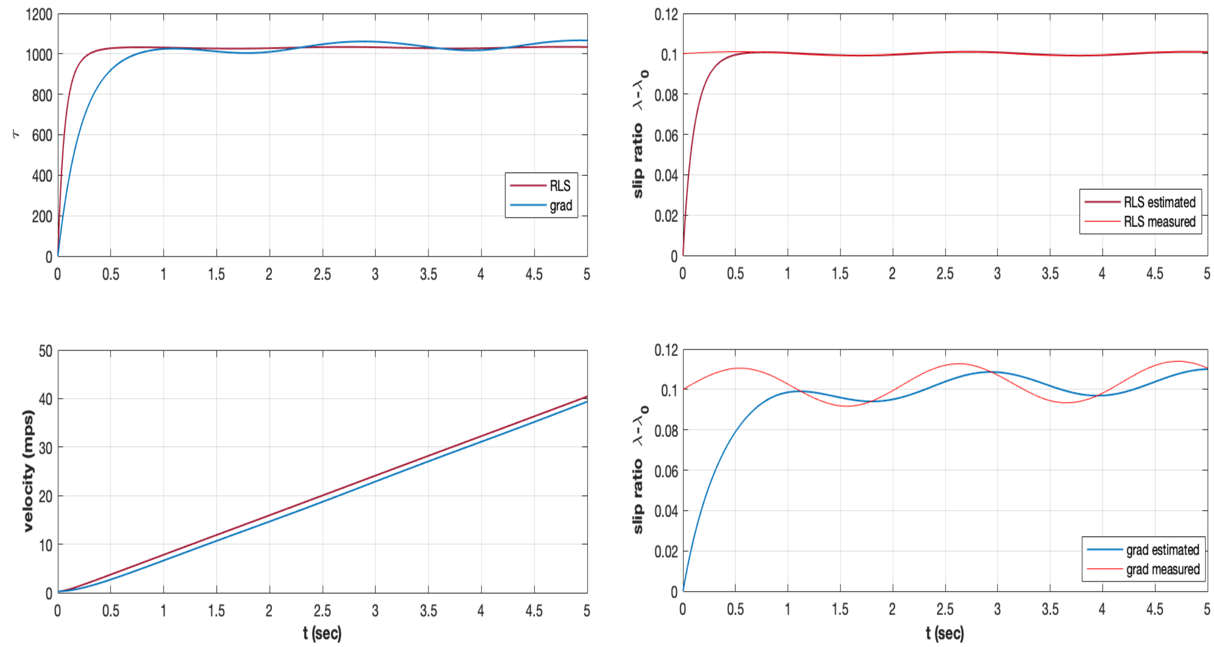


(a) Braking torque and speed results for gradient and RLS based ES.

(b) $\lambda - \lambda_0$ results for gradient and RLS based ES.

Figure 4.23: RLS based redesigned ES results for ABS.

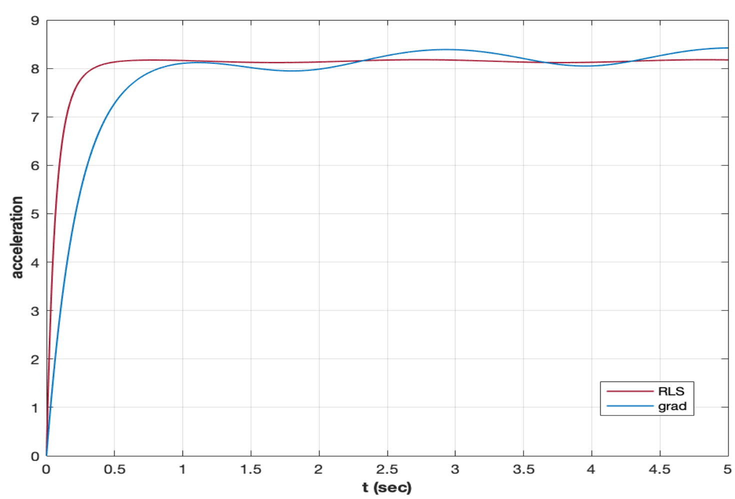


Figure 4.24: Acceleration results for gradient and RLS based ES.

## 4.5 Summary

In this chapter, the formal problem definition for ES of static maps and dynamics systems was given. RLS parameter estimation based ES scheme was studied for scalar and vector parameter systems in each case, utilizing high-pass and low pass filters based on the work of [73].

Secondly, an RLS parameter estimation based ES scheme that does not involve bandpass filtering and considering ES as an estimation problem was introduced for scalar and vector parameter systems in static maps and dynamic systems. Their stability results were presented.

The performance of the proposed RLS based ES designs is examined in simulations for active vehicle safety systems, ABS and TCS. Several driving scenarios such as one road condition, road condition change, are designed to evaluate the capability of the proposed designs in longitudinal vehicle safety systems. Matlab/Simulink and CarSim simulation applications were presented to prove the effectiveness and validity of the proposed schemes.

# Chapter 5

# Conclusion and Future Research

## 5.1 Summary and Conclusions

This thesis has investigated several aspects of RLS parameter estimation based adaptive control and adaptive extremum seeking (ES). After providing a comparative numerical analysis of the use RLS based parameter estimation in adaptive control, with respect to gradient based parameter estimation, a formal constructive analysis framework for integration of RLS based estimation to direct adaptive control has been proposed. The proposed framework follows the typical steps for gradient adaptive law based direct model reference adaptive control, but is based on construction of a new Lyapunov-like function for the analysis.

Later, an RLS estimation based ES scheme is designed and analysed for application to scalar parameter and vector parameter static map and dynamic systems, with established asymptotic convergence to the extremum.

Finally, the proposed RLS parameter estimation based direct adaptive control and ES schemes have been applied to active vehicle safety systems, ACC, ABS and TCS.

## 5.2 Future Research Directions

This thesis has opened several doors for future work. An immediate follow up research topic is formal transient analysis of RLS parameter estimation based direct adaptive control based on the framework developed in Chapter 3.

A second potential future research direction as continuation of this thesis is to conduct a study on adaptive control using ES. Adaptive ES scheme can be used to estimate the parameters of MRAC. RLS parameter estimation based ES block will consider the tracking error as input, and minimizing of the cost function, ES scheme will produce the parameter estimates as output.

A third potential future research direction is detailed formal frequency domain analysis of the RLS parameter estimation based ES schemes developed in Chapter 4.

Another potential future research direction is development of RLS parameter estimation based source seeking algorithms. The main objective of source seeking algorithms is to steer autonomous agents towards the source location of a field of interest (e.g., a radio transmitter, a location of chemical contamination, etc.). Source seeking algorithms allow the autonomous agents to sense or estimate certain information about the field, e.g. the local distribution of the field strength or the gradient of the field strength, and steer the agents, accordingly, towards the source location. RLS parameter estimation based ES schemes can be applied to various such source seeking applications.

# References


[1] Acosta-Lú, C., Gennaro, S. D., and Sánchez-Morales, M. (2016). An adaptive controller applied to an anti-lock braking system laboratory. *Dyna*, 83(199):69–77.

[2] Adetola, V. and Guay, M. (2007). Parameter convergence in adaptive extremum-seeking control. *Automatica*, 43(1):105–110.

[3] Ameho, Y., Niel, F., Defay, F., Biannic, J., and Berard, C. (2013). Adaptive control for quadrotors. In *ICRA Robotics and Automation*, pages 5396–5401.

[4] Anderson, B. D. O. and Johnson, C. R. (1982). Exponential convergence of adaptive identification and control algorithms. *Automatica*, 18(1):1–13.

[5] Ariyur, K., Ganguli, S., and Enns, D. (2009). Extremum seeking for model reference adaptive control. In *AIAA Guidance, Navigation, and Control Conference*, page 6193.

[6] Ariyur, K. B .and Krstic, M. (2003). *Real-time optimization by extremum-seeking control*. John Wiley & Sons.

[7] Astrom, K. J. and Wittenmark, B. (1973). On self tuning regulators. *Automatica*, 9(2):185–199.

[8] Astrom, K. J. and Wittenmark, B. (2013). *Adaptive control*. Courier Corporation.

[9] Atta, K. T.and Johansson, A. and Gustafsson, T. (2017). Accuracy improvement of extremum seeking control. *IEEE Transactions on Automatic Control*, 62(4):1952–1958.

[10] Bae, H., Ryu, J., and Gerdes, J. C. (2001). Road grade and vehicle parameter estimation for longitudinal control using gps. In *Proceedings of the IEEE Conference on Intelligent Transportation Systems*, pages 25–29.

[11] Becker, A., Kumar, P., and Wei, C. Z. (1985). Adaptive control with the stochastic approximation algorithm: geometry and convergence. *IEEE Transactions on Automatic Control*, 30(4):330–338.

[12] Benesty, J. and Huang, Y. (2013). *Adaptive signal processing: applications to real-world problems*. Springer Science & Business Media.

[13] Benosman, M.and Atinc, G. M. (2013). Nonlinear learning-based adaptive control for electromagnetic actuators. In *European Control Conference (ECC)*, pages 2904–2909.

[14] Benosman, M. and Atinc, G. M. (2013). Multi-parametric extremum seeking-based learning control for electromagnetic actuators. In *American Control Conference (ACC)*, pages 1914–1919.

[15] Blackman, P. (1962). Extremum-seeking regulators. In *An exposition of adaptive control*. Macmillan.

[16] Burckhardt, M. (1993). Fahrwerktechnik: radschlupf-regelsysteme. *Vogel-Verlag, Germany*, 1:16.

[17] Canudas-de Wit, C., Tsiotras, P., Velenis, E., Basset, M., and Gissinger, G. (2003). Dynamic friction models for road/tire longitudinal interaction. *Vehicle System Dynamics*, 39(3):189–226.

[18] Carnevale, D., Astolfi, A., Centioli, C., Podda, S., Vitale, V., and Zaccarian, L. (2009). A new extremum seeking technique and its application to maximize rf heating on ftu. *Fusion engineering and design*, 84(2):554–558.

[19] Centioli, C., Iannone, F., Mazza, G., Panella, M., Pangione, L., Podda, S., Tuccillo, A., Vitale, V., and Zaccarian, L. (2008). Maximization of the lower hybrid power coupling in the frascati tokamak upgrade via extremum seeking. *Control Engineering Practice*, 16(12):1468–1478.

[20] Chen, H. F. and Guo, L. (1986). Convergence rate of least-squares identification and adaptive control for stochastic systems. *International Journal of Control*, 44(5):1459–1476.

[21] Chen, W., Tan, D., and Zhao, L. (2018). Vehicle sideslip angle and road friction estimation using online gradient descent algorithm. *IEEE Transactions on Vehicular Technology*, 67(12):11475–11485.

[22] Choi, J. Y., Krstic, M., Ariyur, K., and Lee, J. S. (2002). Extremum seeking control for discrete-time systems. *IEEE Transactions on Automatic Control*, 47(2):318–323.

[23] Chowdhary, G. and Johnson, E. (2010a). Least squares based modification for adaptive control. In *IEEE Conference on Decision and Control*, pages 1767–1772.

[24] Chowdhary, G. and Johnson, E. (2010b). Recursively updated least squares based modification term for adaptive control. In *American Control Conference*, pages 892–897.

[25] Cochran, J. and Krstic, M. (2009). Nonholonomic source seeking with tuning of angular velocity. *IEEE Transactions on Automatic Control*, 54(4):717–731.

[26] Creaby, J., Li, Y., and Seem, J. (2009). Maximizing wind turbine energy capture using multivariable extremum seeking control. *Wind Engineering*, 33(4):361–387.

[27] Dalvi, A. and Guay, M. (2009). Control and real-time optimization of an automotive hybrid fuel cell power system. *Control Engineering Practice*, 17(8):924–938.

[28] Dasgupta, S. and Huang, Y. F. (1987). Asymptotically convergent modified recursive least-squares with data-dependent updating and forgetting factor for systems with bounded noise. *IEEE Transactions on Information Theory*, 33(3):383–392.

[29] De Larminat, P. (1984). On the stabilizability condition in indirect adaptive control. *Automatica*, 20(6):793–795.

[30] De Mathelin, M. F. and Lozano, R. (1997). Robust adaptive identification of slowly time-varying parameters with bounded disturbances. In *European Control Conference*, pages 2300–2305.

[31] Dimogianopoulos, D. and Lozano, R. (1999a). Adaptive control for linear time-varying systems using direct least squares estimation. In *IEEE Conference on Decision and Control*, volume 4, pages 3309–3314.

[32] Dimogianopoulos, D. and Lozano, R. (1999b). Direct least squares estimation for linear time varying systems. In *European Control Conference*, pages 1884–1889.

[33] Dimogianopoulos, D. and Lozano, R. (2001). Adaptive control for linear slowly time-varying systems using direct least-squares estimation. *Automatica*, 37(2):251–256.

[34] Dincmen, E., Guvenc, B. A., and Acarman, T. (2014). Extremum-seeking control of abs braking in road vehicles with lateral force improvement. *IEEE Transactions on Control Systems Technology*, 22(1):230–237.

[35] Dixon, C. and Frew, E. (2009). Maintaining optimal communication chains in robotic sensor networks using mobility control. *Mobile Networks and Applications*, 14(3):281–291.

[36] Drakunov, S., Ozguner, U., Dix, P., and Ashrafi, B. (1995). Abs control using optimum search via sliding modes. *IEEE Transactions on Control Systems Technology*, 3(1):79–85.

[37] Draper, C. S. and Li, Y. T. (1951). *Principles of optimalizing control systems and an application to the internal combustion engine*. American Society of Mechanical Engineers.

[38] Fidan, B. and Camlica, A. (2012). Least-squares based adaptive source localization by mobile agents. In *Allerton Conference on Communication, Control, and Computing*, pages 1286–1291.

[39] Fidan, B., Dasgupta, S., and Anderson, B. D. O. (2013). Adaptive range-measurement-based target pursuit. *International Journal of Adaptive Control and Signal Processing*, 27:66–81.

[40] Fidan, B., Çamlıca, A., and Guler, S. (2015). Least-squares-based adaptive target localization by mobile distance measurement sensors. *International Journal of Adaptive Control and Signal Processing*, 29(2):259–271.

[41] Ghaffari, A., Krstic, M., and Nesic, D. (2012). Multivariable newton-based extremum seeking. *Automatica*, 48(8):1759–1767.

[42] Ghaffari, A., Krstic, M., and Seshagiri, S. (2014). Power optimization and control in wind energy conversion systems using extremum seeking. *IEEE Transactions on Control Systems Technology*, 22(5):1684–1695.

[43] Ghaffari, A., Seshagiri, S., and Krstic, M. (2015). Multivariable maximum power point tracking for photovoltaic micro-converters using extremum seeking. *Control Engineering Practice*, 35:83–91.

[44] Gissinger, G. L., Menard, C., and Constans, A. (2003). A mechatronic conception of a new intelligent braking system. *Control Engineering Practice*, 11(2):163–170.

[45] Goodwin, G. and Sin, K. (2014). *Adaptive filtering prediction and control*.

[46] Guay, M. (2014). A time-varying extremum-seeking control approach for discrete-time systems. *Journal of Process Control*, 24(3):98–112.

[47] Guay, M., Beerens, R., and Nijmeijer, H. (2014). A time-varying extremum-seeking control approach for discrete-time systems with application to model predictive control. *IFAC Proceedings Volumes*, 47(3):1023–1028.

[48] Guay, M. and Dochain, D. (2015). A time-varying extremum-seeking control approach. *Automatica*, 51:356–363.

[49] Guay, M., Dochain, D., and Perrier, M., j. v. n. p. y. Adaptive extremum seeking control of continuous stirred tank bioreactors with unknown growth kinetics.

[50] Guay, M. and Zhang, T. (2003). Adaptive extremum seeking control of nonlinear dynamic systems with parametric uncertainties. *Automatica*, 39(7):1283–1293.

[51] Guler, S., Fidan, B., Dasgupta, S., Anderson, B. D., and Shames, I. (2016). Adaptive source localization based station keeping of autonomous vehicles. *IEEE Transactions on Automatic Control*, 62(7):3122–3135.

[52] Haghi, P. and Ariyur, K. (2011). On the extremum seeking of model reference adaptive control in higher-dimensional systems. In *American Control Conference (ACC)*, pages 1176–1181.

[53] Hellstrom, E., Lee, D., Jiang, L., Stefanopoulou, A., and Yilmaz, H. (2013). On-board calibration of spark timing by extremum seeking for flex-fuel engines. *IEEE Transactions on Control Systems Technology*, 21(6):2273–2279.

[54] Hespanha, J., Liberzon, D., and Morse, S. (2003a). Hysteresis-based switching algorithms for supervisory control of uncertain systems. *Automatica*, 39(2):263–272.

[55] Hespanha, J., Liberzon, D., and Morse, S. (2003b). Overcoming the limitations of adaptive control by means of logic-based switching. *Systems & control letters*, 49(1):49–65.

[56] Hu, C., Yao, B., and Wang, Q. (2010). Integrated direct/indirect adaptive robust contouring control of a biaxial gantry with accurate parameter estimations. *Automatica*, 46(4):701–707.

[57] Hudon, N., Guay, M., and Perrier, M.and Dochain, D. (2008). Adaptive extremum-seeking control of convection-reaction distributed reactor with limited actuation. *Computers & Chemical Engineering*, 32(12):2994–3001.

[58] Ikhouane, F. and Krstic, M. (1998a). Adaptive backstepping with parameter projection: Robustness and asymptotic performance. *Automatica*, 34(4):429–435.

[59] Ikhouane, F. and Krstic, M. (1998b). Robustness of the tuning functions adaptive backstepping design for linear systems. *IEEE Transactions on Automatic Control*, 43(3):431–437.

[60] Ioannou, P. and Fidan, B. (2006). *Adaptive Control Tutorial*. SIAM, Philadelphia, PA.

[61] Ioannou, P. and Sun, J. (1996). *Robust Adaptive Control*. Prentice-Hall, Saddle River, NJ.

[62] Jiang, K. and Victorino, A.C.and Charara, A. (2015). Adaptive estimation of vehicle dynamics through rls and kalman filter approaches. In *IEEE 18th International Conference on Intelligent Transportation Systems*, pages 1741–1746.

[63] Karafyllis, I. and Krstic, M. (2018a). Adaptive certainty-equivalence control with regulation-triggered finite-time least-squares identification. *IEEE Transactions on Automatic Control*, 63(10):3261–3275.

[64] Karafyllis, I. and Krstic, M. (2018b). Adaptive certainty-equivalence control with regulation-triggered finite-time least-squares identification. *IEEE Transactions on Automatic Control*, 63(10):3261–3275.

[65] Khalil, H. K. (2002). *Nonlinear Systems Third Edition*. Prentice Hall, Philadelphia, PA.

[66] Kidouche, M. and Habbi, H. (2010). On lyapunov stability of interconnected nonlinear systems: recursive integration methodology. *Nonlinear dynamics*, 60(1-2):183–191.

[67] Killingsworth, N., Aceves, S., Flowers, D., Espinosa-Loza, F., and Krstic, M. (2009). Hcci engine combustion-timing control: Optimizing gains and fuel consumption via extremum seeking. *IEEE Transactions on Control Systems Technology*, 17(6):1350–1361.

[68] Kristic, M., Kanellakopoulos, I., and Kokotovic, P. (1995). *Nonlinear and Adaptive Control Design*. John Wiley & Sons, INC.

[69] Krstic, M.and Kanellakopoulos, I. and Kokotovic, P. V. (1994). Nonlinear design of adaptive controllers for linear systems. *Automatic Control, IEEE Transactions on*, 39(4):738–752.

[70] Krstic, M. (2000). Performance improvement and limitations in extremum seeking control. *Systems & Control Letters*, 39(5):313–326.

[71] Krstic, M. (2009). On using least-squares updates without regressor filtering in identification and adaptive control of nonlinear systems. *Automatica*, 45:731–735.

[72] Krstic, M., Kokotovic, P., and Kanellakopoulos, I. (1995). *Nonlinear and adaptive control design*.

[73] Krstic, M. and Wang, H. H. (2000). Stability of extremum seeking feedback for general nonlinear dynamic systems. *Automatica*, 36(4):595–601.

[74] Kumar, P. R. (1990a). Convergence of adaptive control schemes using least-squares parameter estimates. *IEEE Transactions on Automatic Control*, 35(4):416–424.

[75] Kumar, P. R. (1990b). Convergence of least-squares parameter estimate based adaptive control schemes. *IEEE Transactions on Automatic Control*, 35(5):416–424.

[76] Lai, T. L. and Wei, C. Z. (1982). Least squares estimates in stochastic regression models with applications to identification and control of dynamic systems. *The Annals of Statistics*, pages 154–166.

[77] Lai, T. L. and Wei, C. Z. (1986). Extended least squares and their applications to adaptive control and prediction in linear systems. *IEEE Transactions on Automatic Control*, 31(10):898–906.

[78] Larsson, S. and Andersson, I. (2008). Self-optimising control of an si-engine using a torque sensor. *Control Engineering Practice*, 16(5):505–514.

[79] Leblanc, M. (1922). Sur l'electrification des chemins de fer au moyen de courants alternatifs de frequence elevee. *Revue generale de l'electricite*, 12:275–277.

[80] Leishman, R., Macdonald, J., Beard, R., and McLain, T. (2014). Quadrotors and accelerometers: State estimation with an improved dynamic model. *IEEE Control Systems*, 34(1):28–41.

[81] Leyva, R., Alonso, C., Queinnec, I., Cid-Pastor, A., Lagrange, D., and Martinez-Salamero, L. (2006). Mppt of photovoltaic systems using extremum-seeking control. *IEEE transactions on aerospace and electronic systems*, 42(1):249–258.

[82] Liu, S. and Krstic, M. (2010). Stochastic source seeking for nonholonomic unicycle. *Automatica*, 46(9):1443–1453.

[83] Luxat, J. C. and Lees, L. H. (1971). Stability of peak-holding control systems. *IEEE Transactions on Industrial Electronics and Control Instrumentation*, (1):11–15.

[84] Matveev, A.and Teimoori, H. and Savkin, A. (2011). Navigation of a unicycle-like mobile robot for environmental extremum seeking. *Automatica*, 47(1):85–91.

[85] Mohanty, A. and Yao, B. (2011a). Indirect adaptive robust control of hydraulic manipulators with accurate parameter estimates. *IEEE Transactions on Control Systems Technology*, 19(3):567–575.

[86] Mohanty, A. and Yao, B. (2011b). Integrated direct/indirect adaptive robust control of hydraulic manipulators with valve deadband. *IEEE/ASME Transactions on Mechatronics*, 16(4):707–715.

[87] Murray, R. (2006). Nonlinear and adaptive control lecture notes.

[88] Narendra, K. and Annaswamy, A. (2012). *Stable adaptive systems*.

[89] Nesic, D., Mohammadi, A., and Manzie, C. (2013a). A framework for extremum seeking control of systems with parameter uncertainties. *IEEE Transactions on Automatic Control*, 58(2):435–448.

[90] Nesic, D., Mohammadi, A., and Manzie, C. (2013b). A framework for extremum seeking control of systems with parameter uncertainties. *IEEE Transactions on Automatic Control*, 58(2):435–448.

[91] Ostrovskii, I. I. (1957). Extremum regulation. *Automatic and Remote Control*, 18:900–907.

[92] Pan, Y., Li, X., and Yu, H. (2016). Least-squares learning control with guaranteed parameter convergence. In *International Conference on Automation and Computing*, pages 132–137.

[93] Papachristodoulou, A. and Prajna, S. (2002). On the construction of lyapunov functions using the sum of squares decomposition. In *Proceedings of the 41st IEEE Conference on Decision and Control, 2002.*, volume 3, pages 3482–3487.

[94] Patra, N. and Sadhu, S. (2015). Adaptive extended kalman filter for the state estimation of anti-lock braking system. In *Annual IEEE India Conference (INDICON)*, pages 1–6. IEEE.

[95] Pavkovic, D., Deur, J., Burgio, G., and Hrovat, D. (2009). Estimation of tire static curve gradient and related model-based traction control application. In *IEEE Control Applications,(CCA) & Intelligent Control,(ISIC)*, pages 594–599.

[96] Peet, M.and Papachristodoulou, A. (2012). A converse sum of squares lyapunov result with a degree bound. *IEEE Transactions on Automatic Control*, 57(9):2281–2293.

[97] Radenkovic, M. and Krstic, M. (2017). Adaptive control via extremum seeking: Global stabilization and consistency of parameter estimates. *IEEE Transactions on Automatic Control*, 62(5):2350–2359.

[98] Rajamani, R. (2011). *Vehicle dynamics and control*. Springer Science & Business Media.

[99] Roberts, J. D. (1965). Extremum or hill-climbing regulation: a statistical theory involving lags, disturbances and noise. In *Proceedings of the Institution of Electrical Engineers*, volume 112, pages 137–150.

[100] Ryan, J. J. and Speyer, J. L. (2010). Peak-seeking control using gradient and hessian estimates. In *American Control Conference (ACC), 2010*, pages 611–616.

[101] Seyedtabaii, S. and Velayati, A. (2019). Adaptive optimal slip ratio estimator for effective braking on a non-uniform condition road. *Automatika, Journal for Control, Measurement, Electronics, Computing and Communications*, 60(4):413–421.

[102] Sternby, J. (1977). On consistency for the method of least squares using martingale theory. *IEEE Transactions on Automatic Control*, 22(3):346–352.

[103] Sternby, J. (1980). Extremum control systems: An area for adaptive control? In *Joint Automatic Control Conference*, number 17, page 8.

[104] Tao, G. (2003). *Adaptive Control Design and Analysis*. Wiley.

[105] Tay, T., Moore, J., and Horowitz, R. (1989). Indirect adaptive techniques for fixed controller performance enhancement. *International Journal of Control*, 50(5):1941–1959.

[106] Vahidi, A., Stefanopoulou, A., and Peng, H. (2005). Recursive least squares with forgetting for online estimation of vehicle mass and road grade: theory and experiments. *Vehicle System Dynamics*, 43(1):31–55.

[107] Van Der Meulen, S., De Jager, B., Veldpaus, F., Van Der Noll, E., Van Der Sluis, F., and Steinbuch, M. (2012). Improving continuously variable transmission efficiency with extremum seeking control. *IEEE Transactions on Control Systems Technology*, 20(5):1376–1383.

[108] Van DerMeulen, S., De Jager, B., Veldpaus, F., and Steinbuch, M. (2014). Combining extremum seeking control and tracking control for high-performance cvt operation. *Control Engineering Practice*, 29:86–102.

[109] Walsh, A., Forbes, J. R.and Chee, S. A., and Ryan, J. J. (2017). Kalman-filter-based unconstrained and constrained extremum-seeking guidance on so (3). *Journal of Guidance, Control, and Dynamics*, pages 1–12.

[110] Wellstead, P. E. and Pettit, N. (1997). Analysis and redesign of an antilock brake system controller. *IEE Proceedings of Control Theory and Applications*, 144(5):413–426.

[111] Xu, L. (2017). The parameter estimation algorithms based on the dynamical response measurement data. *Advances in Mechanical Engineering*, 9(11).

[112] Yao, B. (1997a). High performance adaptive robust control of nonlinear systems: a general framework and new schemes. In *IEEE Conference on Decision and Control*, volume 3, pages 2489–2494.

[113] Yao, B. (1997b). High performance adaptive robust control of nonlinear systems: a general framework and new schemes. In *IEEE Conference on Decision and Control*, volume 3, pages 2489–2494.

[114] Yao, B. (2003). Integrated direct/indirect adaptive robust control of siso nonlinear systems in semi-strict feedback form. In *American Control Conference*, volume 4, pages 3020–3025.

[115] Yi, J., Alvarez, L., and Horowitz, R. (2002). Adaptive emergency braking control with underestimation of friction coefficient. *IEEE Transactions on Control Systems Technology*, 10(3):381–392.

[116] Zhang, C. and Ordonez, R. (2007). Numerical optimization-based extremum seeking control with application to abs design. *IEEE Transactions on Automatic Control*, 52(3):454–467.

[117] Zhang, Y. I. and Ioannou, P. A. (1997). Robustness of the adaptive backstepping controllers for linear systems. In *American Control Conference*, volume 1, pages 746–750.

[118] Zhong, Z., Huo, H., Zhu, X., Cao, G., and Ren, Y. (2008). Adaptive maximum power point tracking control of fuel cell power plants. *Journal of Power Sources*, 176(1):259–269.